Neural Correlates of Motor Learning/Memory in Primary Motor Cortex of Macaque Monkeys

Brian J. Benda

B.S., Aeronautical and Astronautical Engineering
Purdue University
1972

M.S., Structural Mechanics
Stanford University
1976

Submitted to the Division of Health Sciences and Technology
in Partial Fulfillment of the Requirements for the Degree of
Doctor of Philosophy in Medical Engineering

at the
Massachusetts Institute of Technology

Signature of Author .....
Brian J. Benda
May 13,1998

Certified by .....
Dr. Emilio Bizzi
Eugene McDermott Professor in Brain Sciences and Human Behavior
Massachusetts Institute of Technology
Thesis Supervisor

Accepted by .....
Dr. Martha L. Gray
Director, Division of Health Sciences and Technology

Neural Correlates of Motor Learning/Memory in Primary Motor Cortex of Macaque Monkeys

Brian J. Benda

Submitted to the Division of Health Sciences and Technology
in Partial Fulfillment of the Requirements for the Degree of
Doctor of Philosophy in Medical Engineering

Abstract

Motor learning can be described as skill acquisition - an improvement in task performance associated with repetition or practice of the task. Improvement is often characterized in terms of performance parameters such as increased accuracy, increased speed of task execution, decrease in reaction time, or maximization of a motor task outcome measure. That improvement in performance is retained over time suggests that motor learning is associated with a change in the state of the neuromuscular system responsible for controlling and executing the task. To establish a neural correlate of motor learning and memory, I recorded single unit cell activity in the motor cortex of two macaque monkeys while they executed a reaching task. The monkeys were trained to move a manipulandum in the horizontal plane such that a computer-displayed cursor moved from a center to a peripheral target. The location of the peripheral target was randomly selected from a set of eight positions spaced at 45° intervals. Motors attached to the manipulandum produced a velocity-dependent, curl force field that altered the dynamics of the reaching task and created the environment for motor learning. Within a given recording session, each monkey performed the reaching task in three behavioral epochs - first in the null field (no forces), then in the presence of the force field, and finally, again in the null field.

The spike activity of over 150 cells in the arm area of the primary motor cortex was recorded. Nearly half of the cells showed activity with no significant correlation to the task. Another 25% of cells demonstrated activity similar to that reported by other researchers. However, approximately 25% of cells displayed "memory" behavior - activity characteristics in the final experimental epoch (no forces) the same as that seen in the force field. This despite the fact that the dynamic characteristics of the reaching task in the two behavioral epochs were significantly different. Memory behavior suggests the presence of neural circuitry that maintains and reinforces cell activity patterns associated with a learned motor task. Such circuitry may be the neural substrate that brings about the change in neuromuscular system state associated with motor learning.

Thesis supervisor and thesis committee chair:	Emilio Bizzi, M.D. Eugene McDermott Professor in Brain Sciences and Human Behavior
Thesis committee:	Earl Miller, Ph.D. Chi-Sang Poon, Ph.D. Conrad Wall, Ph.D.

Acknowledgments

The work and results described herein represents a fraction of the effort that went into this research. Prior to the first successful cortical recording, over two years were spent designing, fabricating and constructing the laboratory in which the experiments were conducted and testing and verifying the hardware/software that defined and controlled the experimental paradigm and the methods of data analysis. Two monkeys were trained in the reaching task; multiple cell recording systems were tried and evaluated. Although I was involved in all aspects of these developments, I was but one in an outstanding group of technicians, graduate students, post-doctoral fellows, and faculty members who, working together, sometimes well, sometimes poorly, made this research happen.

Francesca Gandolfo was responsible for the hardware and software associated with the psychophysical component of the experiment. She also wrote much of the software used in data analyses. Although also working to complete his own separate thesis research, Matt Tresch brought a great personality and invaluable experience in neurophysiology to the project at a time when his talents were needed most. I always wondered who twisted Matt's arm. C.S. Ray Li redefined the experimental protocol into a consistent paradigm. He worked with me in most of the recording sessions documented here. Dan DiLorenzo set up the microstimulation system to verify recording location in M1. Camillo Padoa Schioppa and Javid Sadr, the new kids on the block, were involved in data analyses. Camillo made significant contributions to the statistical analysis methods used here. James Galagan was involved early in training Marcus, but he wisened up and went on to frogs and the spinal cord.

Special thanks go to Margo Cantor and Sylvester Szczepanowski. Margo ensured that I appreciated and respected the animals with which I worked daily. She performed at least one exorcism at a time when nothing seemed to be going right. Not sure whether the exorcism did any good, but she helped keep me sane. Sylvester transformed the sketches and drawings that I gave him into physical realities. He is truly a wizard.

My committee was great. Emilio Bizzi constantly reminded me that to approach the work as a neurophysiologist, not as an engineer. Chi-Sang Poon and Conrad Wall constantly reminded me to approach the work as an engineer, not as a neurophysiologist. No wonder my hair turned gray. If not for Earl Miller, I think we would still be trying to isolate our first cell. Together they kept me focused, honest, and moving forward. Thank you all.

This was a long and difficult road for me. I cannot begin to acknowledge all of those who touched my life in so many ways over the last several years. I had great spiritual and emotional support from many at the Paulist Center, especially those in the DCG and the Saturday evening music group. The Nancys, Patrick, Leann, Sally . . many others . . thanks. Not only did the HST administration guide me over the multiple hurdles of the program, but, since their offices were just down the hall , they were a source of food, money, office supplies, conversation, consolation. Keiko . . thanks. MJ . . succeed. Angie . . make it happen. Rachel, Kate . . you did make it happen. My family . . I could not have been more blessed.

"What's done cannot be undone, to bed, to bed, to bed."
William Shakespeare

to my son, Evan . . . .

not as an example of what was done . . .

but as an inspiration for what can be done

Table of Contents

Table of contents (continued)

List of Tables

Chapter 5

Appendix A

List of Figures

List of Figures (continued)

List of Figures (continued)

Appendix A

Glossary of Terms

dynamics - branch of mechanics that deals with motion and equilibrium of systems under the action of forces. Forces and torques are examples of dynamic parameters.

extrinsic coordinates - a coordinate system referenced to an origin outside of the body with base vectors independent of body-centered parameters. An example is a Cartesian coordinate system with origin external to the body.

intrinsic coordinates - a coordinate system referenced to an origin attached to the body with base vectors defined in body-centered parameters. An example is a planar coordinate system with origin located at the shoulder joint and base vectors defined by rotation angle of the shoulder and elbow joints.

kinematics - branch of mechanics dealing with pure motion, without reference to the forces involved. Displacement, velocity, and acceleration are kinematic parameters.

minimum jerk trajectory - a hand path whose trajectory minimizes jerk. Jerk is the third derivative of displacement. A point-to-point minimum jerk trajectory is characterized by a straight line path and a symmetric, unimodal velocity history. This is a kinematic description in that kinematic parameters are used to define an optimization function. Minimum jerk trajectories capture the "smoothness" of human reaching movements.

manipulandum - a two-link, mechanical mechanism

minimum torque change trajectory - a hand path whose trajectory minimizes the derivative of torque. A point-to-point minimum torque change trajectory yields a slightly curved hand path and a smooth, unimodal velocity history. This is a dynamic description in that dynamic parameters are used to define an optimization function. Minimum torque change trajectories also capture the smoothness of human reaching movements.

model-referenced adaptive control - a control method wherein an internal model of the system to be controlled is formulated and used to predict the response of the system to the inputs from the controller. The difference between the output of the internal model and the response of the system is used to modify or adapt the internal model.

Glossary of Terms (continued)

psychophysical experiments - within the context of this proposal, experiments that determine the behavior or performance of subjects in the reaching task.

trajectory - the path described by a body moving under the action of forces. The path is usually described in terms of the kinematic parameters of position and velocity histories.

1. Introduction

Motor learning can be described as motor skill acquisition - an improvement in task performance that results from repetition or practice of the task and persists through time. Through motor learning, an individual acquires the temporal and spatial features of movement patterns that are increasingly characterized by pre-programmed processes (Halsband and Freund 1993). This is accompanied by a decrease in sensory and attentional demands. The capacity to acquire a motor skill is a characteristic of the individual and must be distinguished from the ability to perform a task as individual skills often peak at different proficiency levels (Schlaug, et.al. 1994).

Models of motor learning are cast in terms of performance parameters, and the extent a task is learned is indicated by the degree a relevant parameter is optimized. Normally there is a trade-off between speed and accuracy in performance of movements with varying amplitude and accuracy requirements (Sanes, et.al. 1990). Faster movements are often performed with low accuracy; movements that demand high accuracy are often performed slowly. Motor skill acquisition is characterized by both increased speed of task execution and increased accuracy (Fitts 1954, Kihlstrom 1987). Skill learning is typically associated with the appearance of smooth, unimodal, bell-shaped velocity profiles and the formation of reference trajectories for accurate vectors of direction and amplitude (Halsband and Freund 1993). These observations provide the basis for methods that quantify the nature, rate, and extent of motor learning as a function of measurable performance parameters.

The ability to acquire, store, and retrieve motor skills is called procedural memory and is distinct from declarative memory. Whereas declarative memory requires the conscious recollection of events and facts, procedural memory is inferred from the effect practice has on performance. Dissociation between the acquisition of motor skills and mental memory has been demonstrated in amnesic patients where proficiency and rate of motor learning was found to be comparable to that in normal controls (Corkin 1968). Procedural memory, then, operates independently of the hippocampal system (Squire 1992). There is no evidence for a single structure in the brain that plays a role in motor learning comparable to that of the hippocampus in declarative memory. Instead, different aspects of motor learning are distributed throughout the motor system. Observations from patients and nonhuman primates with lesions to the striatum, cerebellum, parietal cortex, premotor, supplementary motor area, and primary motor cortex suggest that these structures must be intact to allow for normal motor skill acquisition (Halsband and Freund 1993).

Novel motor skill acquisition implies that movement segments are formed, modified, and retrieved for the execution of the learned skill. It has been proposed that movement segments develop through synaptic plasticity in the motor cortex (Asanuma and Pavlides 1997). Some motor tasks are difficult to learn and require hundreds or thousands of trials to perfect; other tasks can be learned in a few trials. This suggests that, from a neural plasticity perspective, motor skill acquisition can proceed in two ways - instructional learning, where practice of a motor task brings about a change in an individual's repertoire of spatio-temporal neural firing patterns, and selectional learning, where one-trial learning indicates movement segments are chosen from an existing or naive repertoire (Shenoy 1993).

In summary, then, motor learning proceeds from an early phase requiring sensory guidance, attention, and the development of new neural movement segments toward automatic performance, with sensory monitoring and the appropriate selection of existing neural segments. In the performance domain, smooth, unimodal velocity profiles and preferred trajectories are hallmarks of motor learning.

1.1 Thesis scope

A major challenge in the investigation of motor learning is to establish a link between performance changes seen during skill acquisition and corresponding changes in activity of cells in the central nervous system. The research described here takes on that challenge. More specifically, the goal of this research is to identify cells in monkey primary motor cortex whose behaviors reflect the retention of a previously executed task, whose behaviors reflect motor learning or memory. Such cells could be part of cortical loop circuits that reinforce and consolidate through mechanisms such as long-term potentiation the motor skill acquired.

To accomplish this goal, it is necessary to develop and execute an experimental paradigm that

- creates an environment for motor learning
- defines and measures parameters that quantify performance of the motor task and the extent of learning
- records the activity of cells in monkey primary motor cortex and quantifies the activity with appropriate statistical measures
- correlates motor performance with cell activity and demonstrates (or fails to demonstrate) cellular aspects of motor learning or memory.

The paradigm must combine a psychophysical or behavioral component that defines, monitors, and measures monkey performance in the experimental task with a physiological component responsible for recording cortical cell activity.

As in most science, this work does not stand alone, but is built on the efforts of researchers who have preceded me. The next chapter describes human psychophysical and monkey neurophysiological studies that provide the foundation and incentive for this current effort. Chapter 3 explains the experimental paradigm; data analysis methods are presented in Chapter 4. Chapters 5 and 6 provide results and discussion, respectively.

2. Background

It is reasonable to assume that fundamental principles underlie the control of upper limb movements and the acquisition of skills through motor learning. In their efforts to identify and understand these principles, researchers have employed a variety of experimental techniques. Each technique approaches the understanding of motor control and motor learning from a different perspective.

Human psychophysical experiments study motor control and learning from a performance perspective by quantifying the manner in which people move. Movement is the end result of motor control, and by studying the characteristics of movement, the nature of the controller can be elucidated. Similarly, by studying changes in performance during skill acquisition, the nature of changes in the controller associated with motor learning can be identified. Such studies identify key parameters of movement and behavioral constraints or limits, and provide the fundamental data on which mathematical models of motor control are based.

Anatomical and physiological experiments study motor control from a hardware and connectionist perspective. These studies identify and characterize the components of the controller from muscle actuators, to spinal cord organizational elements, and finally, to high function centers in the cortex. The data associated with the interconnection and activity of these components in normal and pathological conditions provides insights into the manner in which the models of movement control formulated in behavioral studies are physiologically expressed in the central nervous system.

The research conducted here addresses motor control and learning from a combined psychophysical and physiological perspective. Psychophysical data quantifies various parameters of movement within an individual reaching task as well as improvement in performance across repetitions of the task. Improvement in task performance is the hallmark of skill acquisition through motor learning. Cell activity in the primary motor cortex then is correlated with task performance. Since various mathematical models of motor control and learning place emphasis on different movement parameters, cortical activity that strongly correlates with specific parameters supports a model based on the represented parameters. The rate and extent of changes in cortical cell activity as performance of the reaching task improves with practice may provides insights to the mechanisms of skill acquisition and motor learning.

In the sections that follow, a brief review of literature relevant to this research is given. Psychophysical studies with human subjects are described first. These works identify important movement parameters and introduce different models of motor control and learning. One such study, that by Shadmehr and Mussa-Ivaldi (1994), defined the experimental protocol that is replicated in this research. Neurophysiological and imaging studies are then presented. These works describe the manner in which movement parameters may be encoded in cortical and subcortical cell activity and identify the cortical structures active during skill acquisition and motor learning.

2.1 Human psychophysical studies

While watching the reaching movements of subjects, Morasso observed a consistent, simple kinematic pattern. When asked to move their dominant hand toward a number of visual targets, subjects tended to move the hand approximately in a straight line with a bell-shaped tangential velocity profile (Morasso 1981). This description of movement trajectory remained for different amplitudes of movement and for different starting positions of the hand in the workspace. However, when Morasso described these reaching movements in terms of angular rotations of the elbow and shoulder joints, the kinematic patterns varied with hand starting position. These observations of movement kinematics suggest a feature of the motor planning process - reaching with the arm is accomplished through simple, smooth movement patterns described in a reference frame external to the body.

Morasso's work initiated a debate in motor control research that continues today. The argument centers on identifying both the strategy used by the central nervous system (CNS) to define a desired trajectory and the coordinate system in which the trajectory is planned. Briefly stated, what are the parameters and associated coordinate reference frames which, when used in an appropriate optimization function, best describe the observed patterns of movement?

Hogan proposed a model that casts the desired trajectory in terms of kinematic variables defined in an environmental or extrinsic coordinate system. Noting the smoothness of human reaching movements, he proposed an optimization criterion based upon minimizing jerk - the third time derivative of position - as a model to describe one-dimensional movements (Hogan 1984). Using this model, the optimal function describing hand trajectory is a polynomial of the fifth order in time. Given the boundary conditions at the onset and termination of movement and the movement time, the trajectory is completely defined. Hogan found that such a polynomial is sufficient to reproduce the primary kinematic features of one-dimensional

movement - a straight-line transition from initial to final position and a symmetric, bell-shaped velocity profile. Implicit in this model is a hierarchy or separation of motor tasks. At one level, the desired trajectory is planned independently of the musculoskeletal dynamics required to bring about the motion. At another level, the associated torques and forces are generated.

Believing that the CNS control strategy must be related to the dynamics of movement, Uno proposed an optimization function that minimized the sum of the squares of the rate of change of torque integrated over the entire movement - the minimum torque-change model (Uno et al. 1987). This model casts trajectory formation in terms of dynamic parameters defined in an intrinsic or body-referenced coordinate system. When applied to the reaching movements examined by Morasso, the minimum torque-change model provided good agreement. In addition, this model provided better agreement with experimental data than the minimum jerk model when the reaching task was performed at the limit of the arm's workspace, when the task required movement through certain intermediate via points, and when the task was performed against the resistance of a spring (Uno et. al. 1989).

The two models embody fundamentally different strategies to determine a desired reaching trajectory. The minimum jerk model employs a criteria function using parameters defined in extrinsic coordinates. The resulting trajectory is invariant to location of movement in the workspace and movement dynamics. The slight curvature seen in actual hand paths is attributed to imperfections in the control process. The model implies that the movement plan determined in extrinsic space must subsequently be transformed into the intrinsic joint coordinates of the musculoskeletal system.

The minimum torque-change model employs a criteria function with parameters defined in intrinsic coordinates. The deviations from straight-line trajectories seen within different parts of the workspace or in the presence of applied static loads reflect variations in the dynamics of the task - changes in the inertial properties of the arm and changes in the external force environment, respectively. The curvatures in hand paths result, not from inaccuracies in the controller, but directly from the minimization of the criteria function. The minimum torque-change model does not require a separate controller to transform desired positions into torques as trajectory planning and torque definition proceed in the same step.

Various researchers had sought to shed light on this controversy by conducting experiments wherein perturbations were made to either the kinematics or the dynamics of the reaching task.

By uncoupling these two characteristics of movement, their separate effects on hand trajectory can be assessed.

Wolpert, et al. (1995) studied the effect of artificial visual feedback on planar two-joint arm movements. During point-to-point reaching tasks, the visual feedback of hand position was altered so as to increase the perceived curvature of the path. This represents a visually-perceived variation in movement kinematics with no change in movement dynamics. A criteria function specified by hand trajectory in extrinsic space - the minimum jerk model - would predict adaptation to the altered environment by an increase in actual path curvature opposite to the perceived curvature. A criteria function based on movement dynamics - the minimum torque-change model - would predict no adaptation in the hand path since the dynamics of the task did not change. The results demonstrated that increasing the perceived curvature of normally straight movements led to significant corrective adaptation in the curvature of the actual hand path.

Flanagen, et.al. (1995) also conducted research in which they manipulated the mapping between visually-perceived and actual motions. Subjects made point-to-point reaching movements will observing their trajectories on a computer screen. The displayed trajectories showed either movement of the hand in Cartesian coordinates or arm movement in joint angle coordinates. Straight line hand trajectories were visualized as straight paths when displayed in hand Cartesian coordinates. However, because of the nonlinear relationship between hand path and joint rotations, straight line movements of the hand were visualized as highly curved paths when displayed in joint coordinates.

When observing movement trajectories in hand Cartesian coordinates, the subjects' actual hand paths were essentially straight. However, after adaptation to observing movement trajectories displayed in joint coordinates, subjects made motions that were linear as displayed but nonlinear in actual trajectory.

The results of Wolpert and Flanagen are consistent with the hypothesis of Hogan and suggest that a fundamental criteria of motor control is defined in terms of movement kinematics - move such that visually-perceived trajectories are essentially straight and executed with smooth, single-peak velocity profiles. It is interesting to note that straight hand paths and single-peak velocity profiles are evidence of a well-learned motor skill (Halsband and Freund 1993).

Shadmehr and Mussa-Ivaldi (1994) provided evidence that movement kinematics are planned independently of the dynamic conditions in which movements occur. Human subjects made visually-guided reaching movements while holding the end-effector of a robot manipulandum which was capable of producing force fields during the reaching task. Starting from the center of the workspace, subjects made reaching movements toward a target selected randomly from one of eight possible targets located at a constant radial distance and at 45° intervals (0°, 45°, . . . 315°). After the subject had moved to the target, the next target, again selected at random, was presented. During an experiment session, subjects would make hundreds of such reaching movements.

In the absence of external forces (null field), subjects' hand trajectories displayed approximately straight paths and smooth, bell-shaped tangential velocities as described by Morasso (1981), Flash and Hogan (1985), and Uno et al. (1989). However, after the presentation of a force field by the manipulandum, kinematic patterns were distorted by the unexpected and uncompensated forces. Shadmehr and Mussa-Ivaldi further observed that, after a number of movements within the disturbing field, subjects showed a spontaneous adaptation in which hand trajectories converged to the kinematic patterns seen in the null force field. These results are compatible with a theory of kinematic optimization; the same smooth endpoint kinematics were observed under very different dynamic conditions.

The restoration of smooth, unimodal velocity trajectories through practice in the altered force environment suggests the acquisition of a new motor skill by motor learning. To investigate a possible mechanism underlying this process, Shadmehr and Mussa-Ivaldi considered the reaching response made by subjects when the force field in which they were training was suddenly removed. Despite the absence of external forces, hand paths were not straight. Rather, the perturbations from a straight path were approximately mirror images of those observed when the subjects were initially exposed to the field. Figure 2.1 illustrates this effect, showing a) typical initial hand paths in the null force field, b) performance during initial exposure to an external force environment, c) hand paths after training in the force field, and d) initial path in the null field after training in the force field. These results suggest that the motor controller gradually composes a model of the force field, a model that the central nervous system uses to predict and compensate the forces imposed by the environment.

Flash and Gurevich (1991) combined similar experimental studies with a mathematical simulation of the reaching task. The model included parameters that accounted for arm stiffness and viscosity. They found that hand trajectories of the first loaded movements were

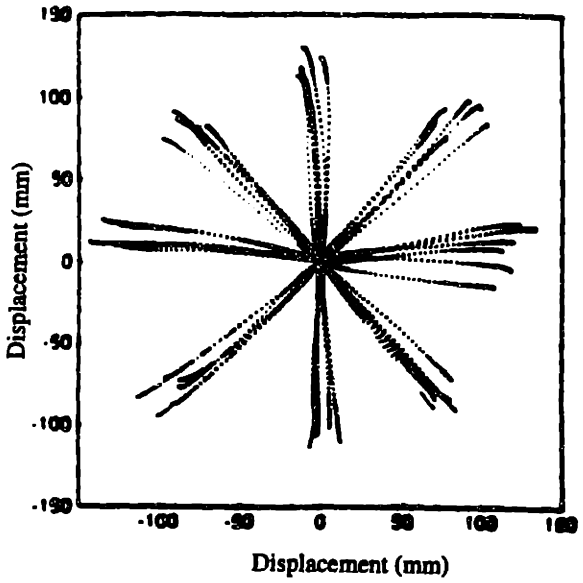

a) Null field

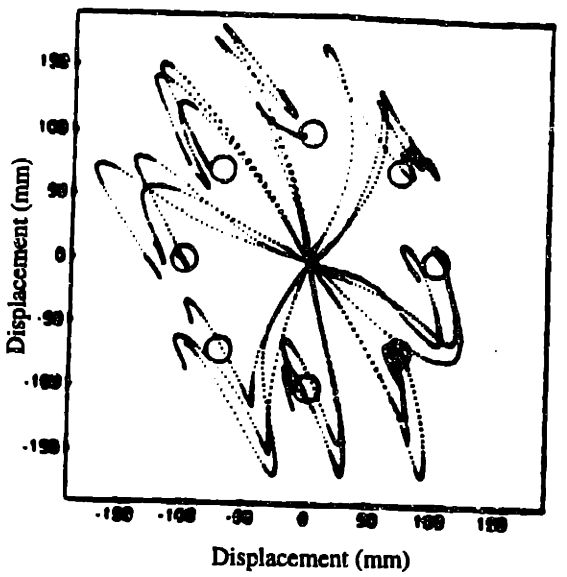

b) Force field, pre-training

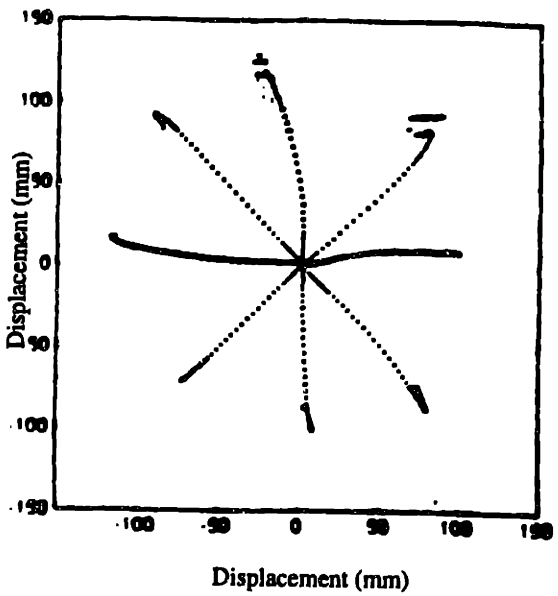

c) Force field, post-training

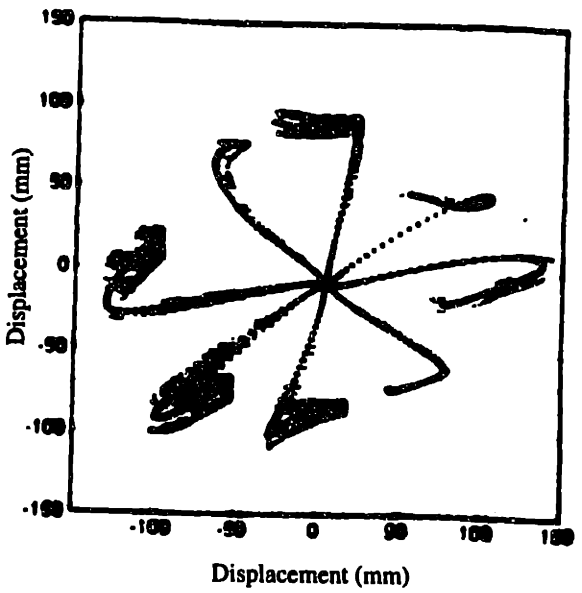

d) Null field, post force field

Figure 2.1 Hand paths for reaching task during experimental epochs a) in null field, b) initially in force field, c) after training in force field, d) initially in null field after force field training

predicted by the model if the same hand path and arm stiffness and viscosity parameters as those used in the generation of the unloaded movements were assumed. In addition, the kinematic characteristics of aftereffects, the hand movement in the null field immediately after adaptation to a force field, indicated that load adaptation might involve the modification of both the kinematic plan and arm impedance.

Further work by Shadmehr and Mussa-Ivaldi (1994) and Ghilardi, et.al. (1995) suggests that learning a visuomotor task in a local area of the work space produces biases in other areas. Dizio and Lackner (1995) showed that adaptation to a novel force environment using the right arm causes a transfer error in endpoint position but not trajectory when reaching movements were made by the untrained left hand. These results suggest that motor adaptation broadly generalizes to motor tasks different than those in which the training took place. Recent work by Gandolfo et al. (1996) provides evidence that motor adaptation extends beyond the local environment to only a limited degree. While performing reaching tasks in the presence of perturbing force fields, subjects were able to compensate for forces experienced at neighboring workspace locations. However, adaptation decays smoothly and quickly with distance from the locations where disturbances had been sensed by the moving limb.

Work by Brashers-Krug et al. (1995) have further investigated the nature of the internal model of movement dynamics and its role in learning and motor memory. They found that repetition of a motor task initiates neural processes that continue to evolve after practice on the task has ended, a phenomenon known as consolidation, and that consolidation of motor memory can be affected by behavioral means. Subjects initially practiced a reaching task in a given force environment. When these subjects returned the next day, their performance in the force field was better than their naive performance, indicating that knowledge of the task had been retained (positive transfer). However, when subjects learned two different force fields in consecutive trials, they experienced a mutual interference between the tasks. Performance in the second task was less than naive performance (negative transfer) and 24-hour retention of the first task was virtually eliminated (retrograde interference). By contrast, nearly one-third of subjects that waited four or eight hours between learning the two tasks showed neither type of interference.

The cited research indicates that the experimental paradigm developed by Shadmehr and Mussa-Ivaldi wherein reaching movements are made in the presence of novel force fields creates an environment that can be used to study motor learning. Within a given day of experimentation, subjects display a temporal variation in performance. Specifically, when initially exposed to a perturbing force, subjects' trajectories reflect corrective movements to the

target and display multi-peak velocity histories. With practice, hand paths straighten and velocity histories return to the unimodal shape seen in the familiar reaching task. Aftereffects, perturbations in hand path seen when forces are initially removed, suggests that the neural system controlling the movement has been altered to reflect the nature and influence of the applied forces. Improved performance of the reaching task on subsequent days indicates that the altered state of the neural system has been retained with time. Such performance clearly exhibits the characteristics of motor learning. For this reason, the experimental paradigm used in this research essentially replicates that developed by Shadmehr and Mussa-Ivaldi.

2.2 Neurophysiological studies of reaching movements

In parallel with human behavioral studies, neurophysiological animal studies have attempted to determine the role of cortical and subcortical areas in the mechanisms underlying reaching by determining how movement parameters are encoded in cell activity. Given the significance of hand motion as a basic aspect of upper limb motor activity, parameters associated with hand motion should be encoded within the central nervous system (Georgopoulos and Ashe). These parameters may include the kinematic variables of position, movement direction and amplitude, the dynamic variables of torque or externally applied force, and the time-varying nature of these parameters.

Georgopoulos et.al. (1984) studied the relationship between active maintenance of the hand at various positions in a 2-D space and the frequency of single cell discharge in motor cortex and parietal area 5. The steady state discharge rate of a majority of cells recorded in the motor cortex varied as a linear function of the position of the hand across the 2-D space, so that the neuronal response was described by a plane. Kettner, et.al. (1988) found a multilinear functional relationship between cell activity and maintained hand position in 3-D space. The preferred orientation for these response planes differed for different cells and varied throughout space. These results indicate that individual cells do not relate uniquely to a particular position of the hand in space. Rather, they encode spatial gradients at certain orientations. Only when the activity of a population of neurons is considered as an ensemble can position in space be uniquely defined.

Several studies have proposed a relationship between the direction of hand motion in 2-D and 3-D space and changes in cell activity in several brain areas, including the primary motor cortex (Caminiti et.al. 1990; Georgopoulos et.al. 1982, 1986, 1988; Kalaska et.al. 1989; Kettner et.al. 1988; Schwartz et.al. 1988), the premotor cortex (Caminiti et.al. 1991; Weinrich et.al.

1984), area 5 of the parietal cortex (Kalaska et.al. 1983, 1990), the cerebellar cortex (Fortier et.al. 1989), and the basal ganglia (DeLong et.al. 1985). The relationship states that when the direction of movement varies over the range of 2-D or 3-D space, cell activity is broadly tuned to movement direction. More specifically, the studies found that 1) an individual cell discharges at a highest rate when hand movement is in a "preferred" direction, 2) cell activity decreases progressively with movement away from the preferred direction, and 3) the preferred direction of a large population of cells is distributed throughout the dimensional space.

The broad directional tuning indicates that reaching in a given spatial direction is based on the activity of different cells with different tuning properties. This population nature was incorporated mathematically by Georgopoulos when he defined a population vector that is the sum of contributions from directionally-tuned cells and that, as a whole, points in the direction of intended movement. Each cell contributes a vector whose direction is in the cells preferred direction and whose magnitude is proportional to the change in cell activity associated with a given movement direction (Georgopoulos et.al. 1983).

There is evidence to suggest that the population vector as a predictor of movement direction remains under different reaching tasks. It has been shown that when the origin of movement changes in the planar workspace, the preferred direction of individual cells shift in an amount related to the angular rotation of the shoulder joint. However, the population vector of cell activity still aligns with the direction of movement (Caminiti et.al. 1990, 1991). Recent work by Scott and Kalaska (1995) also looked at reaching movements with similar hand paths but with different elbow and shoulder postures - a control posture with the monkey's arm in the sagital plane and a second posture with the elbow abducted to nearly the shoulder level. For most directions of movement, there was a statistically significant difference in the direction of the population vector for the two arm postures. Whereas the population vector tended to point in the direction of movement in the control posture, there was a poor correlation between the population vector and movement direction for the abducted posture. These results are inconsistent with those of Caminiti; cortical cell activity that varies with arm position or orientation suggests an intrinsic representation of movement. Mussa-Ivaldi (1988) demonstrated that cortical activity representing muscle-based coordinates can be used to construct accurate population vectors in extrinsic space. These results and their interpretation question the belief that the population vector coding hypothesis can be used to predict the direction of movement of the end point of the limb as represented in an extrinsic coordinate frame.

The vector linking any given initial position in space to a desired target location is defined by both direction and amplitude. Psychophysical studies by Soechting and Flanders (1989a, 1989b) suggest that these parameters are addressed separately by the body's motor controller. Neurophysiological studies have had minimal success in describing relationships between cortical cell activity and movement amplitude. Flament et.al. (1993) demonstrated a correlation between single cell activity and both movement direction and amplitude. The preferred cell direction was very similar for movements of different amplitudes, but overall cell activity increased with a greater range of movement. Cell activity associated with direction of movement occurred prior to the initiation of motion. However, the increase in cell activity correlated to movement amplitude only occurred during the execution of the movement.

That amplitude is encoded by cell activity during movement fails to support the theory that movement kinematics is planned prior to movement execution. For example, defining a minimum-jerk trajectory between two points requires knowledge of two of the following parameters - time of motion, amplitude of movement, peak velocity, or peak acceleration. If such a trajectory is defined prior to movement, then the parameters that specify the trajectory must also be defined prior to movement. That amplitude is encoded in the activity of cells during movement indicates that it is a key parameter not in defining the desired trajectory but rather in monitoring it. Movement amplitude, then, would be part of a sensory feedback system responsible, possibly, for defining movement errors rather than part of a feedforward system responsible for defining an intended trajectory. Psychophysical data still strongly suggests that movement kinematics is planned prior to movement execution; however, extensive neurophysiological studies have yet to identify strong relationships between motor cortical cell activity prior to movement and any set of parameters that would be necessary and sufficient to define apriori a desired hand trajectory.

The influence of externally applied loads on cell activity has also been the subject of extensive study in both single joint and multijoint movement tasks. The experimental paradigms employed in these studies disassociate movement direction and muscular activity by applying static external loads in a movement task, time-varying (dynamic) loads in an isometric task, or dynamic loads in a movement task. Early work by Thach (1978) recorded from cells in the primary motor cortex and the cerebellum while monkeys flexed/extended their wrists to three positions in the presence of a static bias torques. He found that a groups of cells discharged in relation to the applied torque and the cell firing rate was proportional to the magnitude of the load.

In an experimental paradigm similar to that used by Thach, Werner et.al. (1991) found relationships between the activity of groups of cells in the premotor and primary motor areas and the applied static torque. An interesting difference between the two areas pertained to the load range over which the cell modulated activity. Primary motor cortical neurons showed steepest change of firing rates over a limited range of small torques around zero external load; the population average displayed a sigmoidal relationship. Premotor area cells increased their activity over the entire range of applied torques or showed their highest activity with stronger loads. The results suggest differential roles of the two areas in the control of fine versus gross muscular forces.

In an effort to determine whether cell activity was related to movement direction (an extrinsic, kinematic parameter) or muscular activity (an intrinsic, dynamic parameter), Kalaska et.al. (1989) trained monkeys to make reaching movements in the presence of constant bias forces. Results indicated that cell activity in the primary motor cortex reflects the influence of both movement direction and applied load. A preferred direction vector is still encoded in the cell by a gradient of activity as a function of movement direction. Direction of applied load is encoded by changes in the tonic level of cell activity. The magnitude of the tonic activity changes varies with load direction and, as such, defines a preferred load axis. The load axis tended to be in the opposite direction of a cells preferred direction. Kalaska hypothesized that the motor cortex participates in both kinematic and dynamic aspects of movement.

Georgopoulos et.al. (1992) distinguished between static forces required to offset a postural bias force (such as gravity) and dynamic forces that refer to changing force patterns. The total force applied by a monkey in a task would be the sum of these two components. Their findings indicated that cell activity correlated with the dynamic force but not the total force, and they concluded that movement dynamics could be represented at the level of motoneuronal pools by the convergence of dynamic and postural inputs from separate supraspinal structures.

2.3 Neurophysiological and imaging studies of motor planning and learning

Experiments conducted to distinguish cortical activity associated with the planning of movement from those associated with execution have studied the timing of activity with respect to movement onset. Often the experiments require the execution of reaching tasks following a defined delay or hold period of no movement. Cortical activity prior to movement is disassociated from movement-related activity and is implicated in the planning of the desired

motion. Using single-cell recording techniques, these experiments assess whether the planning and execution of motion are facilitated by different cortical areas.

Georgopoulos et.al. (1989) found cells in the arm area of the primary motor cortex whose population vector during a delay period pointed in the direction of the impending movement. Alexander and Crutcher (1990) recorded cell activity in the supplementary motor area and the primary motor cortex prior to an anticipated movement and found preparatory cell activity to be related to the preplanned direction of movement. Most of the preparatory activity was unrelated to the current or anticipated loading conditions. This suggests the planning of movement kinematics, not dynamics. Some cells in the supplementary motor area are active only for a given sequence of motor events (Tanji and Shima 1994). These cells function in a "plan ahead" mode. And finally, di Pellegrino, et.al. (1992) found cells in the premotor cortex of monkeys that discharge in comparable ways both when the monkey executes goal-directed hand movements and when it observes human researchers make similar reaching movements. These results indicate that preparatory cell activity exists in multiple motor cortex areas and suggest that the planning of movement may involve interaction among each of these areas.

Imaging methods such as PET and fMRI can be used to identify both the extent of cortical and subcortical areas active during motor learning and the change in extent as the motor skill is acquired. Karni et.al. (1995) had human subjects execute a finger-to-thumb taping sequence in daily sessions over a period of several weeks. Performance of the task improved both in terms of speed and accuracy until an asymptotic level was reached. By week four, concurrent with asymptotic performance, fMRI images indicated that the extent of contralateral primary motor cortex activated by the practice sequence enlarged compared to the unpracticed sequence. The changes persisted for several months. In a similar finger-taping paradigm, Seitz et.al. (1990) found that, with practice, the character of the movements changed into fast ballistic movements beyond the range that can be corrected during execution by sensory information. In accordance with these changes, the activated field in primary motor cortex grew in intensity. During performance improvement in a pursuit rotor task, Grafton et.al. (1992) found a significance increase in relative cerebral blood flow in the primary motor cortex, supplementary motor area, and pulvinar thalamus. These results suggest a slowly evolving, long-term, experience-dependent reorganization of the adult M1 which may underlie the acquisition and retention of motor skills.

2.4 Summary

The research conducted here addresses whether neurophysiological data in the form of cell activity recorded from neurons in the primary motor cortex of awake monkeys performing reaching tasks can provide insights into the mechanisms used by the CNS to acquire and maintain motor skills. This work does not stand alone; rather, it builds on the efforts of others. Psychophysical studies have provided an experimental paradigm which creates an environment for motor learning. In the paradigm, reaching movements are made in different external dynamic environments. Human performance in the reaching task exhibits changes in hand path and velocity consistent with motor skill acquisition and learning.

Experiments that record single cell activity during reaching have provided a huge amount of data and have lead to a number of statistically-based relationships between cell activity and arm motion. Yet conclusions emanating from these relationships are few and controversial. Nonetheless, the studies provide examples of analysis methods that define activity parameters and quantify the nature of cell behavior. These parameters can then be correlated with behavioral performance measures in the task.

Finally, imaging studies indicate that the primary motor cortex is indeed active during motor learning and the extent and therefore the nature of M1 involvement varies as a skill is acquired. It is reasonable, then, to expect measurable changes in the activity of a population of cells in M1 during execution of the motor learning paradigm used here.

3. Materials and Methods

The research conducted here attempts to identify the manner in which motor learning and memory are encoded in the activity of cells in the primary motor cortex. To this end, there are two distinct yet integrated components of the experimental method. The first addresses monkey psychophysics or behavior in the learning task. This component controls the execution of the reaching paradigm - selects and displays targets, defines timing requirements, and rewards successful trials. It also records the kinematic data of the hand trajectories as the monkey executes the task. The second component of the experiment addresses neurophysiology. Here cortical cell activity during execution of the experimental paradigm is acquired, detected, analyzed, and recorded. These two components and their associated hardware and software are described in the sections below. The specific experiments that provided the psychophysical and neurophysiological data used to evaluate the questions posed in this research are then presented. Finally, data analysis methods are described. These methods quantify task performance and cell activity and provide the basis for the conclusions drawn in this study.

3.1 Psychophysical component of the experiment

The physical apparatus of the experiment replicates the environment used by Shadmehr and Mussa-Ivaldi (1994) in their studies of motor adaptation and learning with human subjects. Their work was described in the previous chapter. The hardware used here was modified to accommodate the use of monkeys as subjects and to allow the recording of cortical cell activity.

Two adolescent *macaca nemestrina* monkeys were trained for use in this study. During the experiment, a monkey sits in a primate chair and holds the handle of a two-link mechanical manipulandum with its right hand. Its right elbow is supported by an arm rest that is part of the primate chair, but the arm and shoulder are otherwise unrestrained. Hand motion is limited to the horizontal plane by the manipulandum.

The manipulandum is a two degree of freedom, low friction mechanism. Angular position measurements are made using optical encoders mounted on the axes of the mechanical joints. Two torque motors mounted at the base of the mechanism are connected independently to each joint via a parallelogram configuration. The motors enable specified forces to be applied to the monkey's hand at the manipulandum handle.

A video display monitor is positioned in front of the monkey, slightly below eye level. The targets of the reaching movements and a cursor representing the manipulandum handle position are displayed on the monitor. Targets are specified by a square of size 12x12 mm^2; the handle position cursor is a square of size 3x3 mm^2. A schematic of the experimental setup is shown in Figure 3.1.

The basic task of the experimental paradigm is a single reaching trial - movement of the manipulandum handle such that the cursor moves from the center target to a peripheral target within defined timing and directional constraints. A target is first displayed at the center of the monitor to induce the monkey to bring the handle of the manipulandum to the center of the workspace. The monkey must maintain the cursor within the center target for a hold period of 1000ms. At the end of the center target hold period, a second, peripheral target appears on the screen. This target is radially placed in a direction with respect to the center target randomly chosen from a set of eight possible locations {0°, 45°, 90°, 135°, 180°, 225°, 270°, 315°}. In the experiment, 0° indicates a hand movement to the right and moves the cursor to the right target; 90° indicates a forward hand movement and moves the cursor up to the top target; etc. The distance between the center and the radially-placed targets on the monitor is approximately 7cm. The time period when both the center and peripheral targets are illuminated is called the delay period. It is variable in length - ranging from 800-1200ms. During this period, the monkey maintains the cursor in the center target. At the end of the delay period, the center target is extinguished. This is the "go" signal and indicates that the monkey should begin moving the manipulandum such that the cursor moves toward the peripheral target. A 7cm movement of the manipulandum handle is required to bring the cursor to a target. The monkey must acquire the peripheral target within 1000ms and must hold the cursor in the target for 1000ms to receive a drop of juice. Once the reward is given, the peripheral target is extinguished and the screen is blank for an intertrial period. The center target is again illuminated, and the reaching paradigm repeats. The timeline for the experiment is shown in Figure 3.2.

Timing and movement direction criteria dictate whether a given reaching trial is accepted. If the monkey leaves the center target before the "go" signal, the trial aborts. If movement time exceeds 1000ms, the trial aborts. If the initial direction of hand movement is not within ±60° of the intended target direction, the trial aborts. These criteria help ensure a level of consistency in the execution of the experimental paradigm.

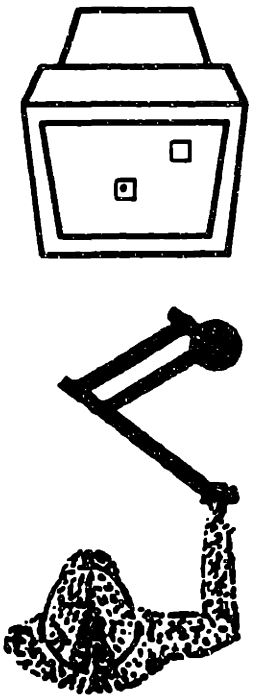

Figure 3.1 Schematic diagram of experimental setup showing computer monitor, manipulandum, and monkey

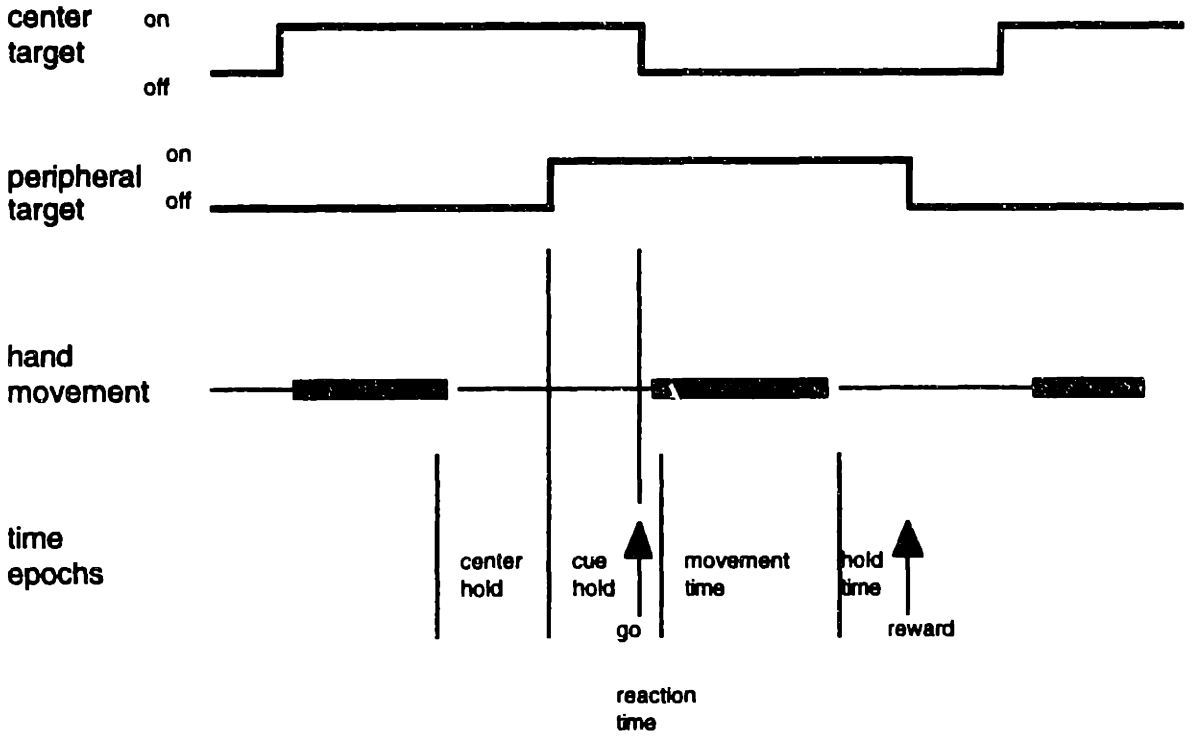

Figure 3.2 Time line for an individual reaching trial

A single reaching trial is divided into distinct time periods. The hold period in the center target is a time of muscle inactivity. Movement does not occur, and since the location of the next target is not known, planning of impending movement cannot occur. Cell activity recorded during this period establishes baseline spike rate. When the peripheral target is illuminated during the delay period, planning can begin. Since movement has not yet commenced, the planning and execution phases are distinct. The "go" signal initiates task execution which itself is divided into a reaction period (from "go" signal to movement onset) and a movement period (from movement onset to acquisition of target). Finally, holding in the peripheral target represents a static condition at a distinct set of radial target locations. The various timing epochs define different periods during which cell activity can be characterized and compared.

On a given day the experimental paradigm is divided into three dynamical phases or behavioral epochs. In the first or "baseline" epoch, the task for the monkey is simply to execute the reaching trial consistent with the constraints of the experimental protocol. No external forces are applied by the manipulandum. Approximately 160 successful reaching trials are made in this baseline epoch. This is the null field condition and establishes nominal performance parameters for that day.

The second phase of the experimental paradigm is similar to the first in the manner in which the targets are displayed and the definition of timing requirements for successful task execution. However, in this phase, the manipulandum applies forces to the monkey's hand. These forces unexpectedly alter the dynamics of the reaching task and create the environment in which learning the novel force field can be studied. The monkey makes approximately 200 successful trial during this "force" epoch.

The applied force field is computed as a function of endpoint or hand velocity:

$$\bar{f} = B\bar{v}$$

where $\bar{v}$ is the hand velocity vector in Cartesian coordinates,
B is a constant matrix representing viscosity of the imposed environment in endpoint coordinates, and
$\bar{f}$ is the vector of forces applied to the hand

In particular, if B is chosen as:

$$B = \begin{bmatrix} 0 & a \\ a & 0 \end{bmatrix}$$

the defined forces may be shown as a vector field over the space of hand velocities (Figure 3.3a). This is a viscous curl field - viscous in that the magnitude of the applied forces is proportional to hand velocity; curl in that force direction is normal to the hand velocity vector. Depending on the sign of "a" in the viscosity matrix B, the direction of the curl field can be either clockwise or counterclockwise. Given a smooth reaching movement 10cm in length with a period of 500ms, a counterclockwise, viscous curl field would produce forces in each moment direction as shown in Figure 3.3b. Note that since applied forces are proportional to hand velocity, the monkey feels no forces while holding the manipulandum stationary either in the center target (center hold time) or in the peripheral target (target hold time).

In the third and final phase of the experimental paradigm, the applied force field is removed, and the dynamics of the task return to that of the null field. This is the "washout" phase in that the influence of the perturbing forces seen in the previous epoch is allowed to fade. Approximately 160 reaching motions are made in this phase of the experiment. At the end of this epoch, the performance of the monkey has returned to that of the initial or baseline epoch.

Work by Morasso (1981), Hogan (1984), and Wolpert, et. al. (1995) suggest that the central nervous system optimizes kinematic parameters as a fundamental quality of motor control. Shadmehr and Mussa-Ivaldi (1994) demonstrated that human reaching movements returned to smooth "straight-line like" paths even in the presence of perturbing forces. The extent that performance of the experimental paradigm by the monkeys mimics that of human subjects indicates the extent that monkeys are a valid model for motor learning within this paradigm.

Although the kinematic requirements of the reaching task are the same over the three epochs, the dynamical requirements are not. The viscous forces applied by the manipulandum in the second epoch require the monkey to invoke muscle strategies different than those used in the first and third epochs where no perturbing forces are applied. Indeed, it is the need to adopt a new muscle strategy within the force field that makes the experiment a paradigm for motor learning.

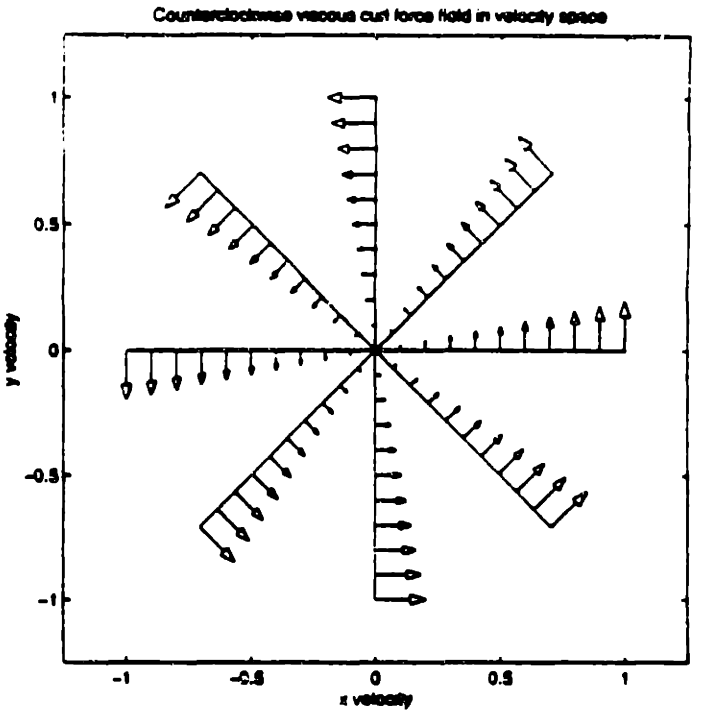

a) counterclockwise viscous curl force field in hand velocity space

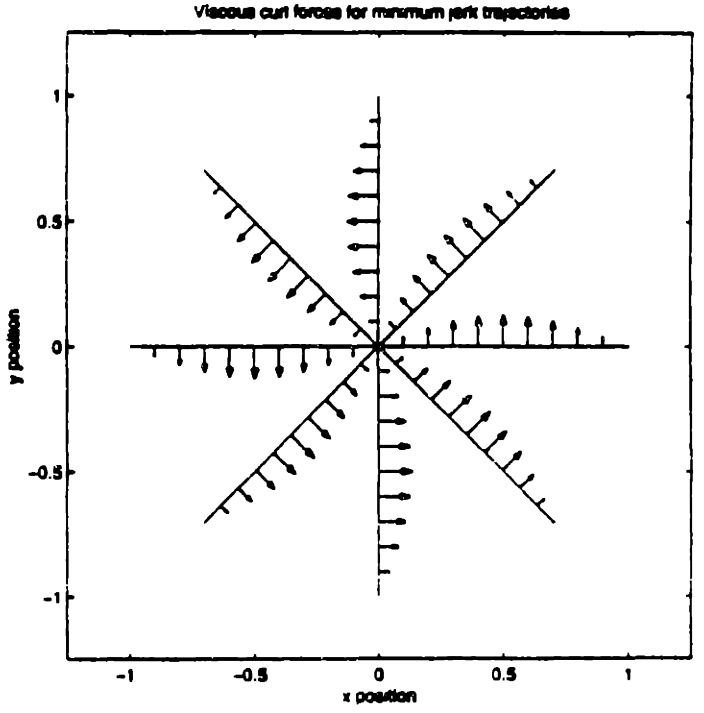

b) External forces applied to a minimum jerk trajectory

Figure 3.3 Counterclockwise viscous curl force field expressed in velocity space and as applied during movements

Since there are no external forces applied during the first and third behavioral epochs of the experimental paradigm, the kinematic and dynamic requirements of the two epochs are the same. Yet there is an important difference. During the intervening epoch, the monkeys learned a new motor task - execute the reaching trial in a perturbing force field. Therefore, the state of the monkeys' control system has changed. Characterizing this change, both in monkey performance and cortical cell activity, is the goal of this work.

3.2 Neurophysiological component of the experiment

The purpose of the neurophysiological component is to record the activity of individual neurons in the primary motor cortex of the monkeys while they perform the reaching task described above. As with the psychophysical part of the experiment, the neurophysiological component involves the design and fabrication of hardware, the development and implementation of software, and the integration of these components within an environment compatible with the demands of an awake, performing monkey.

The physical environment in which the experiment is conducted consists of a 4'x4'x6' enclosure that acts as a Faraday cage, isolating the working space from spurious electromagnetic radiation. The monkey sits in a primate chair within the enclosure; its head is rigidly attached to the chair. Eliminating head movement provides a stable environment for cortical recording; movement artifact is minimized. The monkey is otherwise unrestrained.

The two-link manipulandum extends through a slot in the enclosure into the working area. A bracelet loosely connects the manipulandum to the monkeys' wrist. This prevents the monkeys from completely letting go of the manipulandum. Since applied forces can cause unstable manipulandum movements, it is essential that the monkey continuously adds stability to the system. The video monitor displaying target and manipulandum positions sits outside of the enclosure and is viewed by the monkey through a cutout.

After approximately six months of training in the reaching task, the monkeys were stereotaxically implanted with a titanium head restraint system and a titanium cylindrical recording chamber. Hardware was attached with both bone screws and bone cement. All surgical procedures were performed under aseptic conditions and with full surgical anesthesia. In the immediate postoperative period, the animals received an analgesic and prophylactic doses of antibiotics. The recording chamber was located over the frontal lobe just rostral to the central sulcus to provide access to the arm area of the primary motor cortex (area M1,

Broadman's area 4). As discussed in the background section, this area has been implicated in the planning, execution, and learning of reaching movements. Figure 3.4 illustrates the recording sites based on post-experiment histological evaluation.

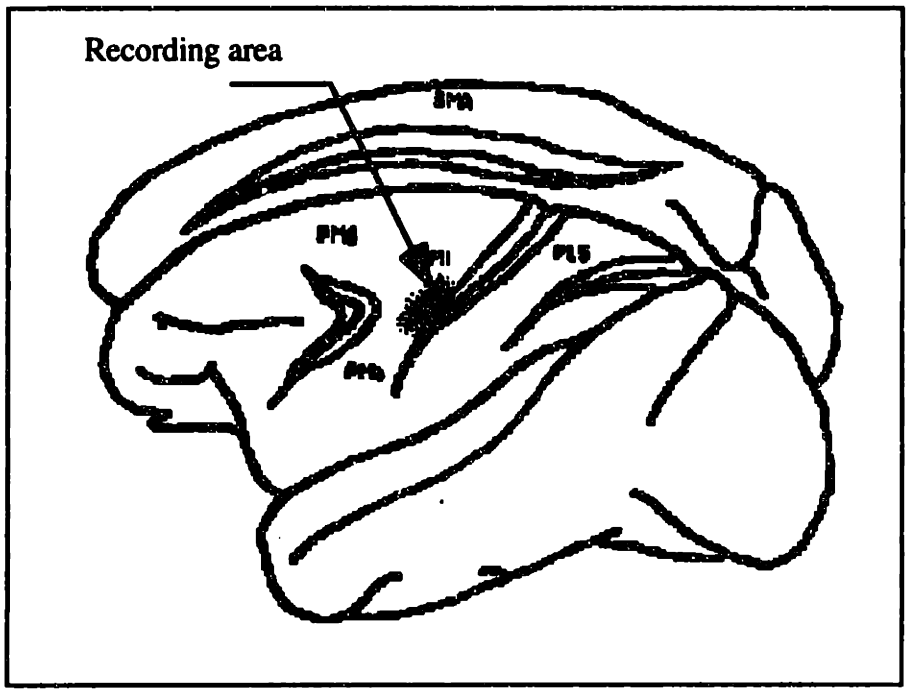

Figure 3.4 Location of recording areas in primary motor cortex

Cortical cell activity was obtained using two recording systems. Initially, a single electrode method was employed. A plastic template sat on the recording chamber and was used to reliably locate the electrode penetration site. A guide tube which attached to the template and extended to a level just above the dura surface provided lateral stability to the recording electrode. The electrode itself slid through the guide tube, its position controlled by a hydraulic microdrive system (David H. Kopf Instruments). All cortical data from the first monkey was obtained using this single electrode system. For the second monkey, a three-electrode system was used. A plastic grid placed on the recording chamber and positioned by a key and groove located the recording site. Guide tubes extended from the grid to the dura surface; each electrode sliding through a separate guide tube. Electrodes were individually advanced by manually-rotated threaded rods. All electrodes were epoxylite-insulated tungsten wire with an average impedance of 2 megaohms (Frederick Haer & Co.).

A preamplifier (AI 401, Axon Instruments, Inc.) locally attached to each electrode provided an initial boost to the strength of the cortical signal. Cables then took the data signal out of the

experimental enclosure to an eight-channel amplifier (Cyberamp 380, Axon Instruments, Inc.) that further boosted the signal and processed it through a 10kHz lowpass filter, a 300Hz highpass filter, and a 60Hz notch filter. Each channel of cortical data was again filtered through a graphic equalizer (Optimus Ten Band Stereo Graphic Equalizer) before being displayed and stored.

Neurophysiological data was displayed, analyzed, and recorded using software developed by DataWaves Technology. Data from each of the electrode channels were continuously acquired at a rate of 25kHz and individually displayed on a software oscilloscope. An event, the occurrence of an action potential, was detected when acquired voltage levels exceeded a specified threshold value. For each detected event, 1.75ms of data were extracted and written to an output file. These 43 data points captured the action potential waveform and allowed for subsequent discrimination between the activity of multiple cells recorded on a single electrode. Only data corresponding to a detected event were recorded for subsequent analysis. This minimized the amount of data stored for any given experiment execution. Output files, then, consist of rows of data records, each row corresponding to a unique event or action potential. Each action potential record has a timestamp to indicate when the spike occurred, data defining the waveform shape, and other descriptors that provide additional information relevant to the experiment.

In addition to data characterizing spike information, output files contain records that indicate key experiment behavioral events. Timestamps and identifiers for events such as the appearance of a target in a specific direction, onset of hand movement, and cursor entry into the target represent timing milestones for a given reaching task. These behavioral data originate with the computer that controls the psychophysical part of the experiment. The data is transmitted via parallel port cables to the hardware that acquires the cortical data. The combination of behavioral and spike data provides the elements required to define the basic descriptors of cell. A schematic diagram showing all the components of the experimental setup is given in Figure 3.4.

3.3 Specific Experiments

Through the application and removal of external force fields, the experimental protocol creates different conditions that allowed for the study of motor learning and memory. The first behavioral epoch establishes baseline psychophysical and neurophysiological data for the reaching task in the null field. Novel force fields alter the dynamics of reaching in epoch two.

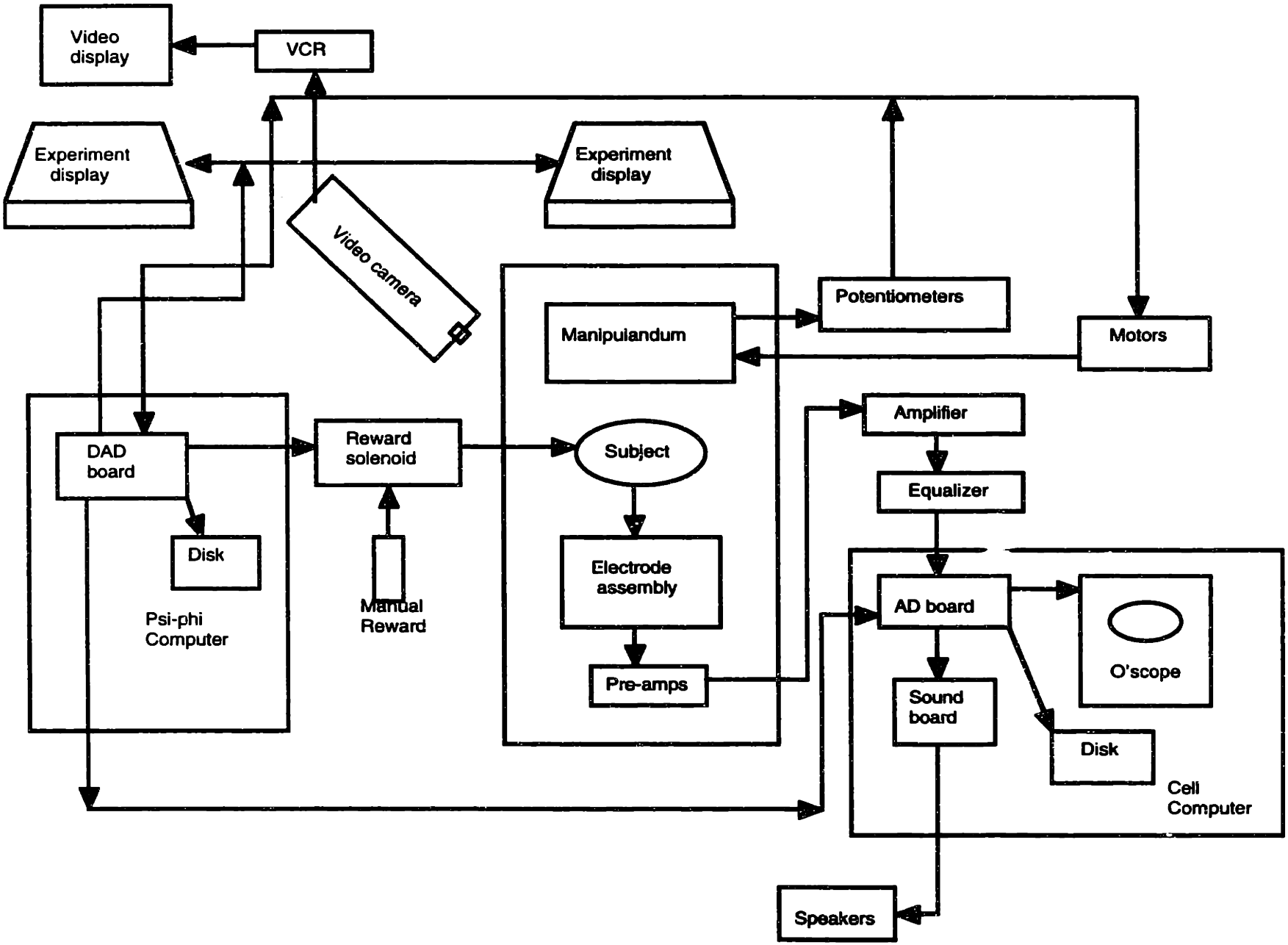

Figure 3.5 Schematic diagram of experimental setup

Human studies indicate that initial hand trajectories are perturbed in a manner consistent with the effect of the applied force field; subsequent trajectories are similar to those seen in the baseline case. The change in hand trajectories with practice in the force field is a quantitative measure of the rate and extent of learning the force environment.

Epoch three of the experiment returns movement dynamics to the baseline condition. In human studies, initial hand trajectories are not straight but reflect the aftereffects of the force conditions learned in the force field epoch. The aftereffects quantify the nature and extent to which the external force field is learned. Within very few movements, aftereffects fade, and hand trajectories return to the smooth, straight-line case. Correlating the performance measures from each of the experiment epochs with changes in cortical cell activity may provide insights to the nature of the developing internal representation of movement dynamics and the impact of this representation on motor learning and memory.

To acquire the psychophysical and neurophysiological data required to address the questions posed by this research, the following experiments were conducted.

3.3.1 First Experiment Set - Learning a Clockwise Force Field

In the initial series of experiments, each monkey was required to learn to execute the reaching task proficiently in the presence of a clockwise force field. As described previously, in a typical experimental session, the monkey first worked in the null field so as to establish baseline behavior for that day. Then, approximately 200 trials were made in the clockwise, viscous field. This was followed by a "washout" series of trials in the null field.

This paradigm was repeated over many days until monkey performance saturated, that is, until learning of the clockwise force field had been demonstrated and had reached steady state levels. By repeating the paradigm many times, it was possible to collect data from a population of cells in the motor cortex and establish trends in cell activity during changes in performance and therefore changes in motor learning.

3.3.2 Second Experimental Set - Learning a Counterclockwise Force Field

The paradigm here mimics that of the first set of experiments in that a single force field will be used repeatedly. In this case, however, the field is counterclockwise, viscous. This series of experiments provides another opportunity to record cell activity while the monkeys learn a

second novel force field. Psychophysical and neurophysiological data collected during the second experimental set augments and compliments the findings of the learning paradigm in the first experimental series.

4. Data Analysis Methods

The methods used to analyze data obtained from both the psychophysical and neurophysiological components of the experiments are described here. The goals of analyses are twofold. First, identify and quantify the parameters that best characterize behavioral performance and cortical cell activity. Second, develop relationships among the parameters that suggest mechanisms for motor adaptation/learning and memory.

4.1 Psychophysical data analysis

Psychophysical data quantify task performance, and, as such, indicate the nature, extent and change in motor learning. Kihlstrom (1987) and Halsband and Freund (1993) suggest that motor learning can be characterized by changes in relevant performance measures, for example, increased peak movement velocity, decreased reaction time, smoother, straighter path trajectories. The goals of psychophysical data analysis, then, are to demonstrate that the changes in task performance seen during execution of the experimental paradigm are consistent with changes seen in motor skill acquisition and motor learning.

The parameters that describe monkey hand kinematics for each reaching movement are manipulandum end-point position and velocity. Manipulandum handle (and therefore monkey hand) position is measured directly by potentiometers mounted on the hardware. Data is collected at a rate of 100Hz. End point velocity is then determined through numerical differentiation.

Performance of the monkey in the experimental paradigm is quantified by parameters based on path and velocity histories for the reaching trajectories. One such parameter is peak hand velocity. The sampling of peak velocity values for all trials within a behavioral epoch will define mean and variance values of that epoch. A one-way analysis of variation (ANOVA) quantifies the significance of changes in peak velocity across the behavioral epochs.

Quantifying learning requires more than assessing changes in average performance across behavioral epochs; it requires demonstrating performance changes from one reaching trial to the next. It has already been suggested that changes in hand paths from trajectories with multi-modal velocity histories to those with unimodal histories are indicative of motor skill acquisition. A challenge, then, is to define an analysis method that can quantify such changes in velocity histories. Such a method is provided by Shadmehr and Mussa-Ivaldi (1994). They

considered the velocity time history of a given reaching movement as a vector. A measure of the similarity of two such velocity sets, U and Y, is a correlation coefficient defined by the ratio of the covariance of the time series and the product of their standard deviations:

$$\rho(U,Y) = \frac{Cov(U,Y)}{\sigma(U)\sigma(Y)}$$

The correlation coefficient can range in values from 1 (two identical velocity histories), to 0 (two orthogonal velocity histories), to -1 (two velocity histories in opposite directions). Essentially the approach calculates a normalized scalar product of two velocity vector sets.

As applied here, the method is as follows. A nominal or average trajectory in the baseline epoch is first determined. Since the monkey is well trained in the reaching task in the null field, the nominal trajectory is relatively straight with a smooth, unimodal velocity history. A correlation coefficient for each trail is then determined by taking the normalized dot product of the specific velocity history with the velocity history from the nominal trial.

Figure 4.1 illustrates the use of the correlation coefficient method. In Figure 4.1a, two trajectory position and velocity histories are shown. The dashed lines represent the nominal trajectory. Note the straight-line characteristic of the path and the smooth velocity history. The solid line is a selected trajectory also in the null field. The similarity in these two trajectories is indicated by the large correlation coefficient. In Figure 4.1b, the dashed line again represents the nominal movement in the null field. However, the solid line is a selected movement to the same target location but with a trajectory perturbed by applied forces. The effect of the forces is seen in the deviated hand path and the multimodal velocity history. The change in task performance suggested by the difference in hand velocity is quantified by the smaller correlation coefficient.

The correlation coefficient as a means of quantifying task performance can demonstrate both short-term and long-term motor adaptation and learning. Human studies suggest that reaching trajectories are perturbed when forces are initially applied but return to smoother, straighter paths with practice in the force field. Such a trend would be indicated by an evolving increase in the correlation coefficient with increasing number of trials executed in the force field.

A summary parameter for daily performance in a force field can be described by a mean and standard deviation of the correlation coefficients calculated for trials executed during the force

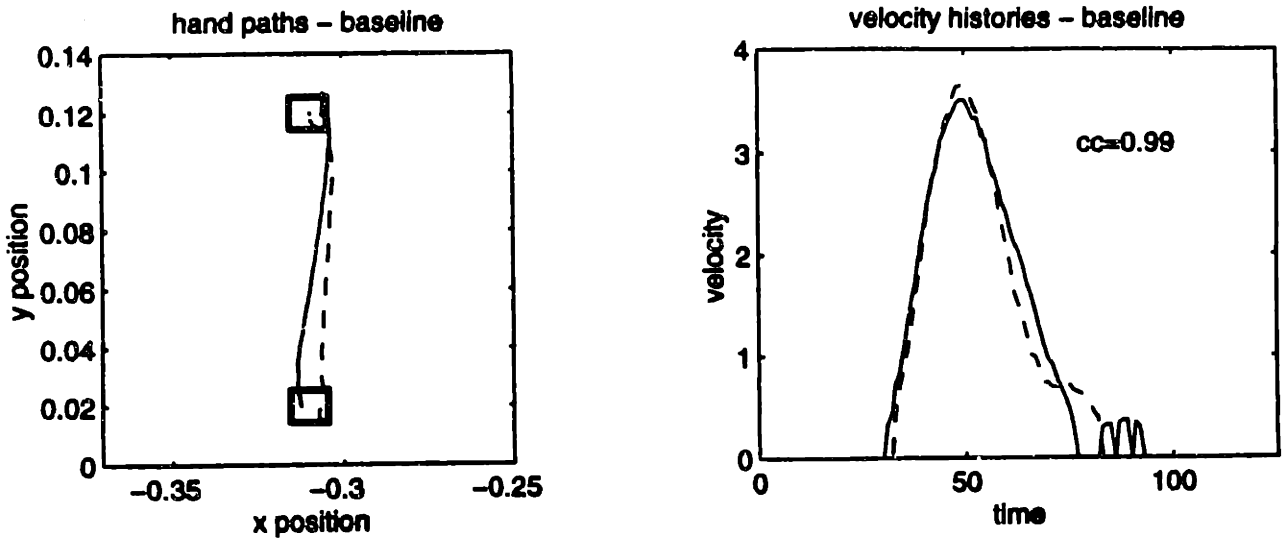

a) comparing selected baseline and nominal baseline trajectories

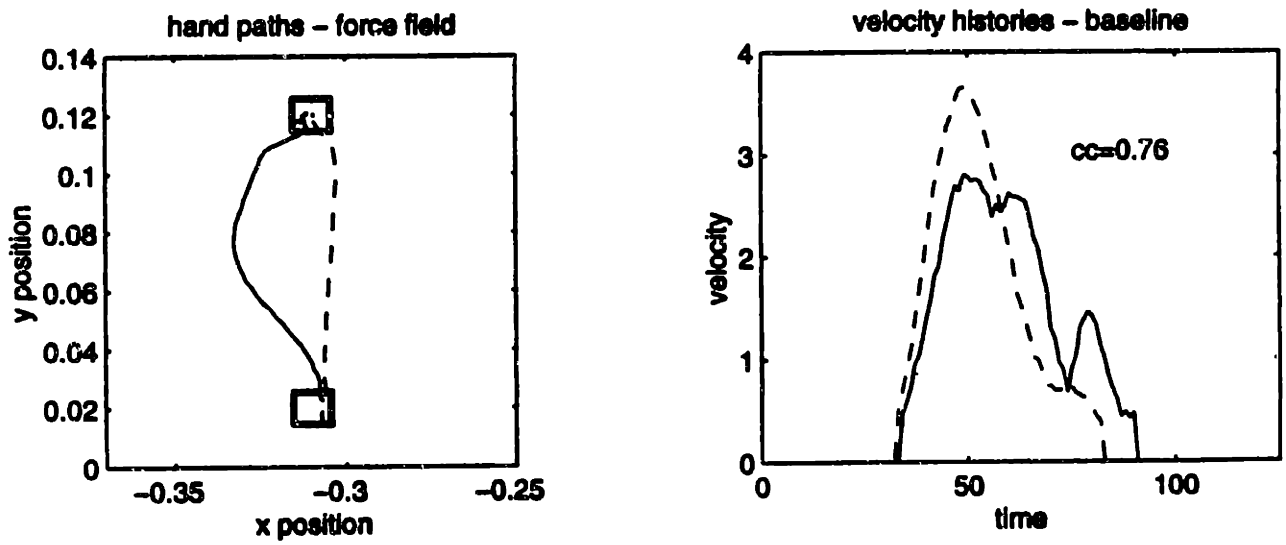

b) comparing selected force field and nominal baseline trajectories

Figure 4.1 Comparisons of hand trajectories and correlation coefficients for baseline and force field trajectories

epoch. When plotted over many days of experimentation, the long-term learning or consolidation of knowledge of the force field is demonstrated.

In summary, then, hand path and velocity histories and peak velocity during the reaching movement are calculated to quantify the change in behavior of the monkey in the reaching task. Motor performance, adaptation, and learning is best described through a method that calculates correlation coefficients based on movement velocity histories. Changes in this parameter most reliably indicates the rate and extent of motor learning.

4.2 Cell data analysis

In its raw form, the neurophysiological data consist of digitized waveforms of each detected spike event, the time at which the event occurred, and the timestamp of events linked with experiment performance, e.g. target on, movement onset, etc. The waveform for each spike is described by 43 values representing 1.75ms of data collected at a rate of 25kHz.

Data collected by a single electrode can correspond to the activity of more than one neuron. Initially then, clustering analysis is performed to identify and separate the data associated with different cells. Each waveform is characterized by a number of parameters - amplitude measures such as peak positive or peak negative values and timing measures such as time to positive peak, time to negative peak, and time between peaks. The waveform signature of a given neuron is a function of the location of the electrode with respect to the cell - its dendrite arbor, soma, or axon - and the distance between the neuron and the electrode. In a stable environment, the waveform of a given neuron remains constant over the experimental recording period. A second neuron demonstrates a different waveform due to a different location and distance to the electrode. The assumption in clustering analysis is that parameters associated with the waveforms from one neuron are different than those from a second cell. When plotted in parameter space, these values will locate or cluster in different regions. By identifying and isolating separate clusters, the activity of separate cells can be identified. The conclusion of multiple cell activity is confirmed by comparing plots of the waveforms shapes.

The clustering process is illustrated in Figure 4.2 which shows the cortical activity recorded on a single electrode during one experimental epoch. The waveform parameters plotted are peak positive amplitude on the ordinate and peak negative amplitude on the abscissa. Each dot represents an individual spike event. Two distinct groups or clusters are evident and suggest the activity of two separate cells. Plotting the waveforms associated with each group confirms

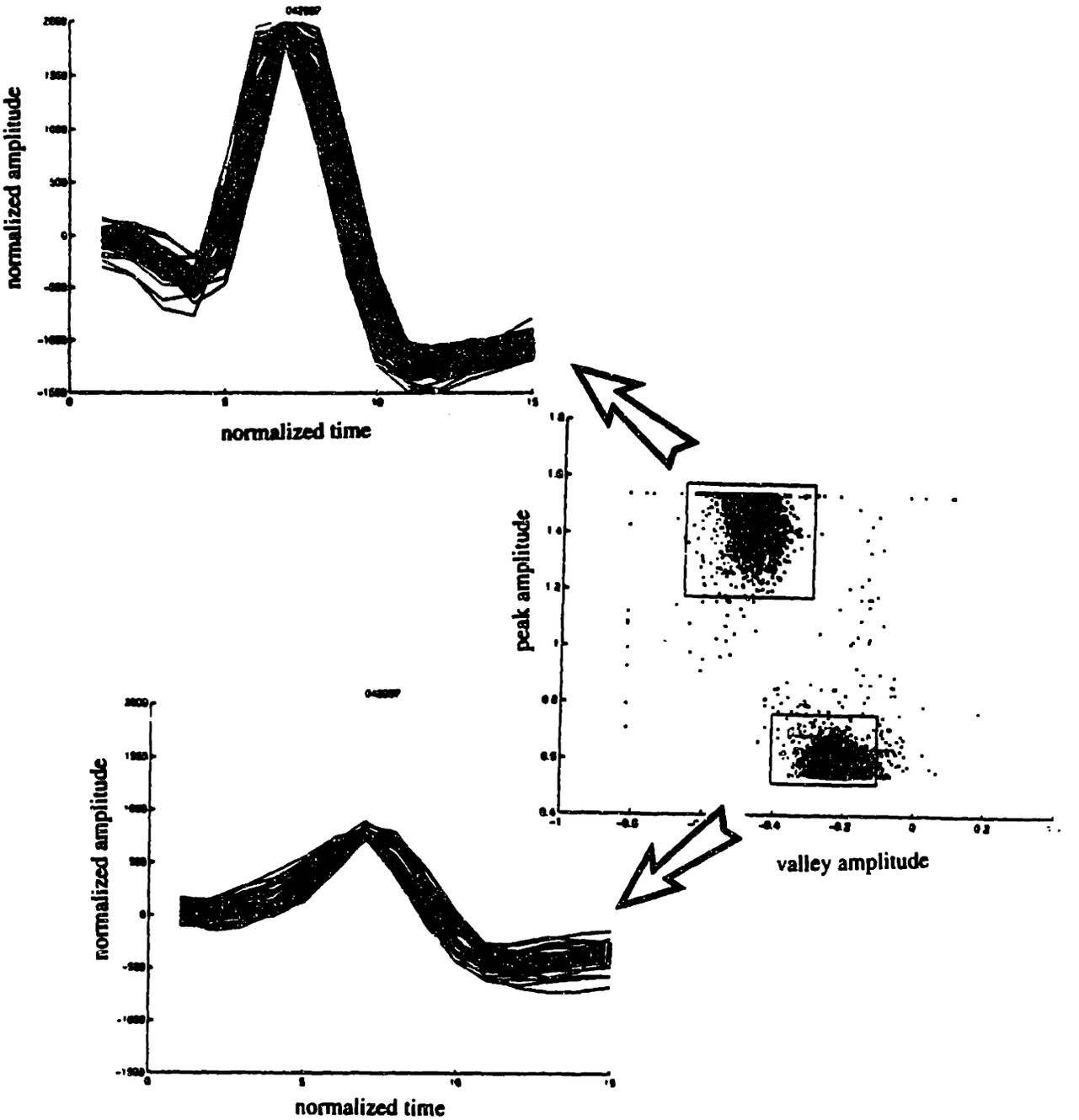

Figure 4.2 Cell clustering method - separating cell activity based on waveform parameters

the consistency of shape within a cluster and the differences between the clusters. That this electrode recorded the activity of two neurons is confirmed.

Once the activity of an individual cell has been identified, it is then necessary to quantify the behavior of the cell in the reaching task. A qualitative description of cell activity is given by raster plots and time histograms. Raster plots show the temporal sequence of spike events and give a qualitative estimate of the frequency of cell activity across time periods for a set of reaching trials in each movement direction. This is shown in Figure 4.3a. Each subplot shows raster diagrams for one of the eight movement directions. The vertical line on each plot indicates the time of movement onset. Each dot represents a spike event at a specific point in time. Cell activity is aligned such that hand movement begins at time t=0. Also shown on the plot are markers that indicate trial milestones: "s" indicates the time the peripheral target is illuminated; "x" marks the time of the go signal; "o" movement onset; "+" peripheral target acquired; and "#" reward.

Time histograms provide a semi-quantitative description of cell activity. These plots start with raster diagrams that show spike activity during several reaching trials aligned to a common time point. The time line is then divided into a number of intervals or bins; each bin is typically 10ms to 50ms in width. Cell activity that occurs within a given bin is summed across the trials and plotted in a bar format. Figure 4.3b shows a histogram representation of the data shown previously as raster plots.

Neither the raster plots nor the histograms provide descriptions of cell activity adequate for hypothesis testing. A numerical description is required. For this work, the basic parameter quantifying cell activity is average firing frequency. By treating the cell discharge as a quasistatic signal and calculating average firing frequency, information is lost about details of the complex temporal variation of discharge during a reaching trial. However, it was chosen as a conservative measure of cell activity, showing less intertrial variability than other measures such as peak instantaneous frequency (Kalaska, et al. 1989).

As described earlier, a reaching trial is divided into a number of time periods:

- center target hold time
- delay time
- movement time
- peripheral target hold time.

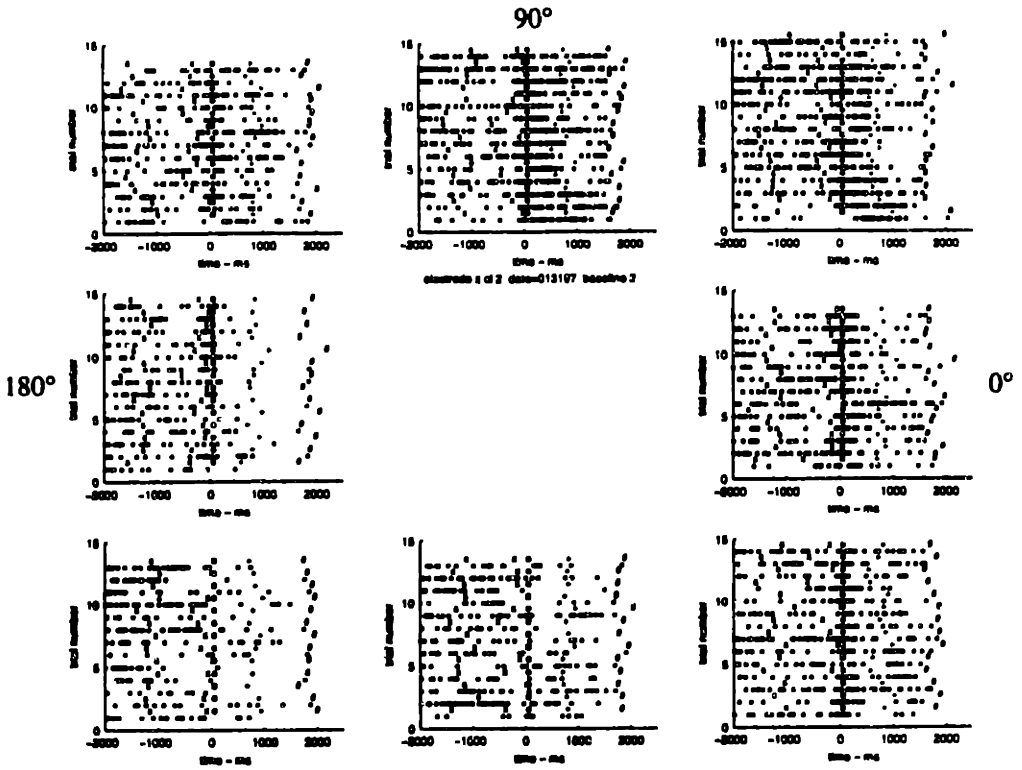

a) raster plots

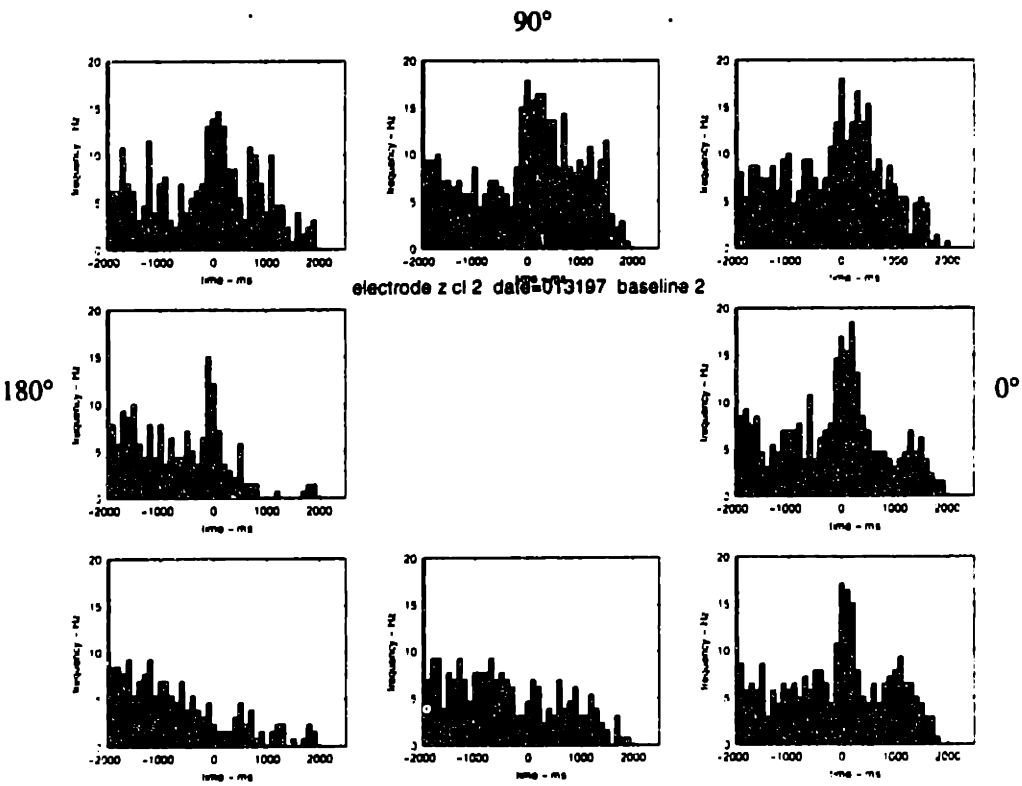

b) histograms

Figure 4.3 Graphical representations of cell activity within a behavioral epoch

For a given time period, average cell discharge is calculated simply by dividing the number of spikes occurring during the period by the period length. Since multiple trials are made in all eight reaching directions, a sampling of frequencies is obtained for each direction of movement. Each sampling is described by a mean and variance. Figure 4.4 illustrates the manner in which this quantitative description of cell behavior is graphically displayed. Four plots are shown, one for each of the reaching trial time periods. In each plot the ordinate is cell firing frequency in Hertz; the abscissa is movement direction in degrees for the reaching task. Zero degrees corresponds to hand movements to the right, 270° corresponds to movement down or toward the monkey. Cell activity is shown as the mean plus-and-minus a standard deviation for each direction. Also drawn is a least-squared-error fit of a cosine function through the mean frequency values.

These "tuning curve" graphs represent the basic description of cell activity while the monkey executes the task in a single dynamic environment. Although comparing tuning curves across behavioral epochs can indicate changes in cell activity, the comparisons are, nonetheless, qualitative in nature. It is necessary to define activity parameters that quantify this graphical representation of cell behavior and provide the basis for statistical analyses that demonstrate the significance of changes in the parameters across the three dynamic environments.

4.2.1 Cell activity measures for a single epoch

Given the graphical representation of cell activity shown in Figure 4.4, two statistical measures are initially applied to assess and quantify cell behavior. First, a one-way ANOVA is conducted to determine whether there is a statistically significant change in cell activity across any of the eight directions of movement for the four time periods of cell activity. These tests assess both cell activity stability and relevance to the reaching task. During the center hold time, the monkey is holding the manipulandum still so as to maintain the cursor in the center target. This condition is static over all reaching trials, regardless of subsequent movement direction or applied load. Cell activity, then, should be constant. For the center hold time period, an ANOVA test of cell activity should show no significant variation with direction. Constant cell activity implies a stable recording environment.

The other time epochs of the reaching trial - delay time, movement time, and peripheral target hold time - are associated with planning and execution of limb movement in a specific target direction or maintenance of the limb at a specific target location. Many researchers have shown that the activity of a majority of cells recorded in the primary motor cortex varies as a

a) center hold time

b) delay time

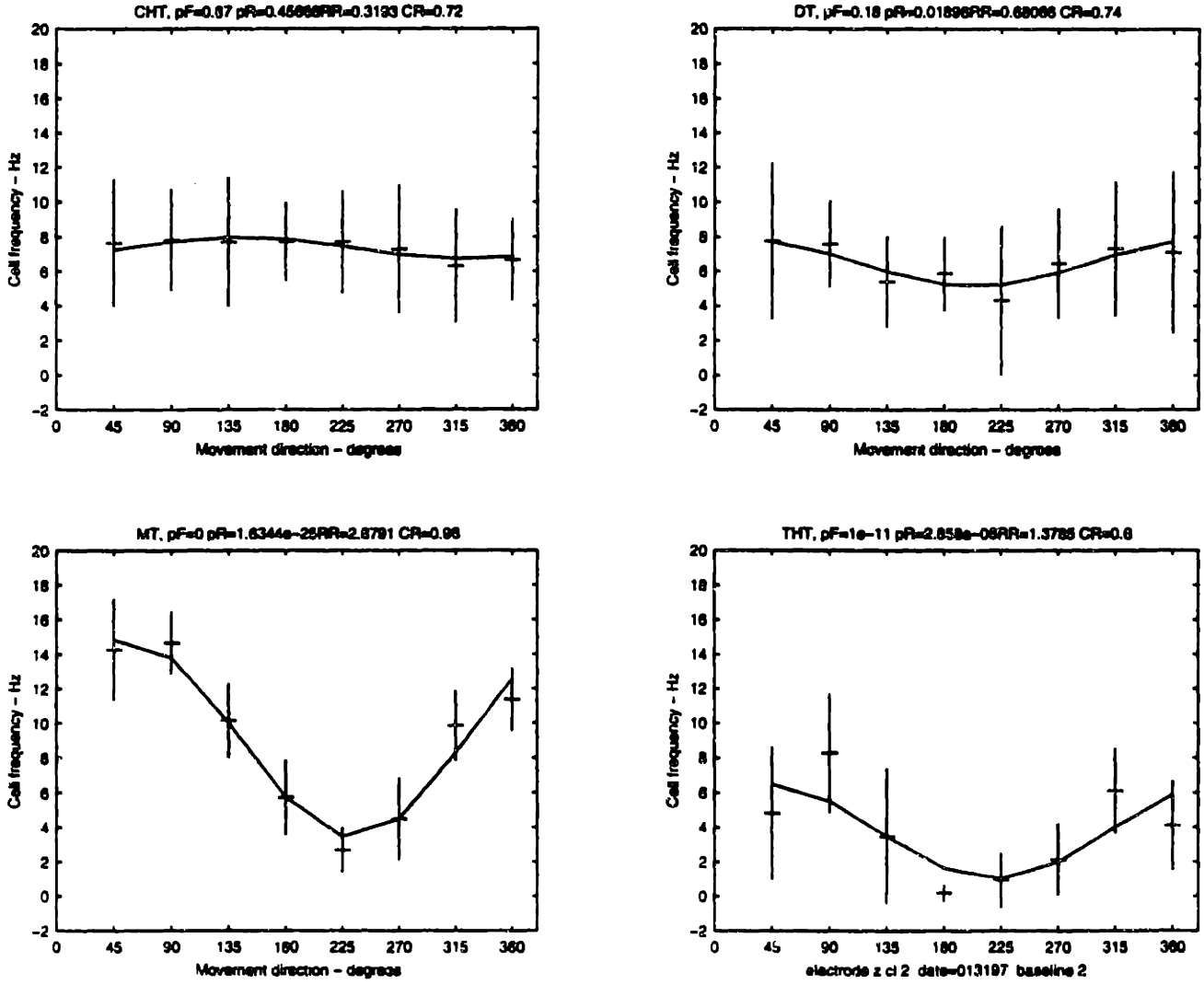

c) movement time

d) target hold time

Figure 4.4 Tuning curves showing cell activity as function of movement direction for a) center hold time, b) delay time, c) movement time, d) peripheral target hold time

function of movement direction. For these time periods, then, an ANOVA test of cell activity should indicate a significant variation with target direction. Cells that do not demonstrate such variations over any time period are assumed to be uncommitted to or unassociated with the reaching task for the force environment considered.

For cells that show significant modulation with movement direction, four parameters are defined to quantify cell activity: mean firing rate, dynamic range, preferred direction of activity, and width or sharpness of tuning. The meaning of each parameter is illustrated in Figure 4.5.

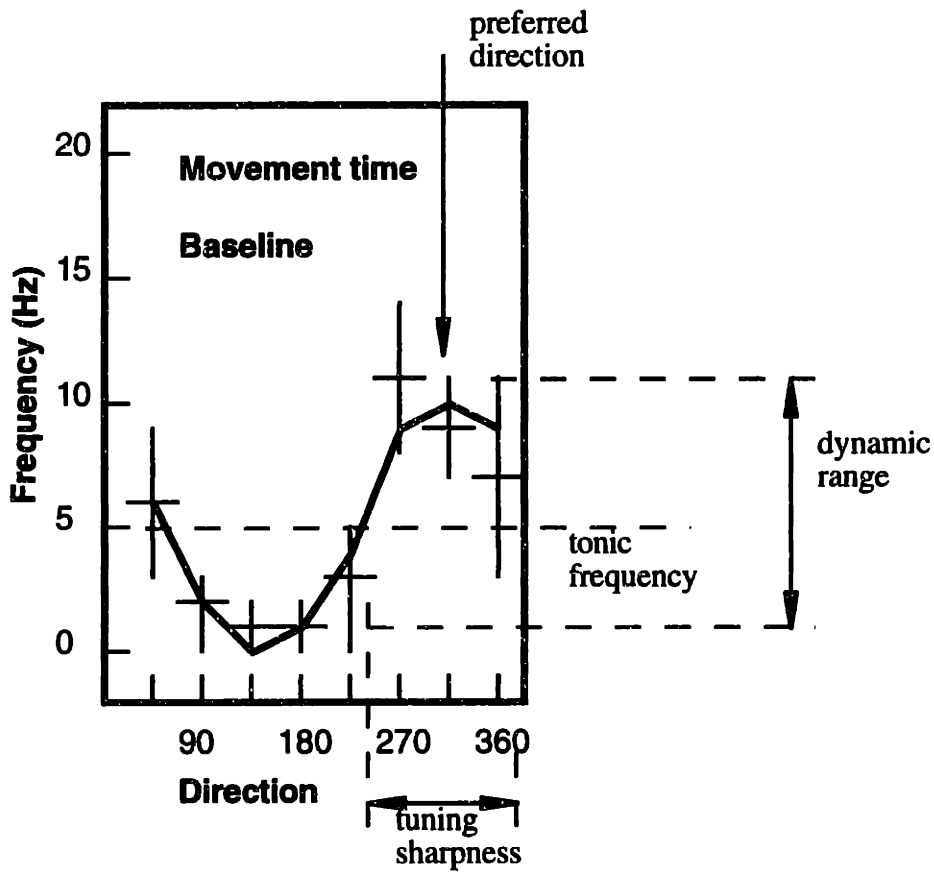

Figure 4.5 Parameters that quantify cell activity within a behavioral epoch

The mean or average firing rate for any time period within a behavioral epoch is simply the mean value of the rates for that period across all reaching trials within the epoch. Dynamic range is the modulation in cell activity about the mean value as a function of movement direction. The parameters for dynamic range are determined from two sampling distributions

corresponding to the directions of maximum (θ_{max}) and minimum (θ_{min}) cell activity. The mean dynamic range is taken as the difference between the mean frequencies for these directions:

$$\varpi_{DR} = \varpi_{\theta max} - \varpi_{\theta min}$$

Preferred direction of cell activity is determined by calculating the sum of vectors representing the activity in each movement direction. The vector for a given direction is determined by scaling the direction unit vector by the mean firing rate (Fisher 1993). Let the vectors

$$\mathbf{e}_1, \mathbf{e}_2, \mathbf{e}_3, \ldots \mathbf{e}_8$$

be unit vectors in the eight movement directions. A vector pointing in the direction of preferred cell activity is given by

$$\mathbf{m} = \frac{1}{\sum_8 M_i}(M_1\mathbf{e}_1 + M_2\mathbf{e}_2 .... M_8\mathbf{e}_8)$$

where M_i is the mean cell discharge frequency in direction i.

Although this method determines the preferred direction of cell discharge, it does not indicate the significance of the direction tuning. The Rayleigh test calculates this significance (Fisher 1993). This method tests whether a cell shows a significant unimodal discharge variation with movement direction against the null hypothesis of a uniform or nondirectional pattern of activity.

The sharpness of tuning is determined by the difference between the two movement direction angles defined by the intersection of a line at the average firing rate and the tuning curve itself.

The four parameters describe the nature of cell activity within a given behavioral epoch. Mean activity parameter values and their variances are calculated from the dependent random variable measured in the experiment - average cell firing rates. Appendix A provides the mathematical details.

Adopting an analysis method of Georgopoulos, et. al. (1983), a cosine curve can be fit to the mean firing frequency data. Cells whose activities are well fit with a cosine function are said to be broadly tuned. Activity peaks in the preferred direction of movement and decreases gradually as movement deviates from this direction. This results in a quantitative description of broadly-tuned cell activity expressed as follows:

$$d(\theta_i) = a_0 + a_1 * \cos(\phi - \theta_i)$$

where $d(\theta_i)$ is the average firing frequency in movement direction θ_i

a_0 is the tonic or mean firing rate

a_1 is the variation of cell activity about the mean

ϕ is the preferred direction of movement

In this work, fitting a cosine curve to cell data is done only to assess the fraction of cells whose behaviors exhibit such broad tuning. The four activity parameters previously described and the statistical analyses that employ these parameters are the basis for all conclusions regarding cortical representations of motor learning and memory.

4.2.2 Variation of cell activity across epochs

The previous section identified mean firing rate, dynamic range, preferred direction, and sharpness of tuning as parameters that describe cell activity within a behavioral epoch. Each activity parameter is quantified by a mean value and a variance based on spike activity recorded during the reaching trial time epochs (center hold time, delay time, movement time, and peripheral target hold time) for each of the force epochs (baseline, force field, and washout). The statistical analysis methods described in Appendix A are used to assess the significance of changes in activity parameters across the behavioral epochs. The natures of such changes then define classifications of cell behavior for the experimental paradigm.

5. Results

The purpose of psychophysical data analysis is to characterize performance of the reaching task and to demonstrate that changes in performance suggest skill acquisition through motor learning. It is shown below that, indeed, changes in task performance within a single experiment session and across multiple sessions are consistent with those seen during motor skill acquisition. Specifically, with practice in a force field, monkey hand paths are straighter and velocity histories are smoother. Such trajectories suggest a more-skilled movement executed in a feed-forward manner by the neural control mechanisms.

Cell data analyses demonstrated changes in activity across the dynamic environments of the reaching task. The nature of the changes were different for different subsets of cells. This led to defining three categories of cell activity that were then correlated with reaching task performance.

The experimental paradigm generated a huge amount of psychophysical and neurophysiological data during nine months of recordings. All data were subject to the analyses described in the previous chapter. It is not practical, however, to present all analyses in depth. The data plots alone fill many, large binders. Rather, in the sections that follow, selected data are shown. Detailed results from the analysis of psychophysical data for a limited number of experiment sessions are presented. These illustrate typical changes in performance seen across force epochs within a single experimental session and characterize performance changes across multiple days of exposure to the novel force fields. For neurophysiological data, the analyses of the activities of two cells are presented in detail. This illustrates the step-by-step process applied to all cell data that begins with isolating single-cell activity and continues with quantifying cell behavior in terms of activity parameters and conducting statistical analyses to identify changes in activity across behavioral epochs. Cell analysis culminates with a table that, for each analyzed cell, identifies significant activity changes across the epochs and labels cells based on the relationship between the nature of these activity changes and the kinematic or dynamic characteristics of the behavioral task.

5.1 Performance of the reaching task

Within a given day's experiment session, performance of the reaching task by the monkey changes. Performance varies within a behavioral epoch, for example, across trials in a baseline condition, and, more significantly, it changes across epochs from baseline to force fields to

washout. Performance also changes from day to day as the monkey's exposure to a perturbing force field increases.

5.1.1 Task performance within a single session

Performance in the baseline epoch defines nominal behavior for the monkey. This is a null-force condition: no perturbing forces are applied. Since the monkeys are highly trained in this epoch, reaching trajectories should reflect the characteristics of a well-learned task - straight hand paths and smooth, unimodal velocity histories. Figures 5.1 gives actual hand paths for one monkey in all eight directions of movement for the baseline epoch. Four plots are show corresponding to four different experiment sessions during a two-month period. Compare to Figure 2.1a - hand paths are not as straight as those executed by human subjects performing essentially the same task (Shadmehr and Mussa-Ivaldi 1994). Within a given day there is clear inter-trail variation in paths to each target - a finding consistent with that reported by Scott and Kalaska (1995). As seen in Figure 5.2, this variability does not suggest a systematic bias toward a specific curvature in path. The center plot of Figure 5.2 shows the mean hand paths in each movement direction for the four days. The mean paths are tending toward straight trajectories. The figure also shows velocity histories for the nominal trajectories. The location in the figure of each velocity plot with respect to the center graph corresponds to the direction of movement; the plot to the right of center shows data for movement to the right. Velocity histories are typically smooth and unimodal. Peak velocities are approximately 0.3m/s in all directions; movement times average 600-700ms. Such consistent performance supports the belief that the monkey is well-trained in the baseline task.

In the second behavioral epoch, forces are imposed on the reaching task by the manipulandum. These force change the dynamics of the task and force the monkey to adopt a different movement strategy to reach the target. Deviations from straight hand paths and unimodal velocity histories quantify the perturbing effect of the novel forces. As the monkey acquires the skill to perform the task in the presence of the forces, such deviations should diminish.

Figure 5.3 illustrates typical trajectory data from a single experimental session for initial trials in a counterclockwise force field. The center plot shows several individual hand paths in each movement direction. The influence of the force field is clear; there is a systematic bias in hand path reflecting the effect of the counterclockwise, viscous forces. Surrounding the center graph are plots of the corresponding velocity histories. Compare these data with the history

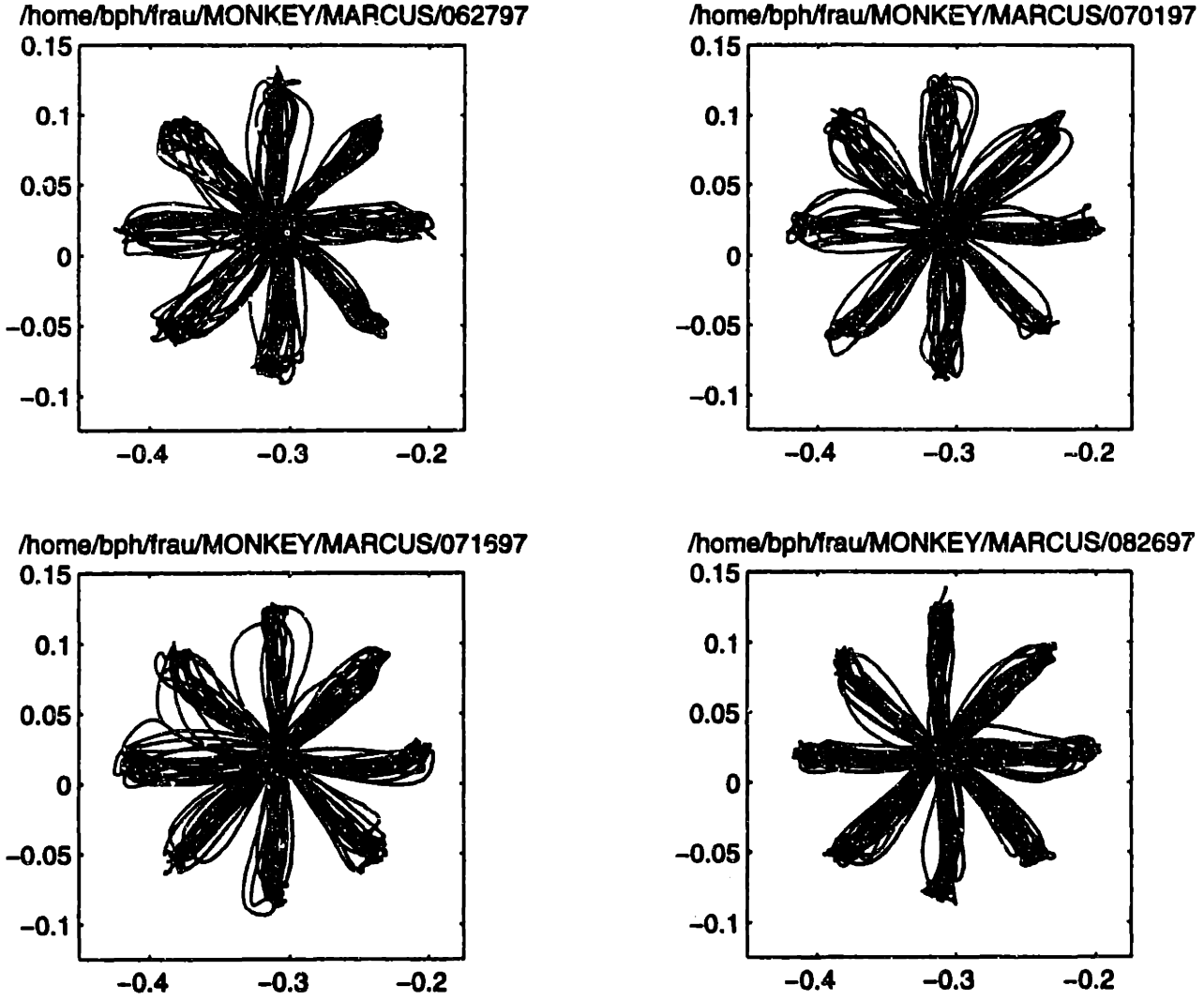

Figure 5.1 Hand paths in baseline epoch on four selected days

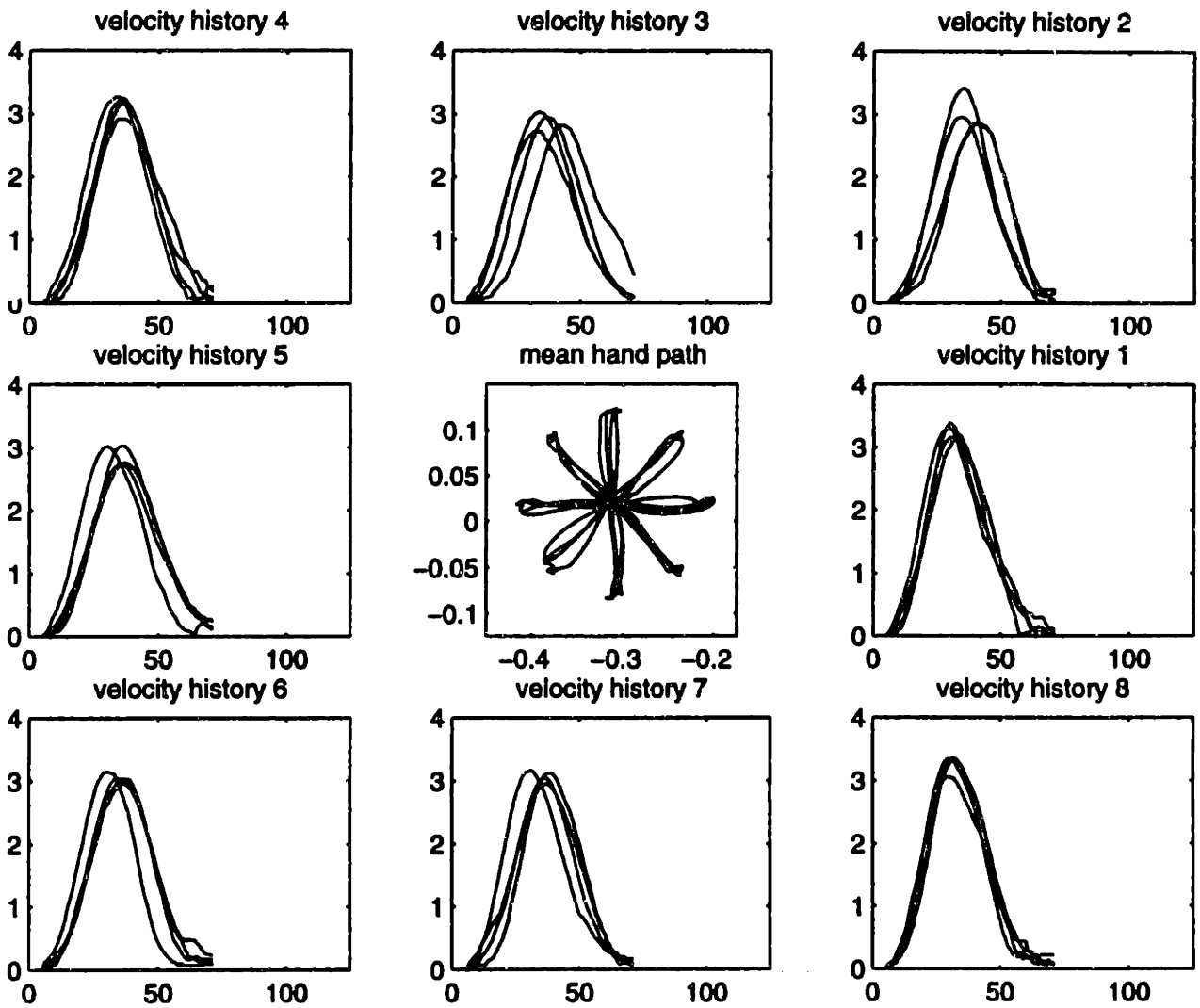

Figure 5.2 Nominal hand paths (center plot) and nominal velocity histories in each movement direction for data in Figure 5.1

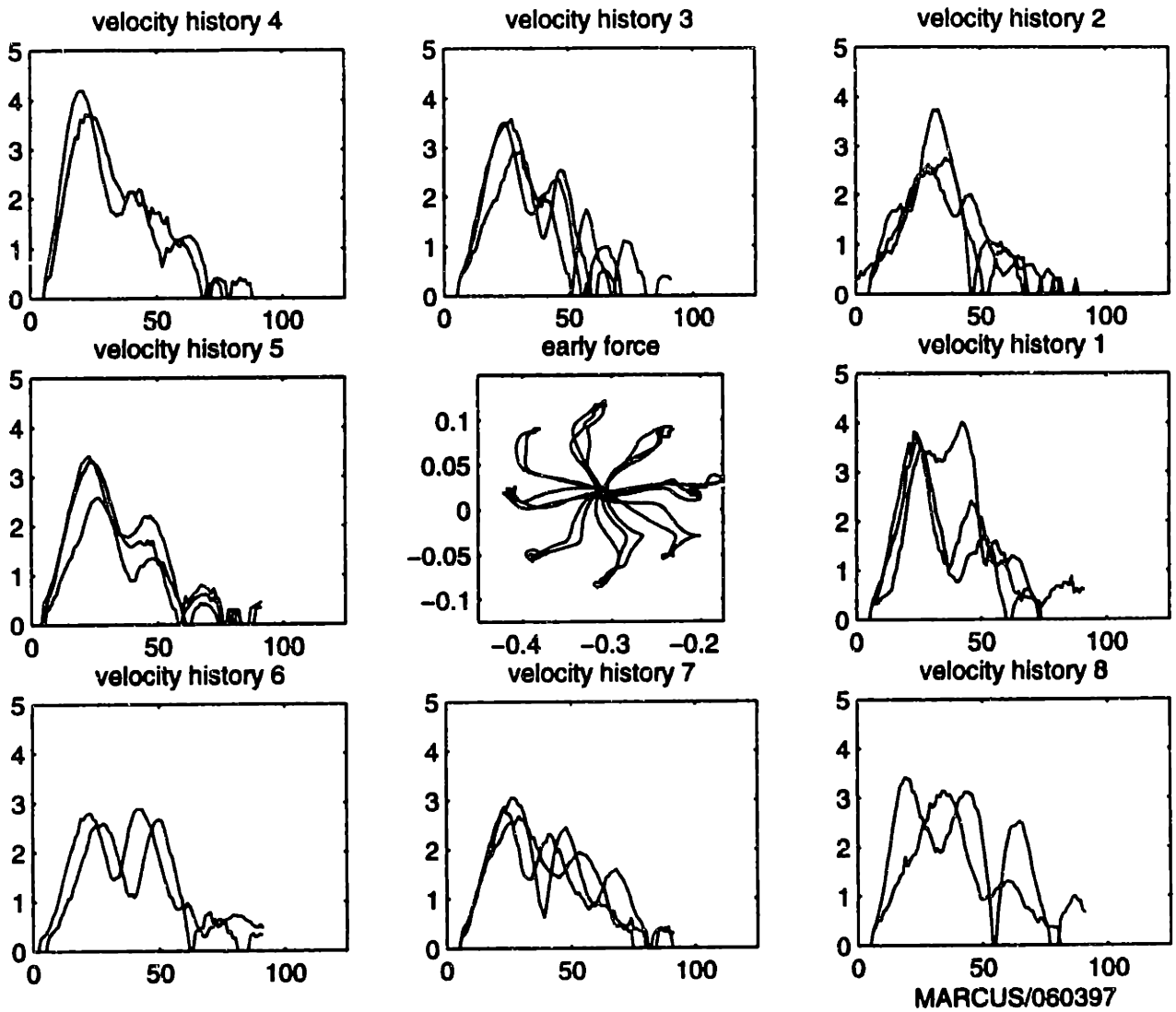

Figure 5.3 Typical trajectories for initial trials in a counterclockwise force field demonstrate perturbing influence of forces

plots of Figure 5.2. Reaching trajectories made early in the force epoch display velocity histories with multiple peaks and increased movement time. Both hand paths and velocity histories indicate that multiple corrective movements are made to acquire the target. This suggests an unskilled or primitive execution of the task.

Approximately 200 trials are performed in the force field. By so doing, the monkey practices the reaching task in this dynamic environment. If skill acquisition through motor learning results from this practice, then hand trajectories should become more like those seen in the baseline case - straighter paths and smoother velocity histories. Understand that the experimental paradigm provides no incentive for the monkey to alter the manner in which the task is executed. Reaching movements that acquire the peripheral targets with multiple corrective actions are rewarded just as direct movements that smoothly acquire the targets. Changes in performance, then, reflect the implicit nature of motor learning.

Figure 5.4 shows data for several individual trials late in the force epoch. The hand paths seen in the center plot still reflect some influence of the counterclockwise force field, but the paths are now much straighter than those seen early in the force epoch. The velocity histories demonstrate a dominant velocity peak, a clear reduction in the number of peaks, and a reduction in movement time. These changes in performance suggest increased proficiency in task execution; these changes suggest skill acquisition through motor learning.

The force epoch is followed by the washout period. In this last epoch, the perturbing forces are removed and the dynamics of the task return to the null condition seen in the baseline period. Although the nature of the reaching task in the washout period is the same as that in the baseline case, the nature of the monkey is different. Specifically, the state of the system controlling the reaching movement has been altered by repeated practice of the task in the force field of the previous behavioral epoch. The control system has been modified by motor learning. The influence of the altered control system state is seen in the initial movements made by the monkey in the washout period. Figure 5.5 illustrate these movements. The hand paths are not straight but reflect a bias in the clockwise direction. Velocity histories are multimodal and indicate longer movement times compared to baseline movements. This bias of trajectories early in the washout period is called aftereffects. Using mathematical simulation and movement data from human subjects, Shadmehr and Mussa-Ivaldi (1994) showed that such aftereffects can result by invoking in the null force condition a control strategy consistent with that developed in the force epoch. The nature of aftereffects, then, reflects the altered state of

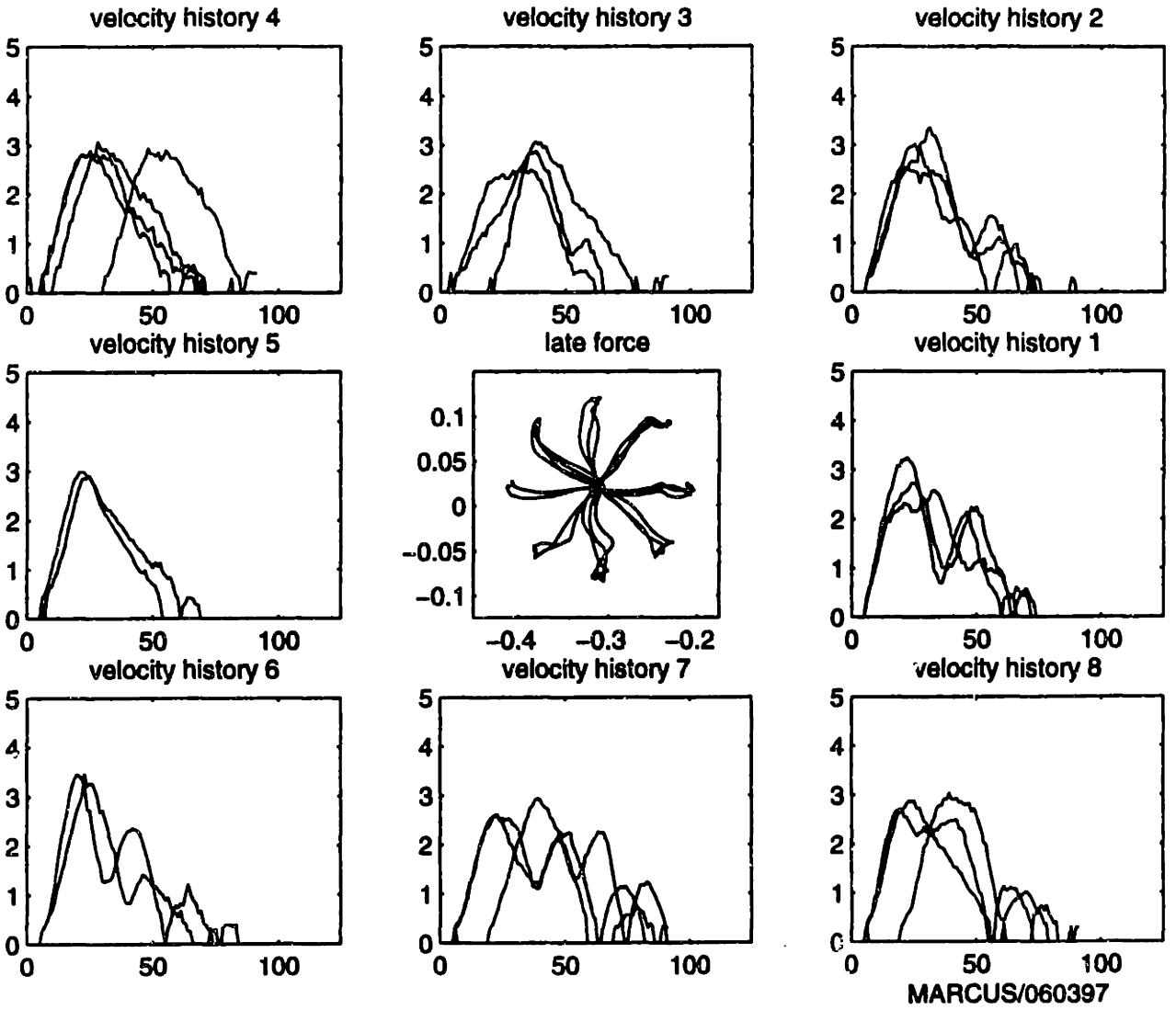

Figure 5.4 Typical trajectories for trials late in a counterclockwise force field show an improvement in performance

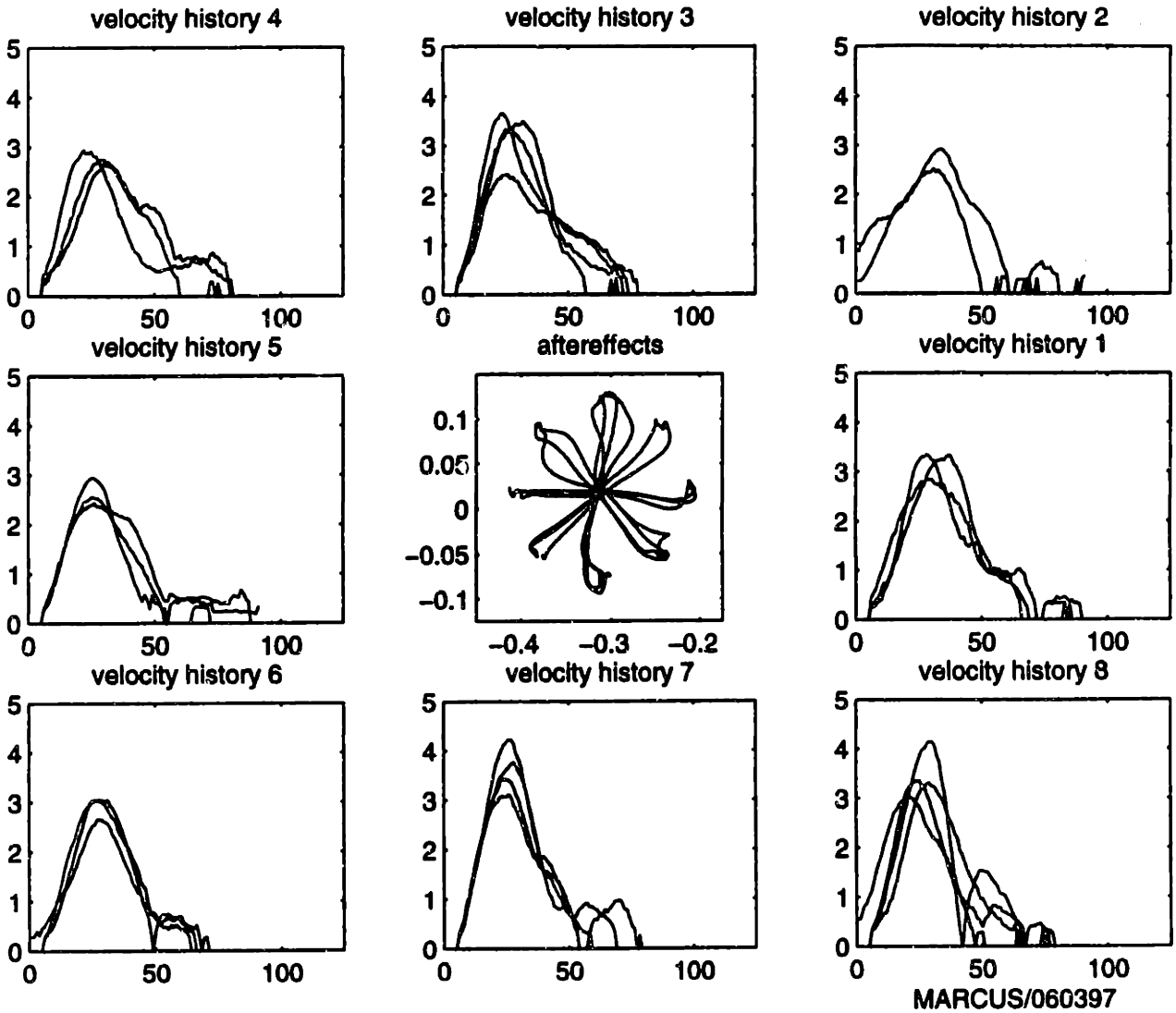

Figure 5.5 Typical trajectories for trials early in the washout period demonstrating aftereffects

the movement control system and quantifies the extent to which the dynamic environment of the force epoch has been learned.

Aftereffects fade within several trails, and reaching movements in the washout epoch soon are characterized by relatively straight hand paths and smooth velocity histories. Figure 5.6 shows data for individual trials late in the washout epoch.

Plots of individual reaching trials, both hand paths and velocity histories, graphically illustrate the effect of novel forces on reaching movements. However, during the course of a single experiment session, the monkey makes several hundred reaching trials. Over multiple weeks of exposure to a force field, the over 10,000 such movements are made. It was necessary, then, to develop a more compact summary statistic that describes performance in a reaching task.

Two such statistics were identified and described in the previous chapter - peak tangential velocity and a velocity-based correlation coefficient. Changes in peak tangential velocity can indicate motor learning; peak movement velocity increases with skill acquisition. Figures 5.7 and 5.8 show peak velocity data as a function of behavioral epoch for the two monkeys tested. Units for velocity are tenths of meters/sec. The four graphs shown on each figure correspond to four different experiment sessions. Each of the three behavioral epochs, baseline, force field, and washout, are divided into an early and late period. Thirty trials are selected from each period and corresponding peak velocities are calculated. Peak velocity data are then displayed as solid bars representing the mean peak velocity and error bars for the standard deviation. A comparison of peak velocities for the two periods of the baseline epoch (BLe and BLl) demonstrate consistency of performance within the nominal task. Performance in the early force field period (FFe) is more influenced by the applied forces than that in the late period (FFl). Early washout trials (AE) reflect aftereffects; late washout trails (WO) demonstrate nominal performance characteristics.

Despite the changes in the reaching task dynamic environments across the behavioral epochs, and despite the clear changes in hand path and velocity histories seen earlier, the peak velocity of movement does not significantly vary across behavioral epochs either within a single session or across multiple days of exposure to a given force field. Peak velocities within the baseline epoch are consistent (compare BLe and BLl) and change little from day-to-day. Also, there is no significant difference between the peak velocities in the well-trained baseline epoch and the peak velocities seen early in the novel force field epoch (FFe). Nor are there significant

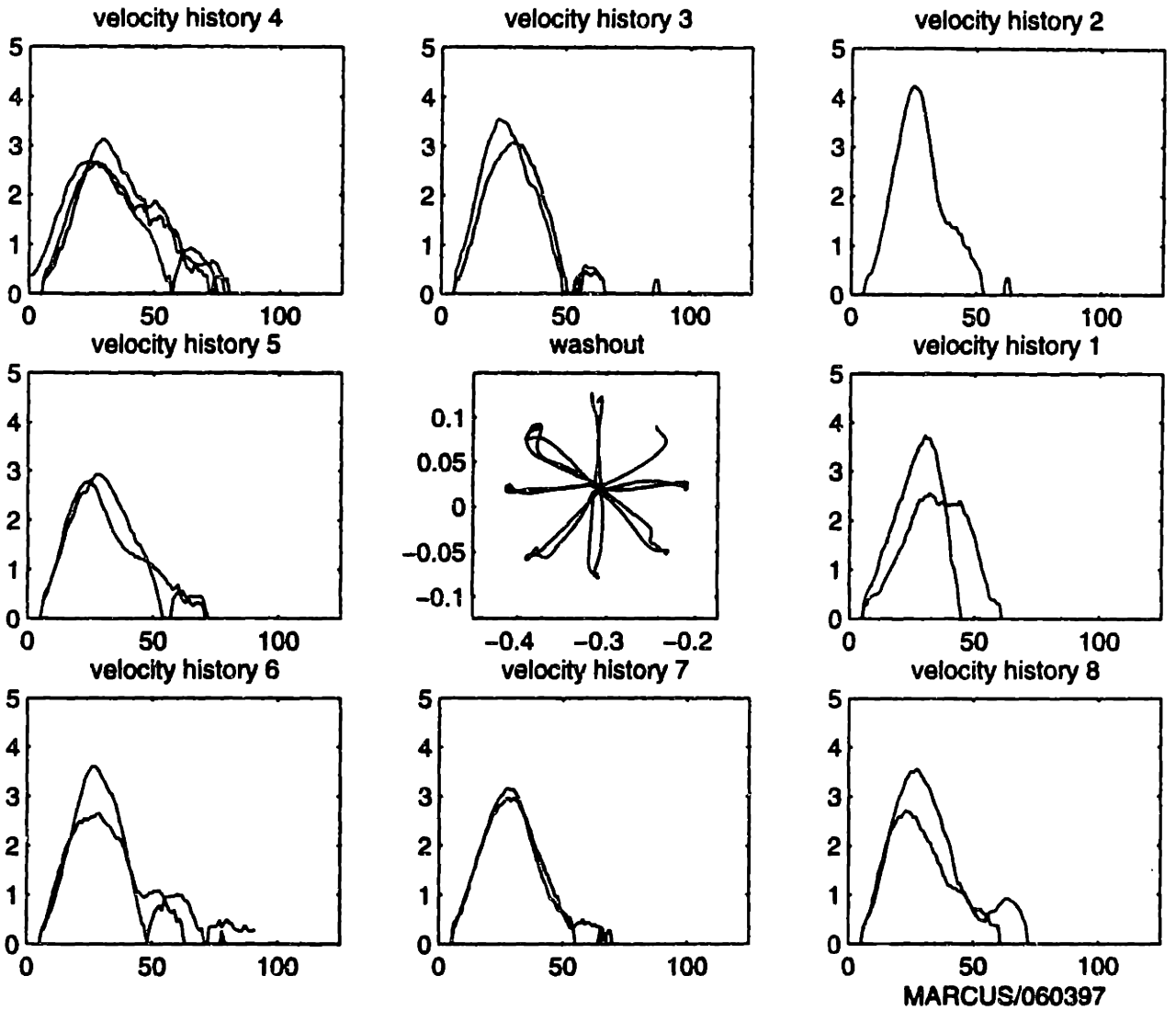

Figure 5.6 Typical trajectories last in washout period show a return to nominal performance in the task

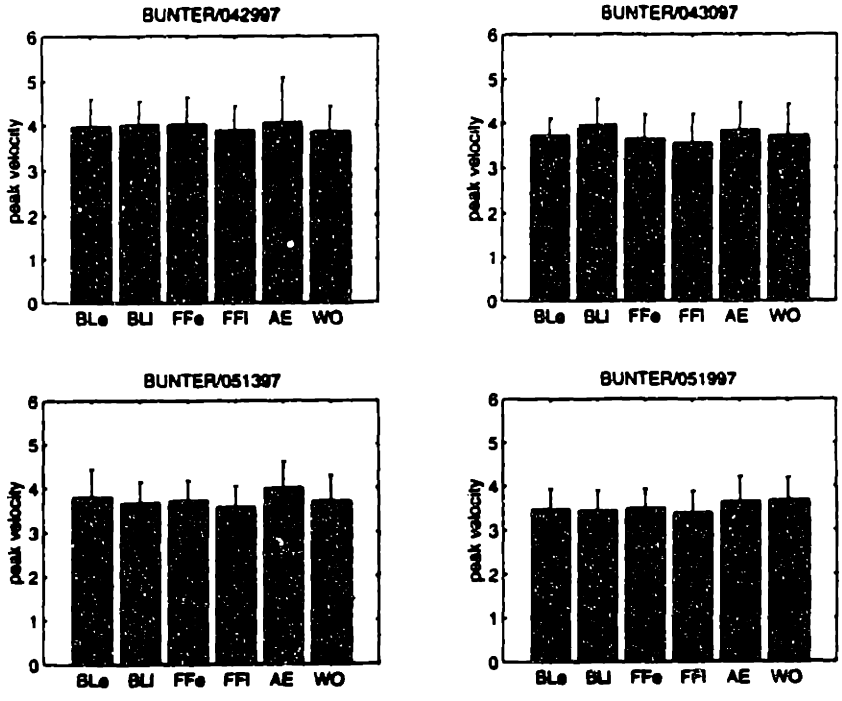

Figure 5.7 Peak velocities over the three behavioral epochs - monkey 1

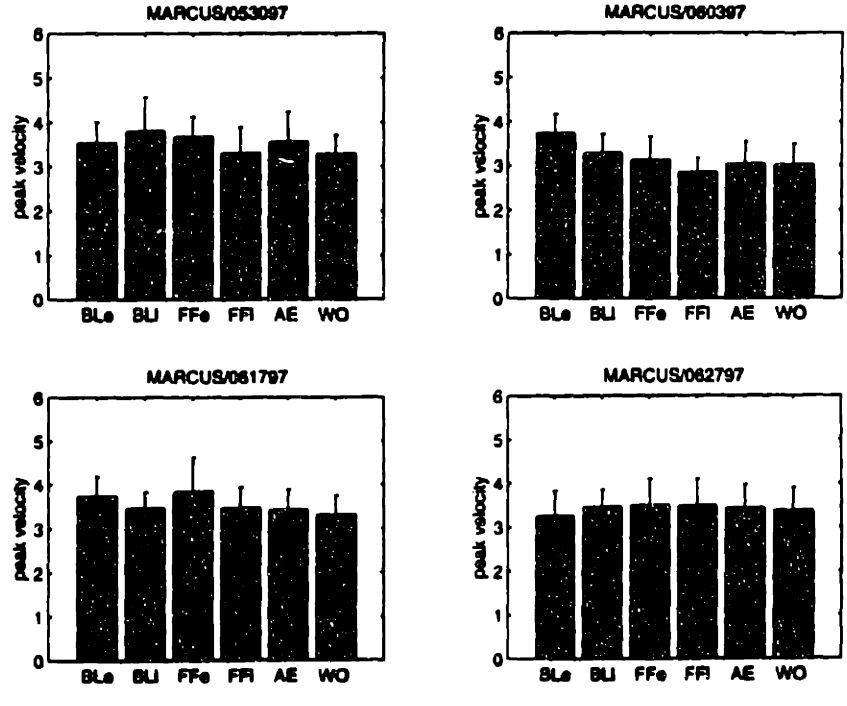

Figure 5.8 Peak velocities over the three behavioral epochs - monkey 2

differences between early performance in the force field and performance later in the epoch (FFl) after the monkey has had considerable practice. Although changes in peak movement velocity can be an indicator of motor learning, it appears that, in the present experimental paradigm, this parameter does not demonstrate the changes in performance seen in task execution.

The correlation coefficient represents a more sensitive measure of reaching trial performance. It is based not on a single peak velocity value, but on a scalar product between two velocity history vector series. For each reaching trial, a correlation coefficient is calculated. Differences between the unimodal velocity history seen in a well-trained movement in the baseline epoch and the multimodal velocity history seen in a perturbed movement during the force epoch are quantified by a lower correlation coefficient for the untrained trial.

Figure 5.9a-d illustrates the correlation coefficients calculated for experiment sessions over a two-week period. The sessions range from early in the monkey's exposure to the novel force field to late or increased exposure to the field. Correlation coefficient values are plotted along the ordinate; the abscissa is reaching trial number. Divisions between the three behavioral epochs are indicated by vertical lines. An exponential curve is fit to the data in each epoch and plotted. The fit acts like a filter, eliminating much of the variability in the data yet demonstrating performance trends.

Although there is some variability in the data, performance of the reaching task in the baseline epoch over all days is consistently high. Correlation coefficients exceed 0.9 for 88% of the trials in the epoch. An exponential curve fit to the data is essentially linear and flat. The monkey is clearly well-trained and performing the baseline task accurately and consistently.

Performance in the force field is markedly different. Consider Figure 5.9a - an experiment session early in exposure to the force field. Average performance in the force field epoch drops compared to the baseline case, and there is a significant increase in the scatter or variability of the data. The fitted curve shows a monotonic increase from a correlation coefficient approximately 0.80 to a plateau value of approximately 0.87. This increase suggests an improvement in performance with practice in the force field. Similar performance trends are seen in subsequent experiment sessions (Figure 5.9b-d). Note, however, that with increased exposure to the force field, the monkey achieves a plateau in fewer trials and the plateau itself trends to a higher performance level.

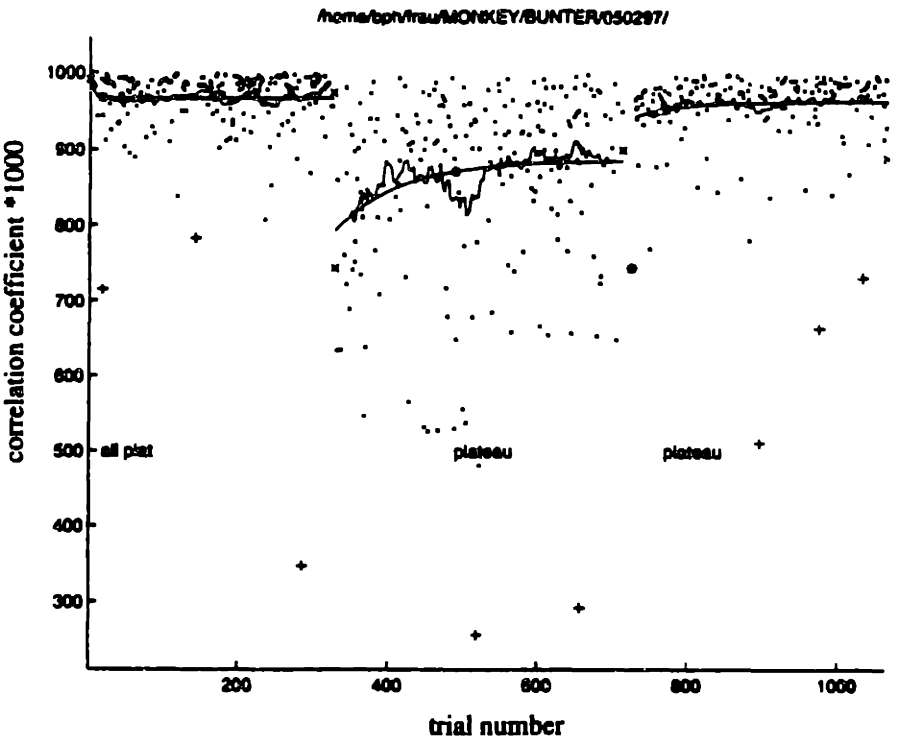

a) correlation coefficients for experiment session - early force field exposure

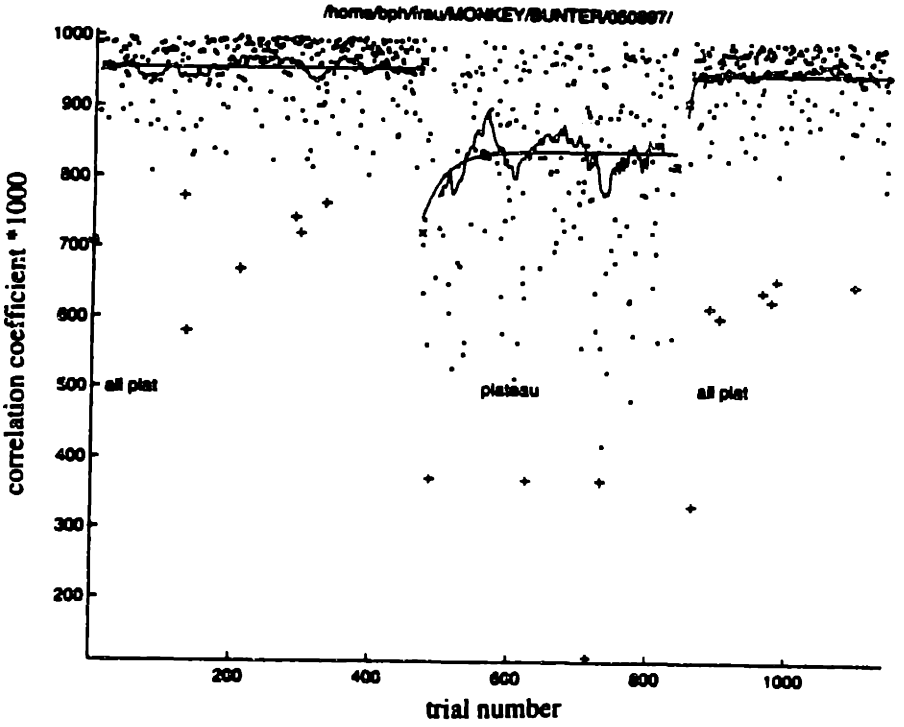

b) correlation coefficient for experiment session - mid force field exposure

Figure 5.9 Correlation coefficients for multiple experiment sessions over exposure to the counterclockwise force field

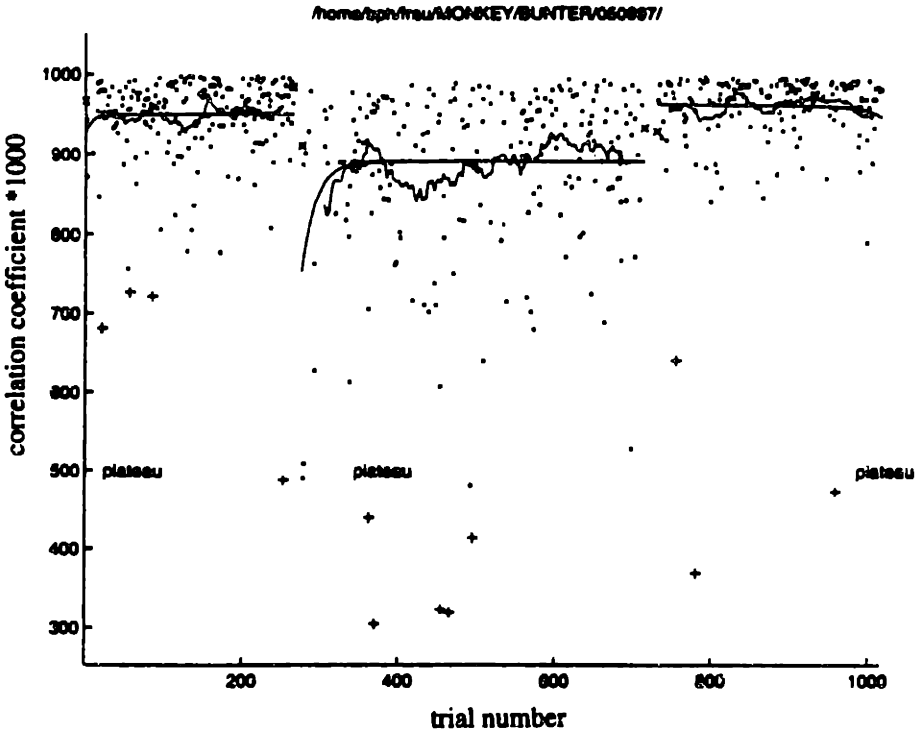

c) correlation coefficients for experiment session - mid force field exposure

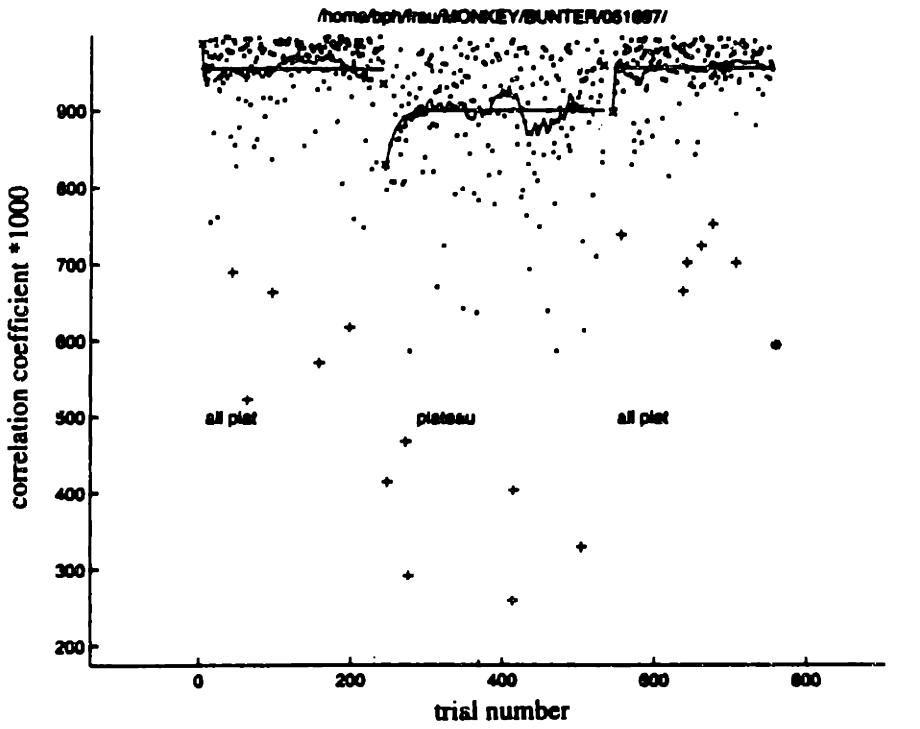

d) correlation coefficient for experiment session - late force field exposure

Figure 5.9 Correlation coefficients for multiple experiment sessions over exposure to the counterclockwise force field

The last behavioral epoch shown in the figure is the washout period. Average performance is similar to that seen in the baseline epoch - high coefficient values and reduced data scatter. In some of the plots, lower performance is seen early in the washout epoch. This reflects the aftereffects - the influence of the learned force field on the initial trials in the washout period.

5.1.2 Task performance across multiple days

The previous section demonstrated significant variation in task performance within a single experiment session. There is skilled performance in the baseline and washout epochs. With practice in the force field, performance transitions from less skilled to more skilled - an indication of motor learning. This performance trend in the force field is not static. It changes with increased exposure to the force field over multiple experiment sessions.

Figures 5.10 and 5.11 capture both the constancy and variability of performance for the two monkeys, respectively. In each figure, three plots are shown. The first demonstrates performance of the task in the baseline epoch; the second shows performance in the force field; the third, performance in the washout period. An ordinate point represents the mean of the correlation coefficients for all trials in the given behavioral epoch in a single experiment session. This is plotted against the number of experiment sessions. A second-order polynomial is fit to the data to demonstrate the change in mean correlation coefficient across sessions exposed to a given force field. Data is shown for each monkey working first in a clockwise force field over multiple sessions then in the counterclockwise force field over multiple sessions.

The skilled behavior of both monkeys in the baseline epoch is evident in data that demonstrate consistently high mean correlation coefficient values and low variances (Figure 5.10a and 5.11a). There is no significant change in performance within this epoch over weeks of experimentation. Nor is there change in baseline performance as the perturbing force field changes from a clockwise field to a counterclockwise field. Clearly, both monkeys are well-trained in the baseline task.

Figures 5.10b and 5.11b demonstrate for the two monkeys changes in performance during the force epoch with increased exposure to the force fields. Mean performance is low when the monkeys are initially exposed to the clockwise field. With daily exposure to the field, mean performance improves. However, after several weeks, a plateau in performance is reached.

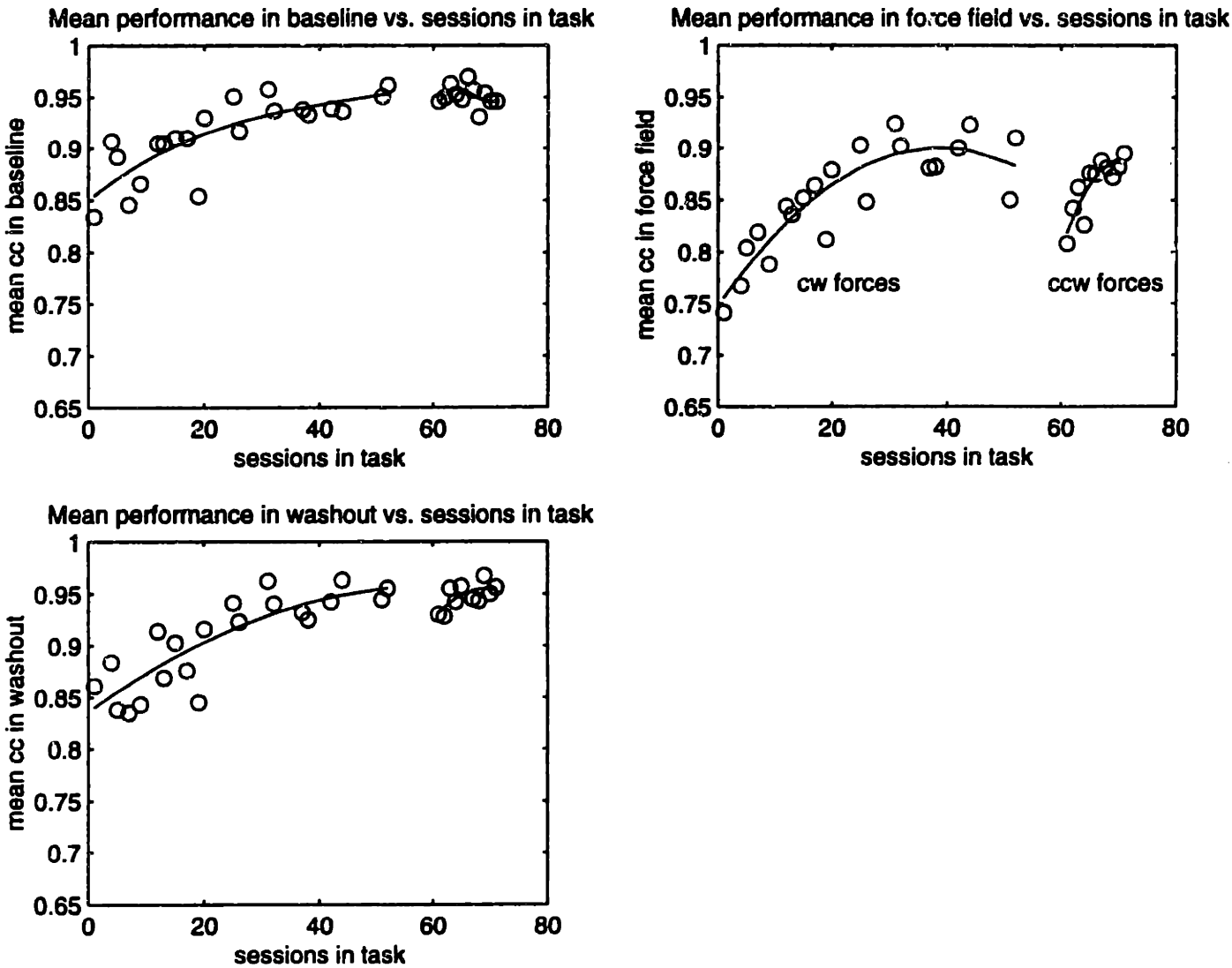

Figure 5.10 Average task performance for monkey 1 - mean correlation coefficients in baseline, force field, and washout epochs versus sessions in field

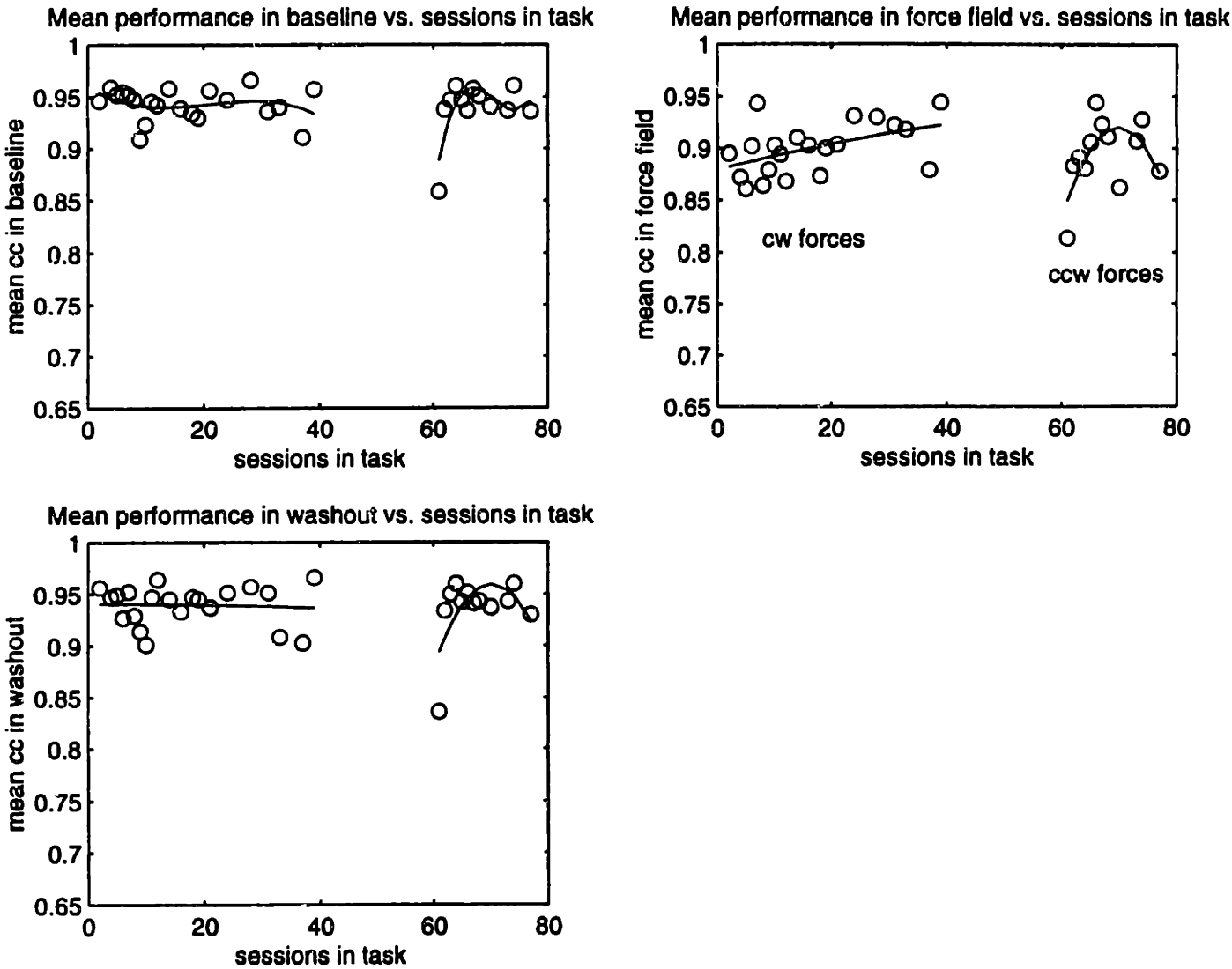

Figure 5.11 Average task performance for monkey 2 - mean correlation coefficients in baseline, force field, and washout epochs versus sessions in field

Continued exposure to the clockwise field does not lead to an improvement in task execution. The monkey has learned the reaching task in the clockwise field to its best ability. At this point, the counterclockwise force field is introduced. Mean performance in this novel force field drops to levels comparable to those seen during early exposure to the clockwise forces. Again, performance improves with increased exposure to the counterclockwise field until a plateau level is reached. Note the higher rate of improvement seen in both monkeys for performance in the second force field. At plateau performance, the monkeys are well-trained in the counterclockwise force field.

Execution of the reaching task in the washout epoch is summarized in Figures 5.10c and 5.11c. Performance is again at high mean levels with smaller variances. This is comparable to that seen in the baseline task.

The psychophysical data demonstrates changes in performance of the reaching task for the two monkeys both across force conditions and over time. The monkeys are skilled in executing the task in the baseline period. The application of a viscous, curl force field creates the environment for motor learning. Within a day's experiment session, performance in the novel field is initially low, but improves with practice. Hand paths become straighter; velocity histories become smoother. Such behavior is the hallmark of motor skill acquisition through motor leaning. Some aspect of the learned skill is retained over time as mean performance in the force field increases with increased exposure to the field over successive experiment sessions. Finally, performance in the force epoch reaches a plateau; the monkey is executing the task to its best ability.

5.2 Evaluation of cell activity

The purpose of cell data analysis is to characterize changes in cell activity both across behavioral epochs within an experiment session and over multiple days of executing the motor learning task. In this work, the activity of 185 cells was recorded. For each cell, data analysis is a multistep process - isolate an individual cell's activity from the continuous stream of voltage data recorded by an electrode, characterize and quantify the activity across the behavioral epochs of the experimental paradigm, identify changes in activity that relate to changes in task performance, demonstrate the significance of these changes through statistical analysis.

5.2.1 Cluster analysis

The first step in the analysis process, isolating individual cell activity, is perhaps the most critical. The method used to isolate cell activity through cluster analysis was described in the previous chapter. The goal of cluster analysis is to ensure that each set of spike events considered as an individual unit in subsequent analyses accurately represents the full activity of a single, stable cell. Waveform shape, the shape of a neuron's action potential as recorded by the electrode, is the basis for evaluating accurate single-cell isolation and stability. The waveform shape for an individual cell must be well defined, unique, and constant over the duration of the experiment session. A set of spike events with multiple shapes suggests that the activity of more than one cell is included. This data set is then reanalyzed to separate the multiple waveforms and thereby separate the activities of multiple cells. Waveform shapes that change significantly over the course of an experiment session suggest a lack of recording stability - relative movement between the electrode and cortex that results in the loss of one cell and the acquisition of another. Such cell data cannot be analyzed further.

The activity of all cells recorded in this work was analyzed to ensure the accuracy of single cell isolation. Waveform shapes recorded during early and late periods of each behavioral epoch were plotted and compared. Only those datasets with unique and constant waveforms were considered for subsequent analyses. Figures 5.12 and 5.13 illustrate typical waveform sets representing the activity of two individual cells. In each plot, the ordinate is a normalized waveform amplitude measure and the abscissa is a normalized time measure. Shapes recorded early and late in the a) baseline, b) force field, and c) washout epochs are plotted. As can be seen for both cells, there is minimal variation in waveform shapes across the behavioral epochs.

5.2.2 Raster plots and histograms

Once single-cell activity is defined, it is necessary to quantify and display the data in a manner consistent with the experiment paradigm. The two primary treatments defined in the psychophysical component of the experiment are direction of movement to the peripheral targets and external force environment. Cell activity, then, is presented as a function of these treatments.

Single cell activity in its most basic form is given by raster plots and histograms. Both graphical forms demonstrate the temporal nature of cell activity during the reaching task.

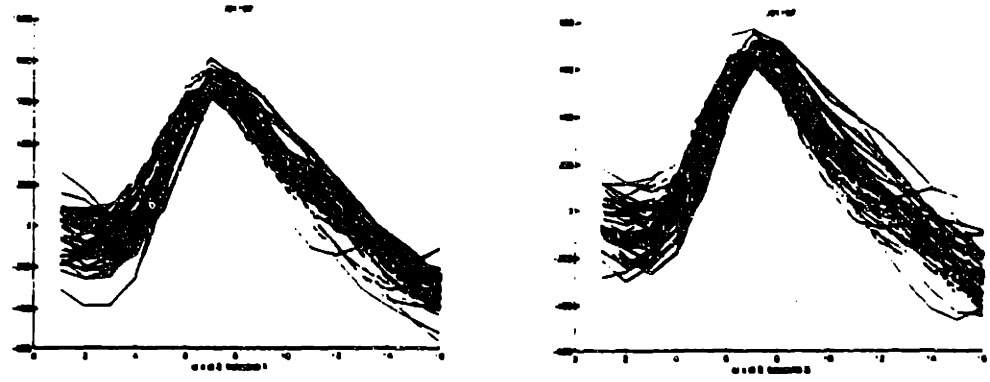

a) Waveforms in baseline epoch

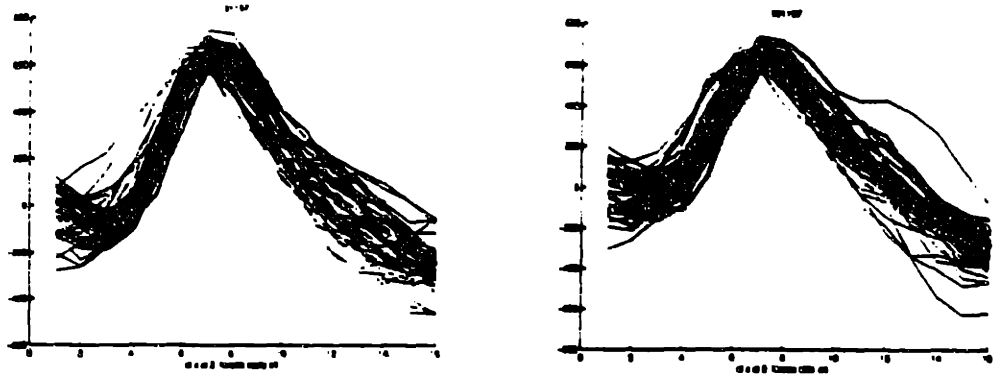

b) Waveforms in force field epoch

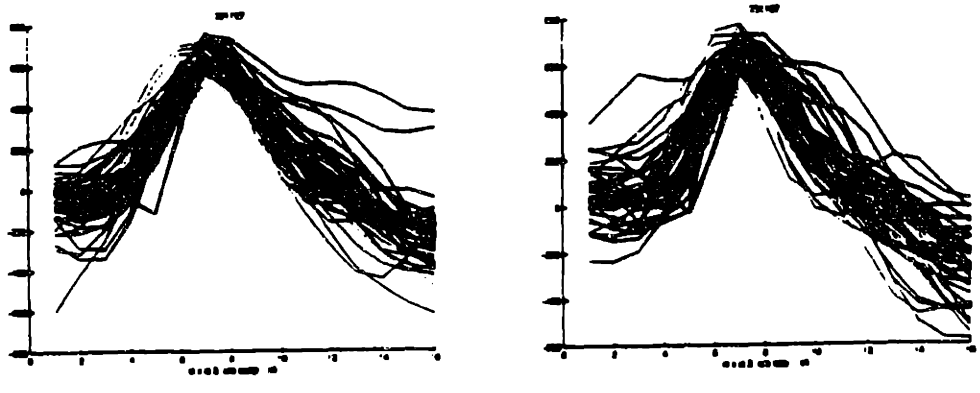

c) Waveforms in washout epoch

Figure 5.12 Cell waveforms demonstrate stability of recording across behavioral epochs - cell 1

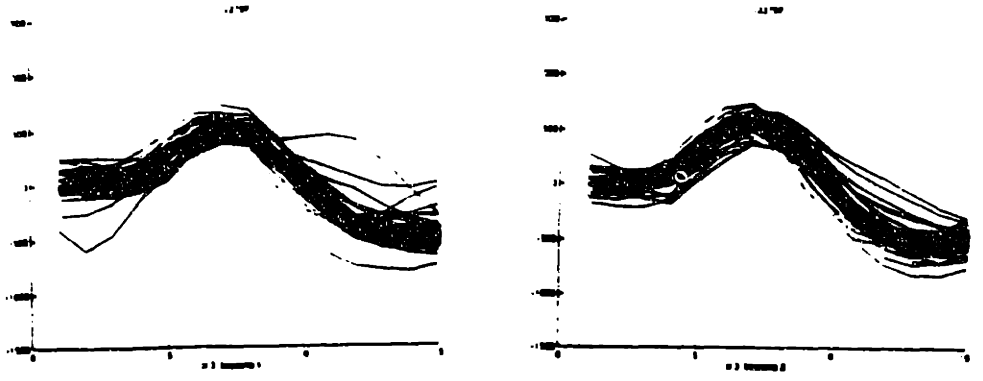

a) Waveforms in baseline epoch

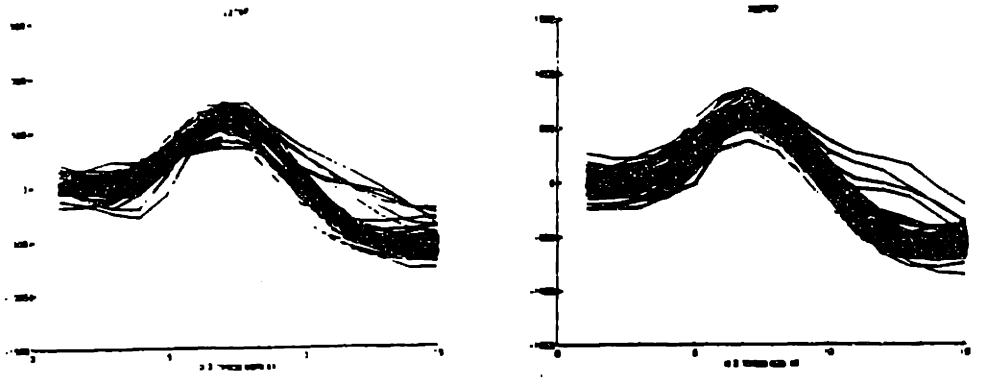

b) Waveforms in force field epoch

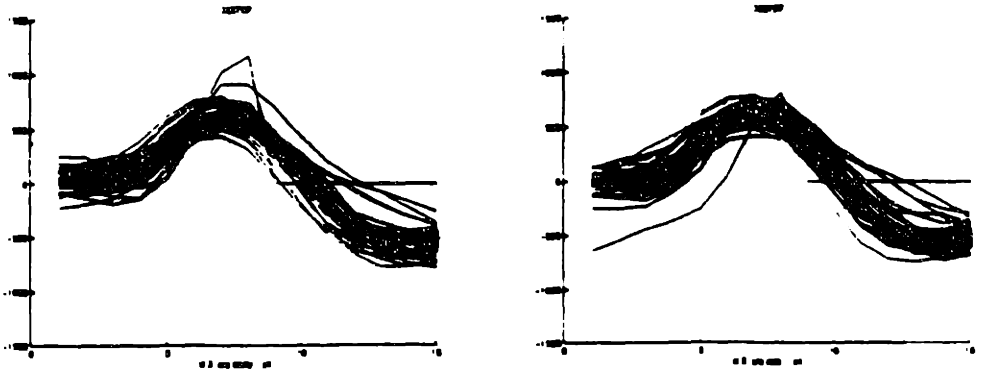

c) Waveforms in washout epoch

Figure 5.13 Cell waveforms demonstrate stability of recording across behavioral epochs - cell 2

Raster plots show the time sequence of individual spike events for a set of individual reaching trials. In a histogram analysis, spike activity in each of multiple reaching trials is first temporally aligned with a common trial event. The timeline is divided into number of intervals or bins. The histograms display the sum across multiple trials of spike activity within each bin.

Raster plots and histograms can be drawn such that cell activity for reaching movements to each target direction is individually displayed. Separate plots are then made for the three behavioral epochs. Figures 5.14 and 5.15 show the activity of two cells in both raster plot (top) and histogram (bottom) formats for a) baseline epoch, b) force field, and c) washout periods. The location on the figure of each raster plot/histogram indicates the corresponding movement direction. Plots located to the left of center show cell activity for reaching movements to the left (180°) target; plots down from center correspond to movements toward the target at 270°.

Even in these basic graphical forms, trends in cell activity are seen. Consider the cell in Figure 5.14. In the baseline epoch (Figure 5.14a), the cell is most active during the perimovement and movement periods. There is minimal activity in the center hold and delay times and low activity during the peripheral target hold time following movement. The frequency of cell activity during movement varies as a function of reaching movement direction. The cell fires at a higher frequency for reaching movements in directions 135° to 225°. Cell activity in the force field epoch (Figure 5.14b) is similar to that seen in the baseline period. Activity is limited primarily to the movement period; average firing rate for the cell is about the same. Cell activity again varies as a function of movement direction. Note, however, that maximum activity seems to have shifted to movements in directions 45° to 180°. Activity in the washout period (Figure 5.14c) is similar in all respects to the activity seen in the baseline epoch. The effect of the experimental paradigm on this cell's activity seems to be a shift in preferred movement direction from baseline to force field periods and from force field to washout periods.

The cell in Figure 5.15 shows different trends. Average activity in the baseline period (Figure 5.15a) is high with most activity occurring during the perimovement, movement and peripheral target hold periods. There appears to be some modulation of activity with movement direction, though the modulation is not great. By comparison, average cell activity in the force field epoch (Figure 5.15b) is much lower, and there is a clear direction of maximum cell activity.

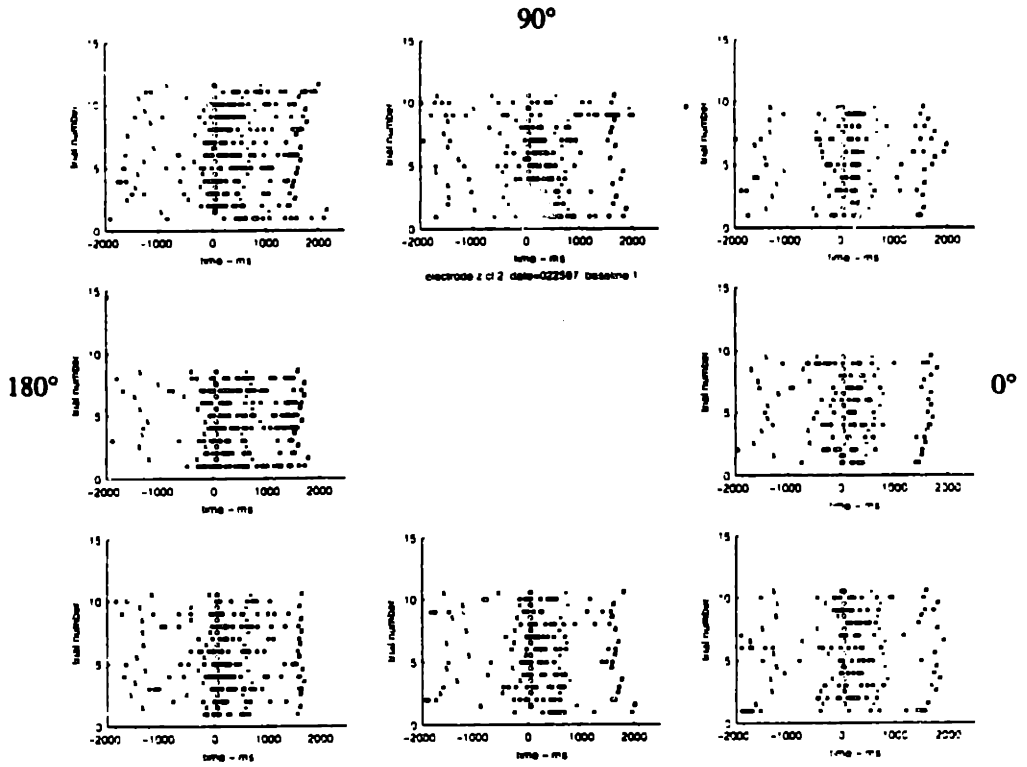

a) raster plots

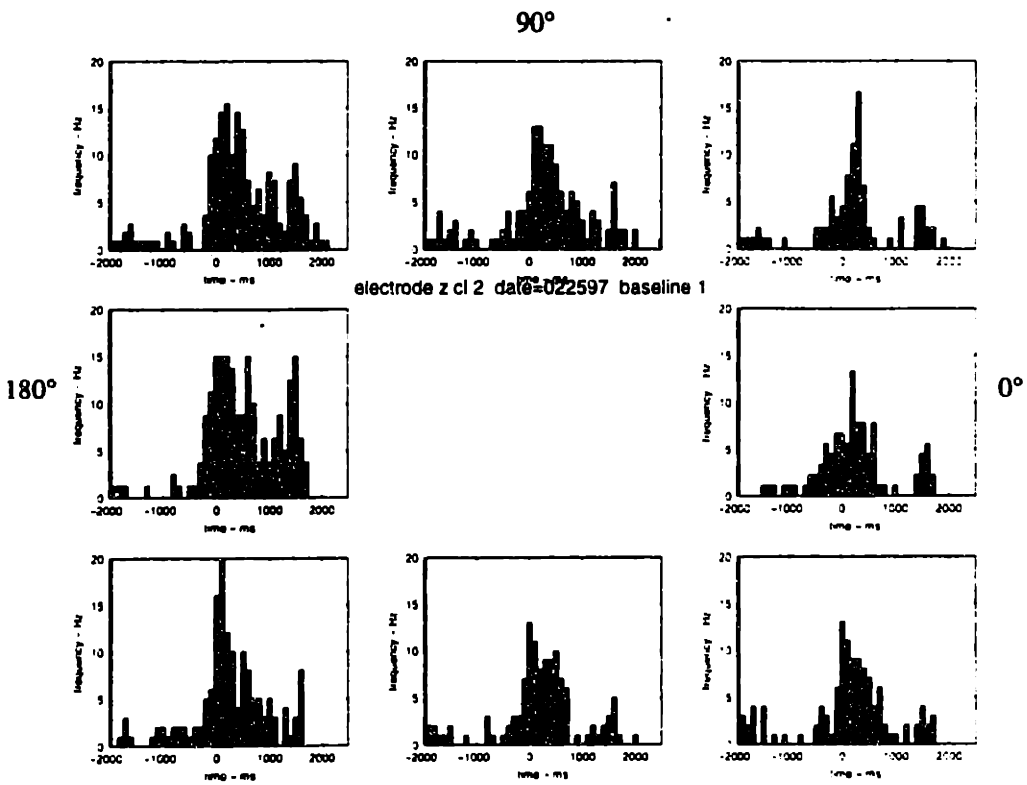

b) histograms

Figure 5.14a Raster plots and histograms for cell 1 - baseline epoch

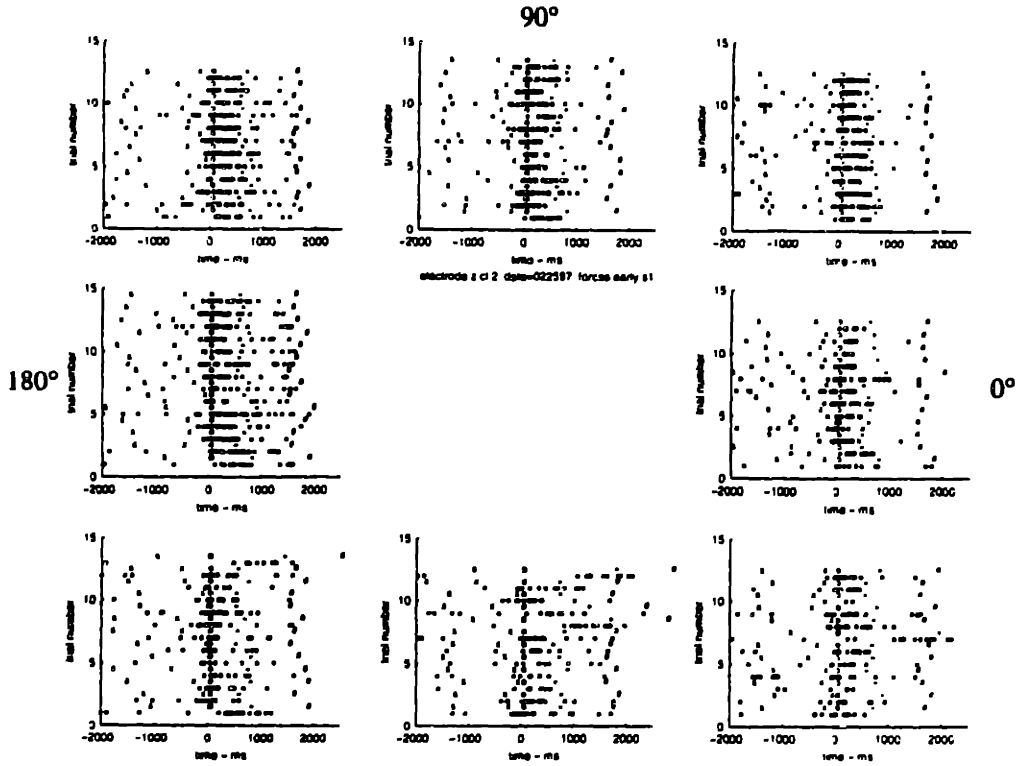

a) raster plots

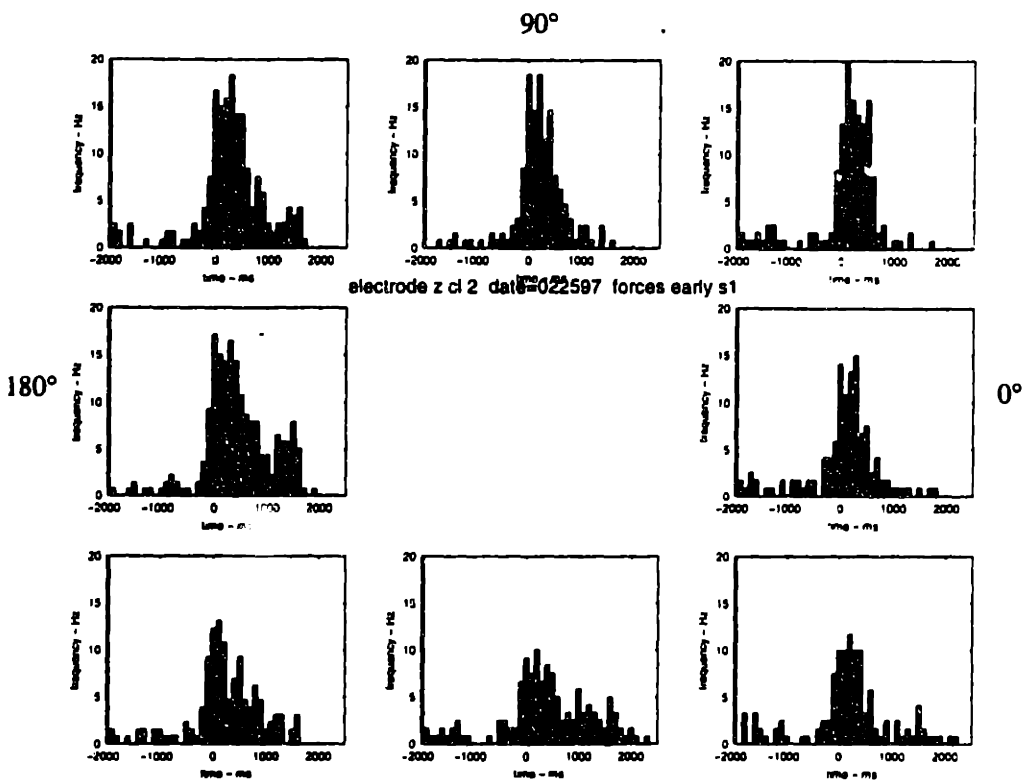

b) histograms

Figure 5.14b Raster plots and histograms for cell 1 - force field epoch

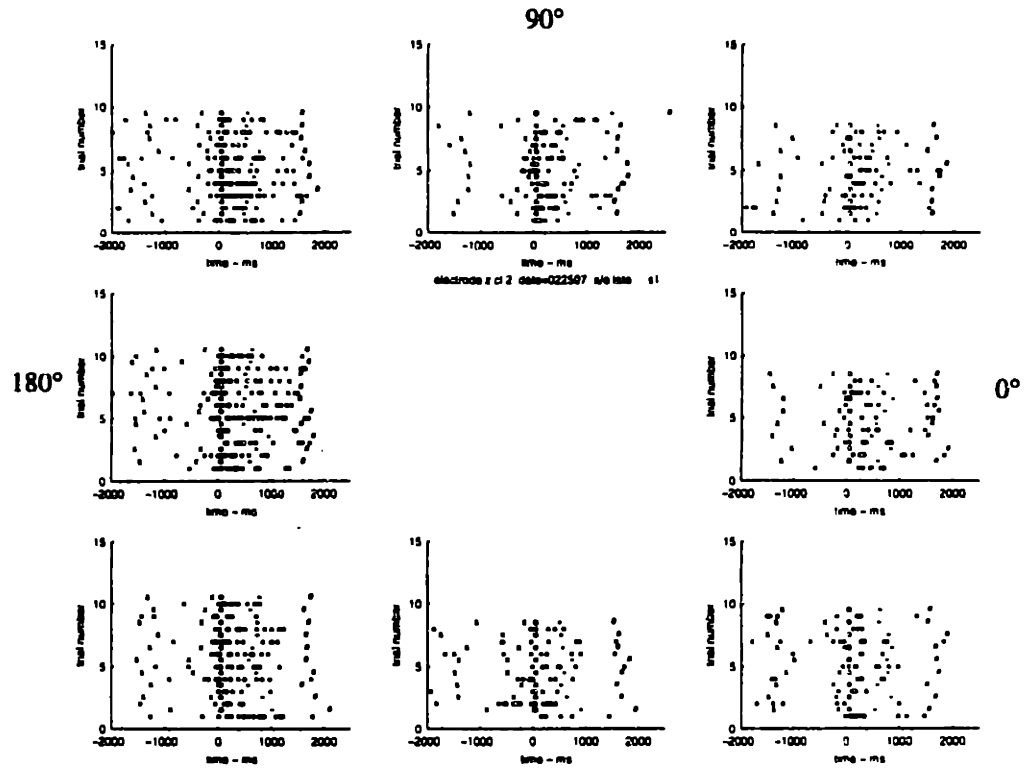

a) raster plots

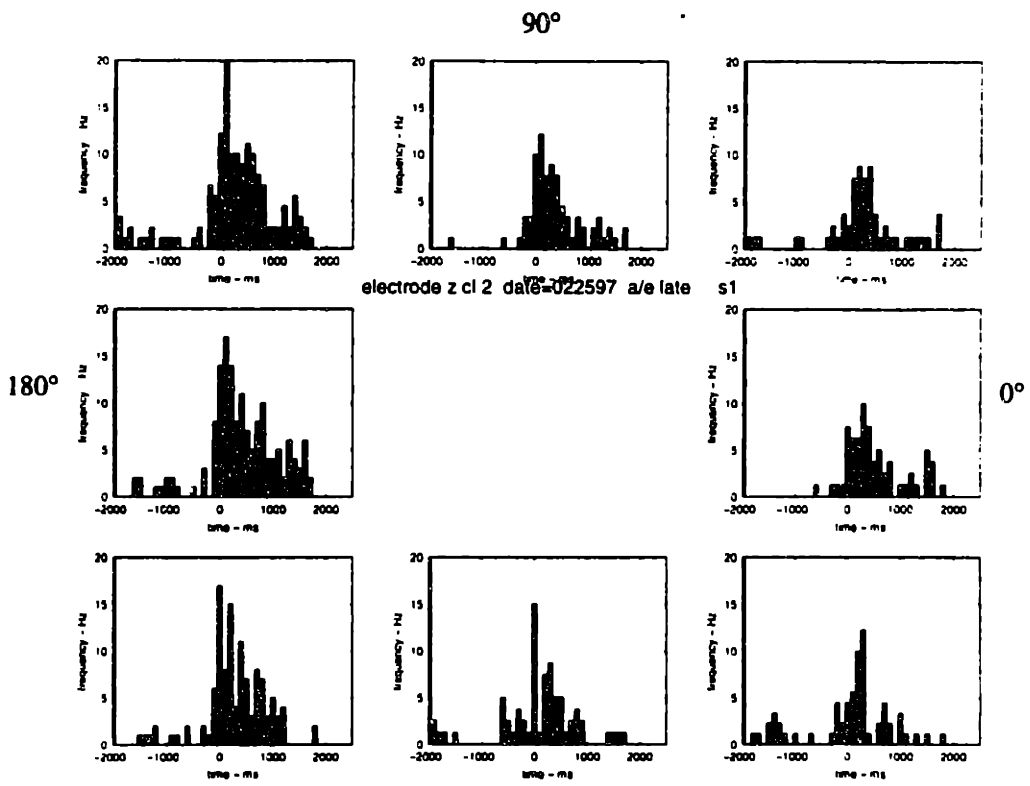

b) histograms

Figure 5.14c Raster plots and histograms for cell 1 - washout epoch

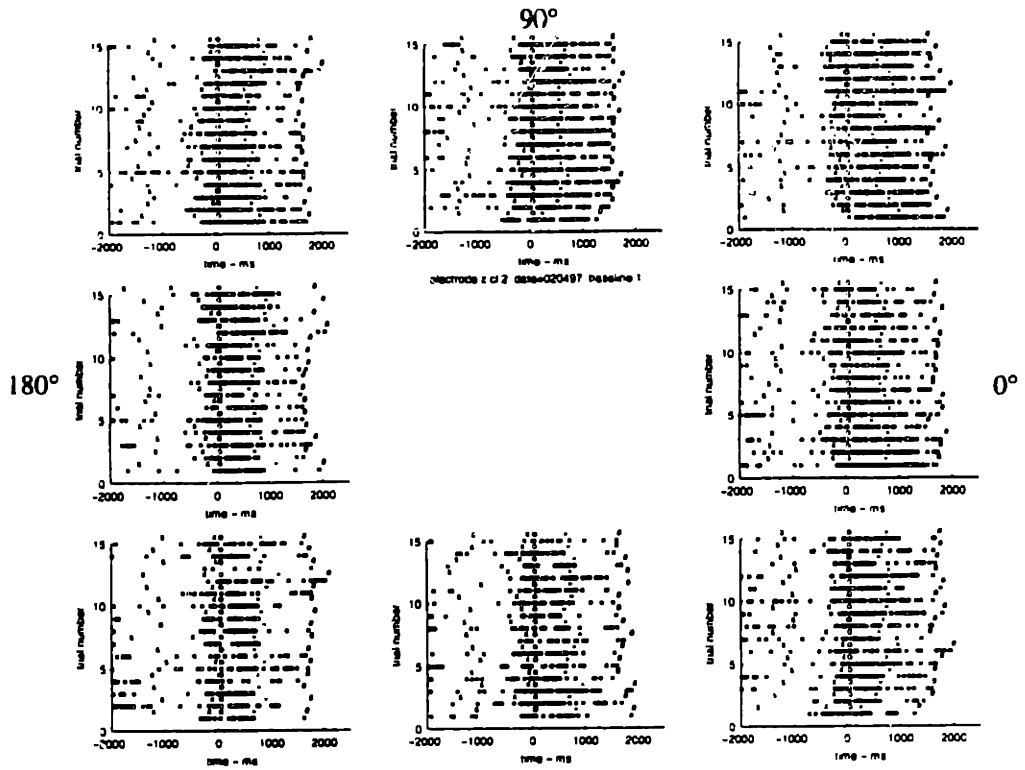

a) raster plots

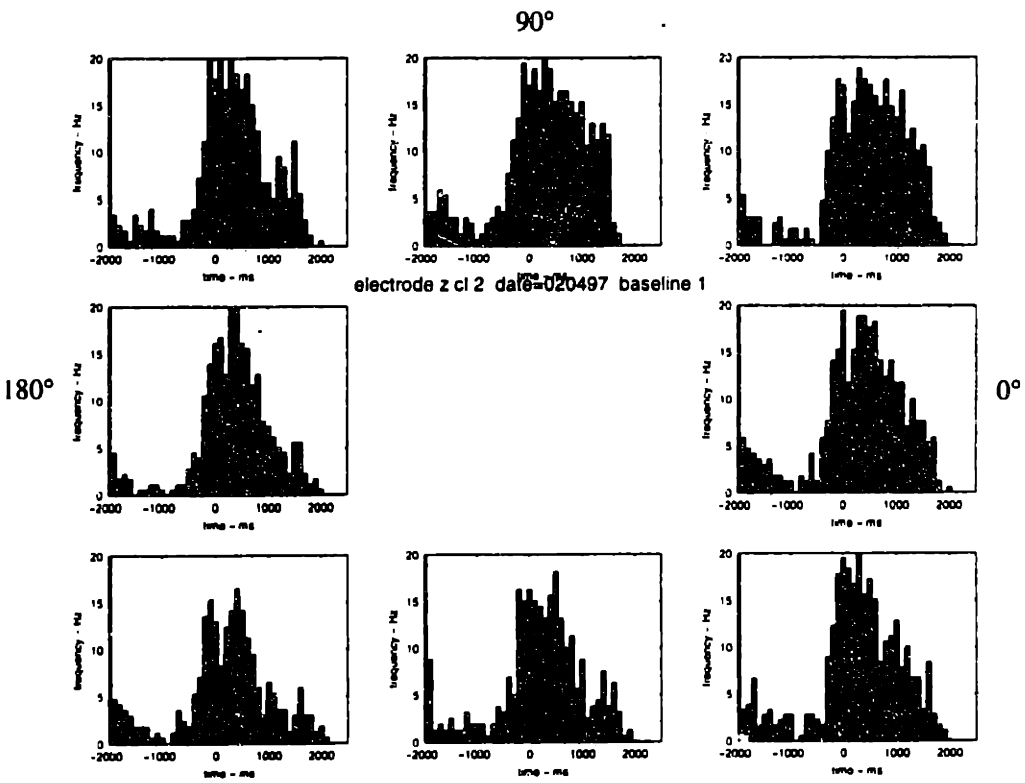

b) histograms

Figure 5.15a Raster plots and histograms for cell 2 - baseline epoch

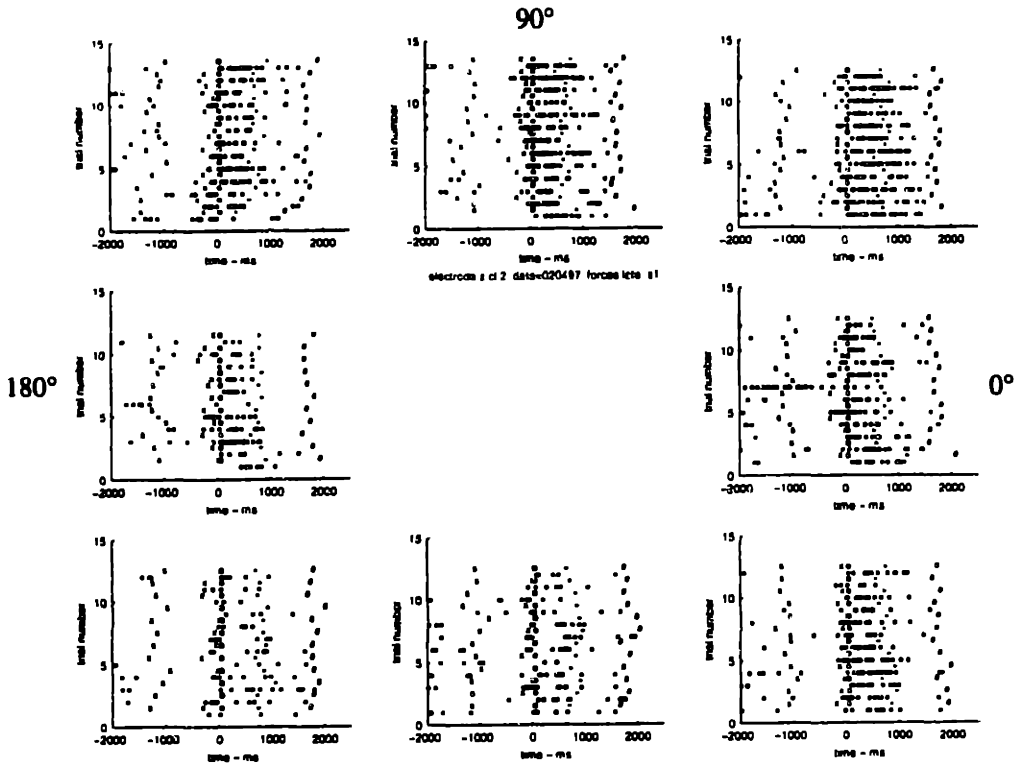

a) raster plots

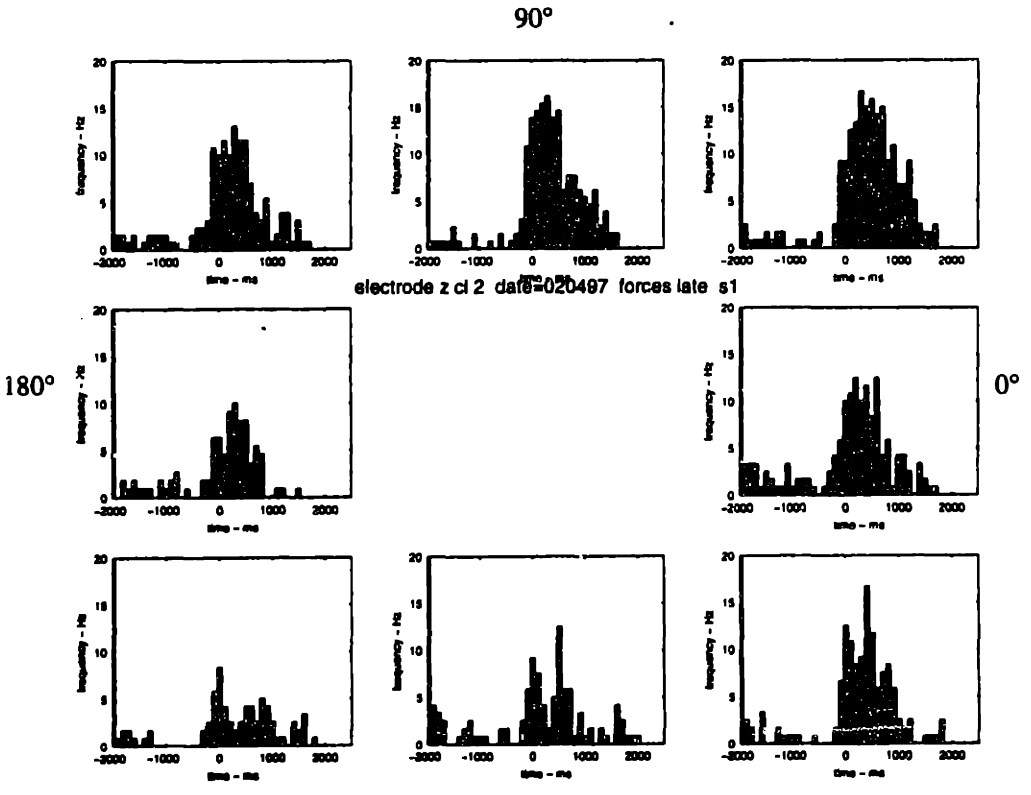

b) histograms

Figure 5.15b Raster plots and histograms for cell 2 - force field epoch

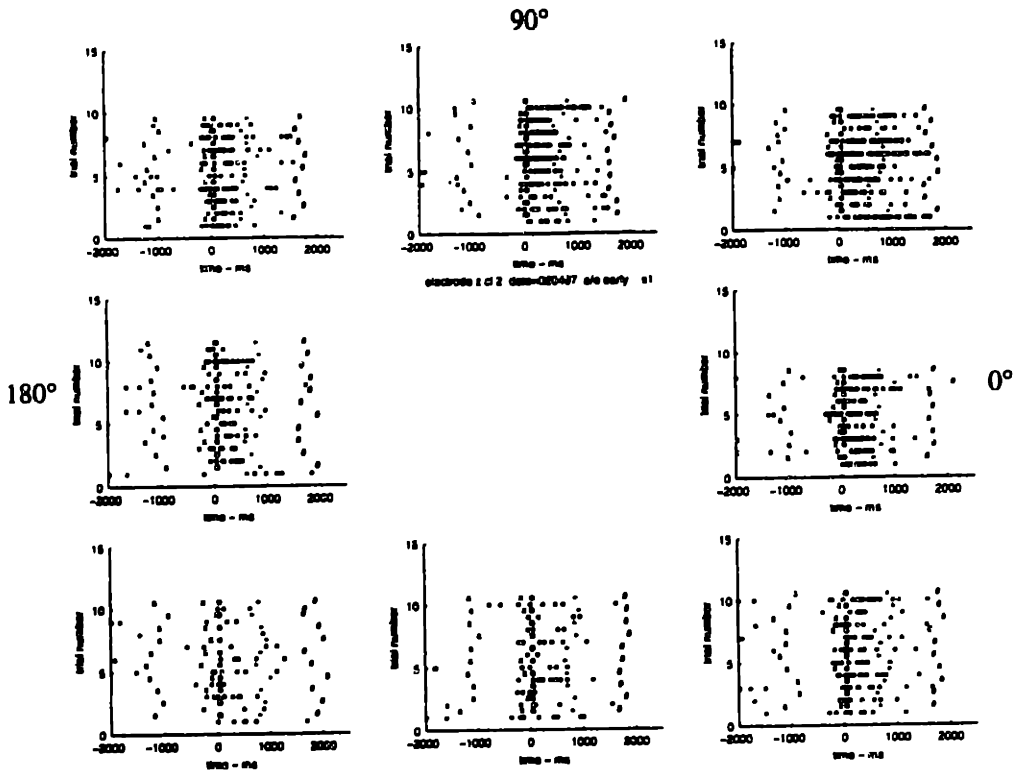

a) raster plots

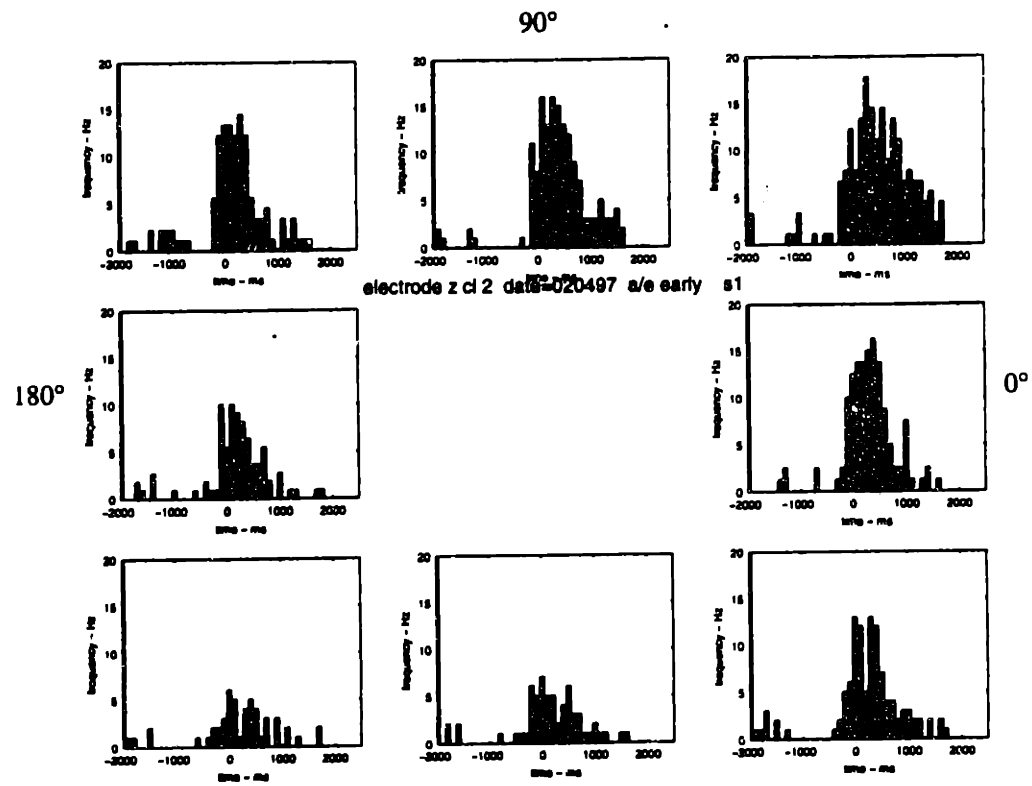

b) histograms

Figure 5.15c Raster plots and histograms for cell 2 - washout epoch

This trend persists in the washout period (Figure 5.15c). For this cell, then, the change in cell behavior across the force epochs is marked by a decrease in activity post baseline epoch.

5.2.3 Tuning curves

The raster plots and histograms provide evidence that executing the experimental paradigm has a physiological effect. There are measurable changes in cell activity within the task; however, the plots themselves do not adequately describe the nature of the change. It is necessary to describe cell activity in a more quantitative form. Consider the recorded data. For each behavioral epoch, multiple reaching movements are made to targets in eight directions. Within a reaching trial, time intervals of interest are defined - center hold time (cht), delay time (dt), movement time (mt), peripheral target hold time (tht). For the activity of a given cell, an average firing rate is calculated for each interval by counting the number of spikes recorded during the interval and dividing by the interval period. This calculation is repeated for all reaching trials. The result is a sampling of average firing rates in Hertz calculated as a function of time interval and movement direction. The mean and standard deviation of each sample are calculated and plotted as a function of movement direction. The resulting function is called a tuning curve. This analysis process is applied to cell activity in the three behavioral epochs.

Figures 5.16 and 5.17 are examples of the series of graphs that result from such an analysis. The data displayed are for the same two cells shown in the previous figures and are presented for the a) baseline, b) force field, and c) washout epochs on successive pages. The four graphs shown for each epoch correspond to cell activity during the center hold time, delay time, movement time, and peripheral target hold time periods. To illustrate change in cell activity with movement direction, a cosine curve is fit to the mean data and plotted.

Consider the upper left plots in Figure 5.16a-c - cell activity during the center hold time period. The center hold time is a period of inactivity for the monkey. Movements are neither being planned nor made. This condition is constant over all behavioral epochs; there is no task-related reason for cell activity to change during this time period. Uniform cell activity during this epoch suggests cell recording stability. As seen in the graphs, activity during the center hold period is constant over the three behavioral epochs.

There is no movement during the delay time; however, since the intended target is displayed, planning of the impending movement can be made. Cell activity during this period may relate to movement planning and could be sensitive to changes in the dynamic environment in which

a) center hold time

b) delay time

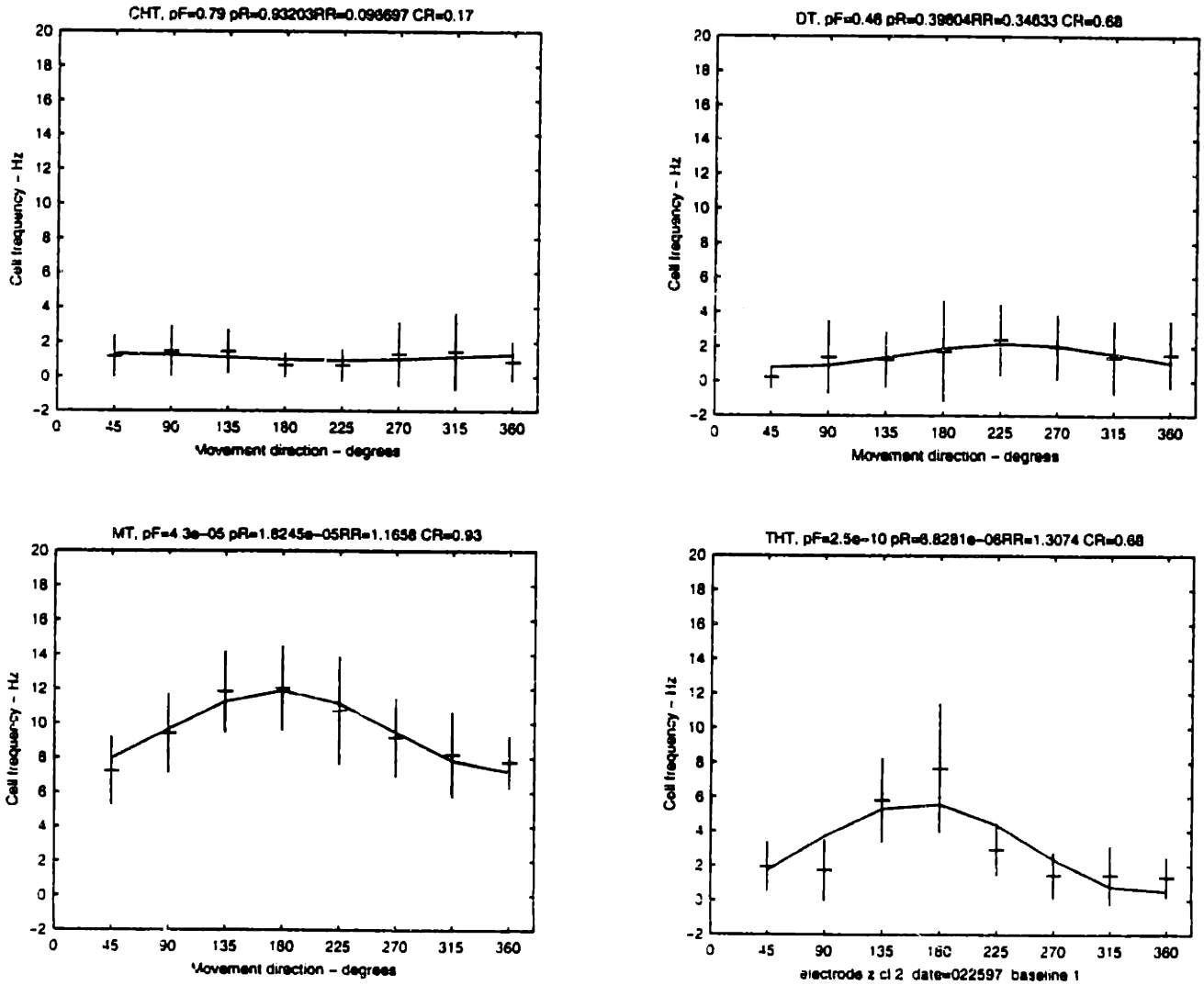

c) movement time

d) target hold time

Figure 5.16a Tuning curves showing cell 1 activity during baseline epoch as function of movement direction for a) center hold time, b) delay time, c) movement time, d) peripheral target hold time

a) center hold time

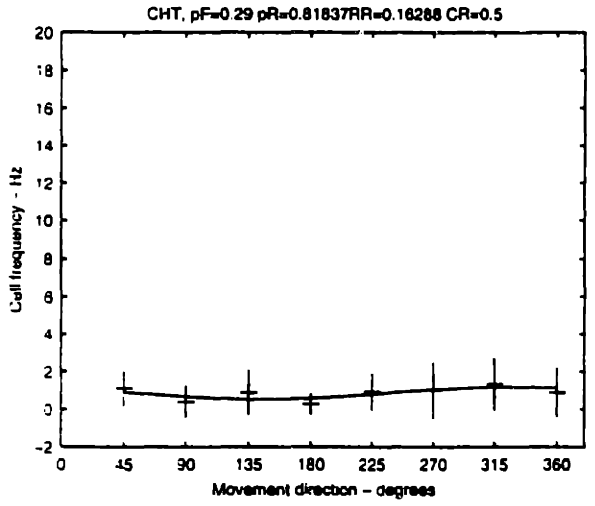

b) delay time

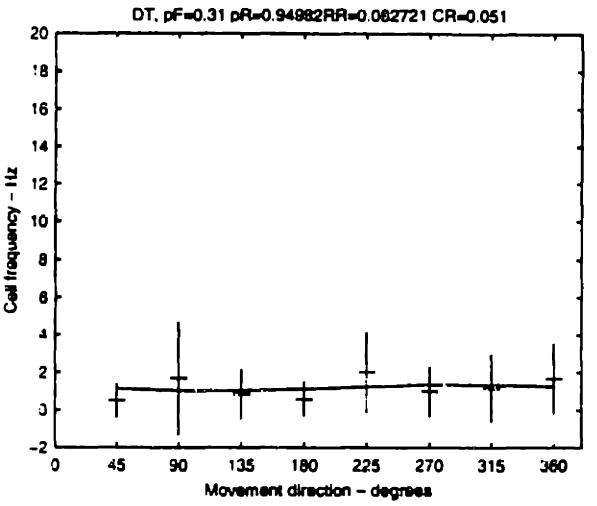

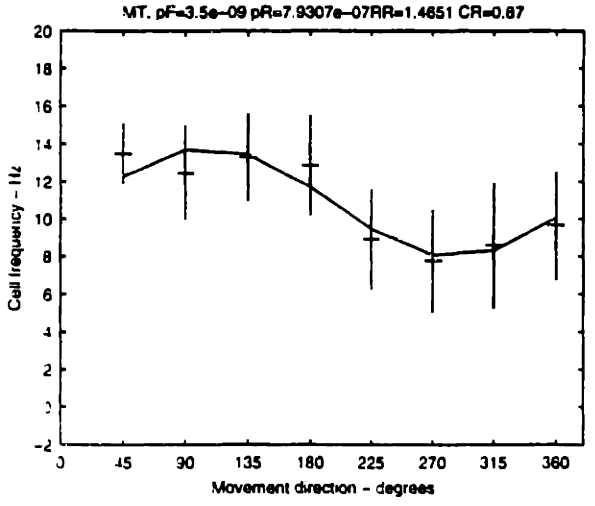

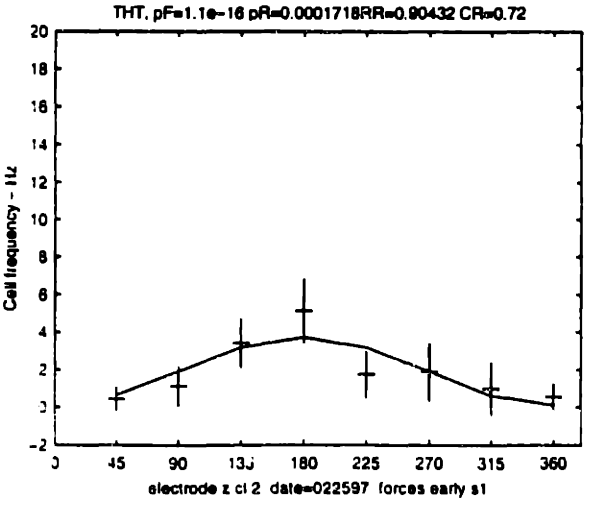

c) movement time

d) target hold time

Figure 5.16b Tuning curves showing cell 1 activity during force field epoch as function of movement direction for a) center hold time, b) delay time, c) movement time, d) peripheral target hold time

a) center hold time

b) delay time

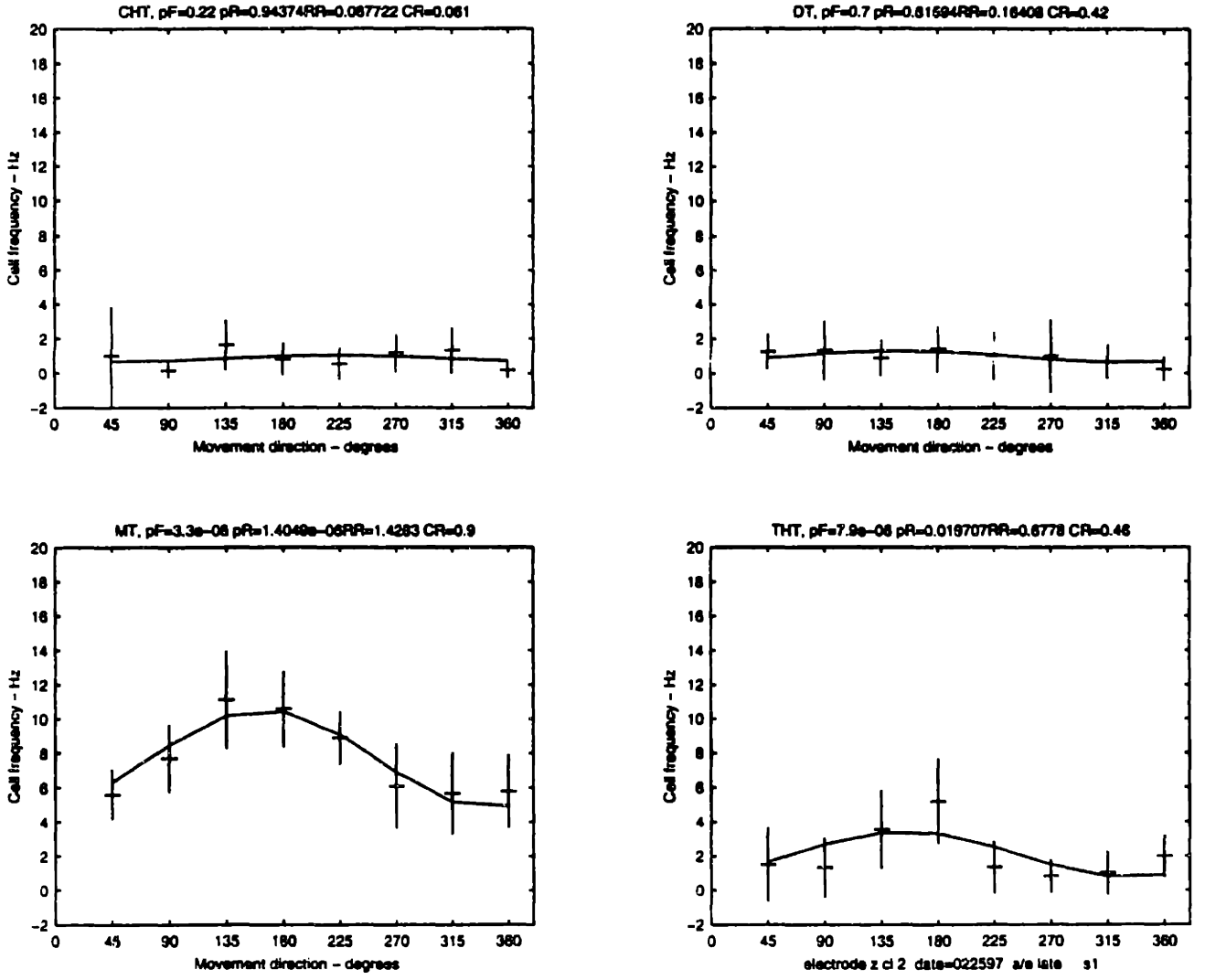

c) movement time

d) target hold time

Figure 5.16c Tuning curves showing cell 1 activity during washout epoch as function of movement direction for a) center hold time, b) delay time, c) movement time, d) peripheral target hold time

the task is executed and the effects of motor learning. For the cell data shown in the upper right plot in Figure 5.16a-c, no significant modulation in activity is seen within the delay period for any behavioral epoch. The minimal cell activity exhibited during the center hold and delay times is consistent with the observations of the raster plots/histograms of Figure 5.14.

As seen in the lower left plots, cell activity is highest during movement time. This period is defined as the interval from 200ms prior to arm movement onset to end of movement in the peripheral target. Activity is broadly tuned with movement direction, displaying a direction of peak activity and a smooth decrease in activity for movements in other directions. Note that although the average cell firing rate across the behavior epochs remains constant at approximately 8-10Hz and the modulation of activity about the average (dynamic range) is about 4Hz, the preferred direction of activity appears to shift from near 180° in the baseline, to near 100° in the force field, then back to 180° in the washout period. These observations quantify in a more specific manner the trends seen in the raster plots and histograms.

Figure 5.17a-c shows activity data for a second cell in the same format. As with the previous cell, activity during the center hold and delay periods is low for all three behavioral epochs and shows little modulation with movement direction. For the baseline epoch, there is significant activity during both the movement time and peripheral target hold time (Figure 5.17a). Activity during movement is modulated by movement direction, but the modulation is not great. Activity in the target hold time shows significant modulation with direction and is maximum when the monkey holds in the target at 90°. Within the force field epoch (Figure 5.17b), average activities during movement and target hold times drop. Compared to the baseline epoch, modulation of activity as a function of direction during the movement time is greater in the force epoch. Activity in the washout period (Figure 5.17c) is similar to that seen in the force field. Again, these results are suggested by the raster plot and histograms of Figure 5.15.

5.2.4 Statistical analysis

The tuning curves of the previous figures demonstrate cell activity over behavioral epochs in a manner more quantitative than a raster plot or histogram presentation. The nature of activity change is more apparent. To confirm trends seen in the plots, statistical analyses are conducted. The methodology was described previously. Cell activity within each behavioral epoch is first assessed. Modulation in activity with movement direction and the significance of

a) center hold time

b) delay time

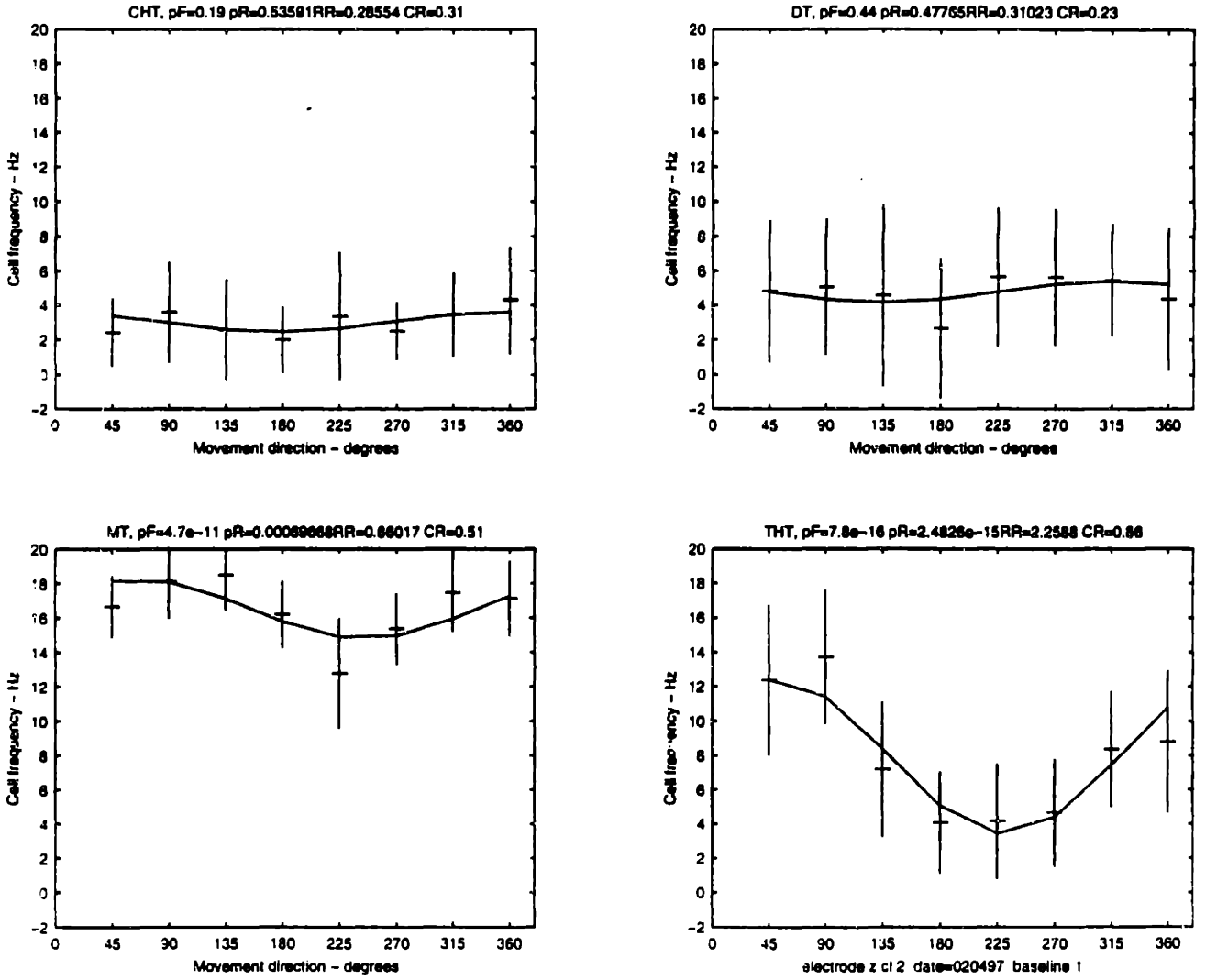

c) movement time

d) target hold time

Figure 5.1 a Tuning curves showing cell 2 activity during baseline epoch as function of movement direction for a) center hold time, b) delay time, c) movement time, d) peripheral target hold time

a) center hold time

b) delay time

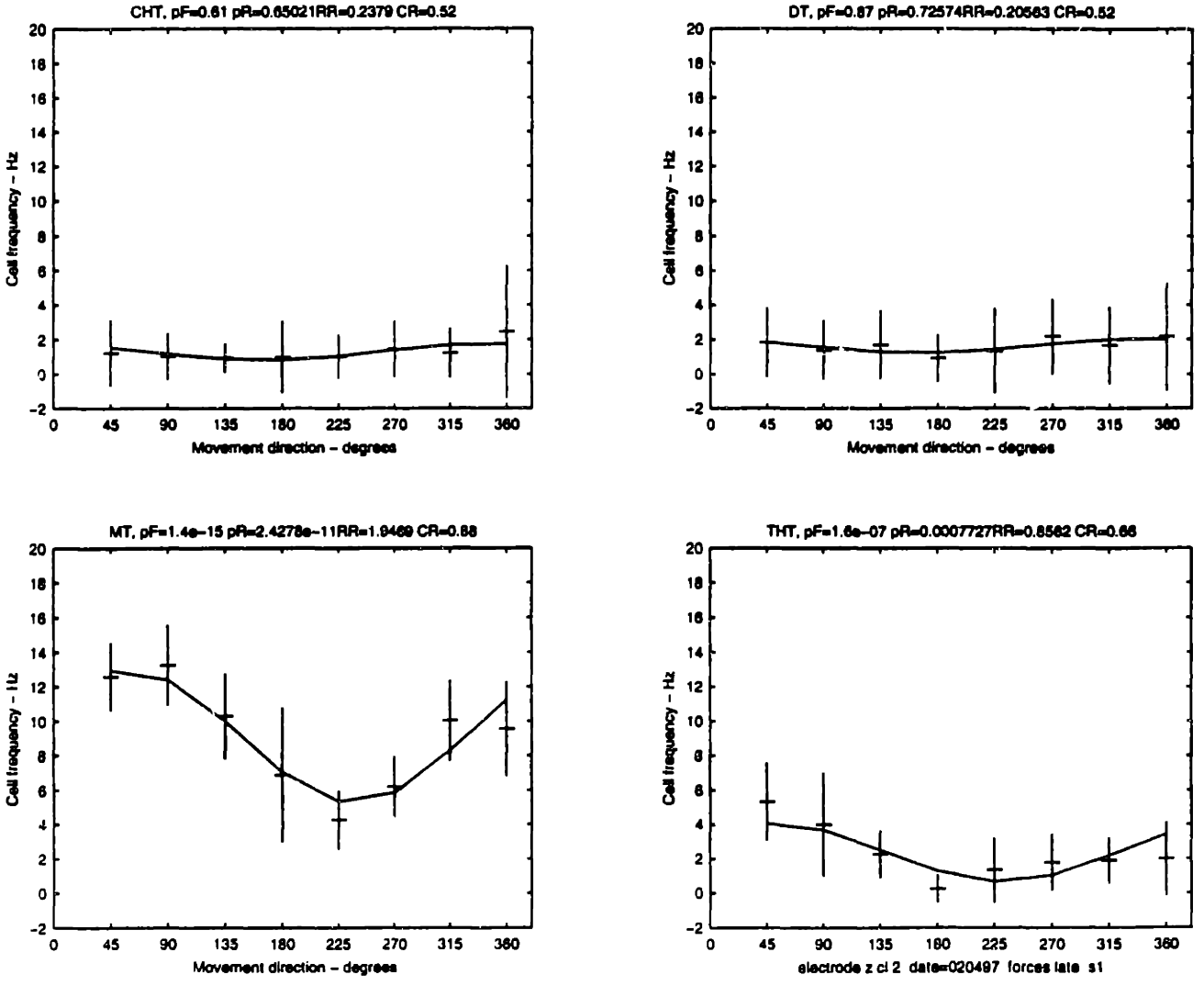

c) movement time

d) target hold time

Figure 5.17b Tuning curves showing cell 2 activity during force field epoch as function of movement direction for a) center hold time, b) delay time, c) movement time, d) peripheral target hold time

a) center hold time

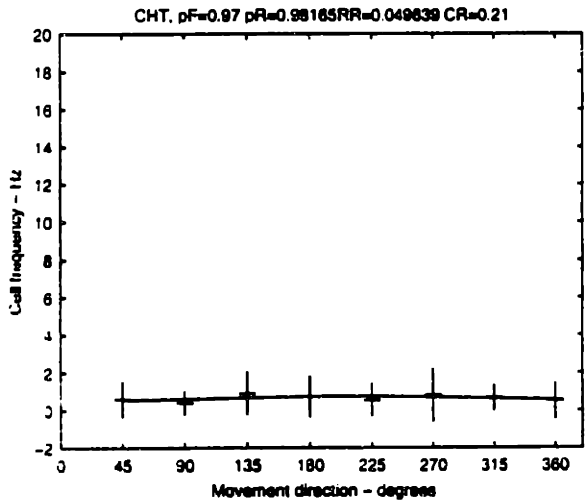

b) delay time

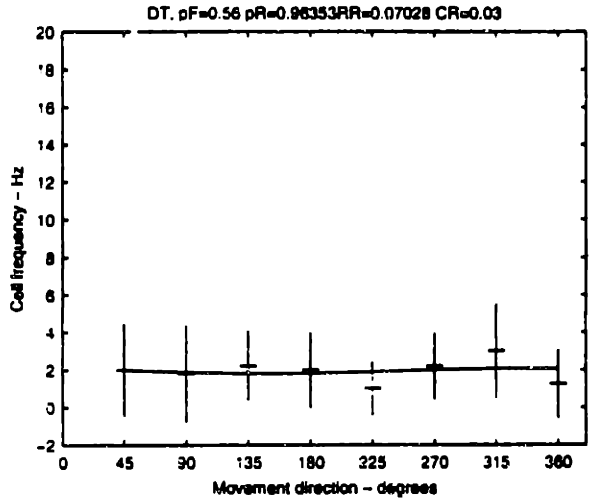

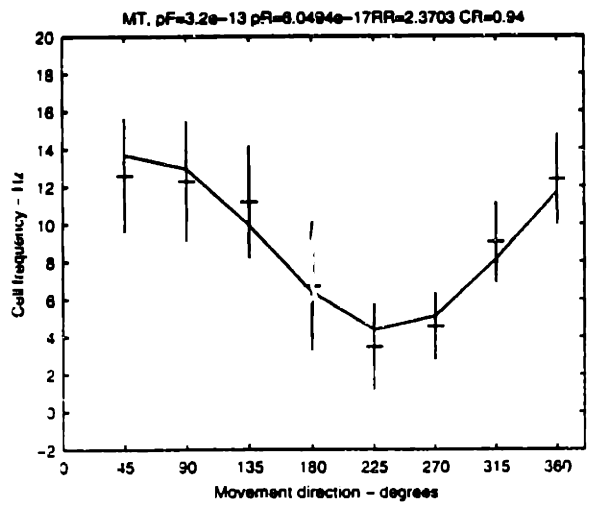

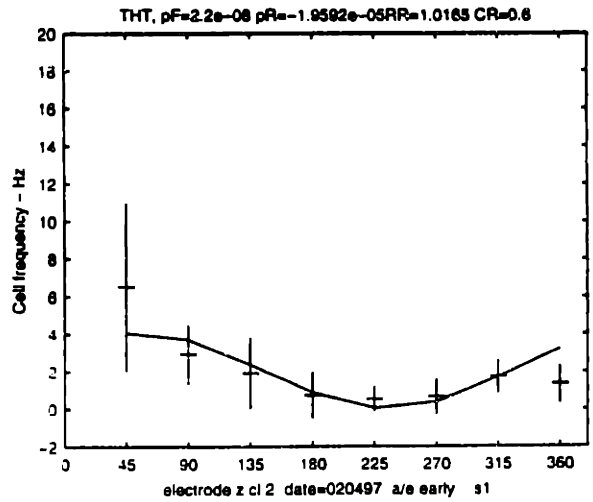

c) movement time

d) target hold time

Figure 5.17c Tuning curves showing cell 2 activity during washout epoch as function of movement direction for a) center hold time, b) delay time, c) movement time, d) peripheral target hold time

a preferred direction are assessed through a one-way ANOVA and a Rayleigh test, respectively. A cell's activity must be modulated by movement direction and must display a preferred direction of activity for some time period in at least one behavioral epoch to be considered for further analysis. If a cell's activity does not exhibit such relationships, it is considered to be unrelated to the experiment task.

P-values for the ANOVA direction test (indicated by "pF=") and the Rayleigh preferred direction test (indicated by "pR=") are included in the labels above the individual plots in Figures 5.16a-c and 5.17a-c. They are summarized in Tables 5.1 and 5.2 for the two cells analyzed in detail here. The statistical analyses confirm some of the trends seen in the graphical presentation of the data. For neither cell is there modulation in activity with movement direction nor a preferred activity direction for any epoch during the center hold or delay time periods. Both cells exhibit significant activity variation with movement direction and a strong direction of maximum activity over all epochs during the movement and peripheral target hold times. Further statistical analysis is therefore limited to these later two time periods.

Cells whose activity demonstrate a significant change within the task are analyzed to assess the nature of the change across the three behavioral epochs. An 8D gaussian analysis is performed first to determine whether changes across the epochs are significant. Then, cell activity within an epoch is characterized by four parameters - average firing rate, dynamic range, preferred direction of activity, and tuning sharpness. These parameters and their variances are calculated as a function of mean firing rates in each direction of movement. By assessing the significance in changes to these parameters, the nature of change in cell activity across the behavioral epochs is better described.

Table 5.3 gives the mean value and variance for the four activity parameters describing cell 1 activity during the movement period. Values are given for the baseline, force field, and washout epochs. Statistical analysis results in the form of p-values and statistical significance for paired t-tests across the behavioral epochs are shown in Table 5.4. Cell activity and associated activity parameters are significantly different between two epochs under the following conditions:

- 8D gaussian $p<0.05$
- average firing rate $p<0.01$
- dynamic range $p<0.05$
- preferred direction $p<0.05$

Table 5.1 Significance of direction modulation and preferred direction for cell 1 - p value comparisons

	Baseline epoch		Force field epoch		Washout epoch	
	direction modulation (ANOVA)	preferred direction (Rayleigh)	direction modulation (ANOVA)	preferred direction (Rayleigh)	direction modulation (ANOVA)	preferred direction (Rayleigh)
center hold time	0.79	0.93	0.29	0.82	0.22	0.94
delay time	0.46	0.40	0.31	0.95	0.70	0.82
movement time	0.00	0.00	0.00	0.00	0.00	0.00
target hold time	0.00	0.00	0.00	0.00	0.00	0.02

Table 5.2 Significance of direction modulation and preferred direction for cell 2 - p value comparisons

	Baseline epoch		Force field epoch		Washout epoch	
	direction modulation (ANOVA)	preferred direction (Rayleigh)	direction modulation (ANOVA)	preferred direction (Rayleigh)	direction modulation (ANOVA)	preferred direction (Rayleigh)
center hold time	0.19	0.53	0.61	0.65	0.97	0.98
delay time	0.44	0.48	0.87	0.73	0.56	0.96
movement time	0.00	0.00	0.00	0.00	0.00	0.00
target hold time	0.00	0.00	0.00	0.00	0.00	0.00

Table 5.3 - Statistical parameters for activity during movement period - Cell 1

Activity parameter	Behavioral epoch					
	Baseline		Force field		Washout	
	mean	variance	mean	variance	mean	variance
average rate	9.80	0.04	10.25	0.05	8.00	0.04
dynamic range	5.32	0.55	6.65	0.53	5.62	0.47
preferred direction	165.5	49.7	120.3	57.4	162.3	37.3
tuning sharpness	0.86	0.007	1.19	0.010	0.94	0.008

Table 5.4 - Significance tests across behavioral epochs for movement time activity - Cell 1

Parameter	Baseline vs Force field		Baseline vs Washout		Force field vs Washout	
	p-value	sig?	p-value	sig?	p-value	sig?
8D gaussian	0.03	yes	0.88	no	0.00	yes
average rate	0.14	no	0.00	yes	0.00	yes
dynamic range	0.20	no	0.76	no	0.30	no
preferred direction	0.00	yes	0.73	no	0.00	yes
tuning sharpness	0.01	yes	0.50	no	0.06	no

- tuning sharpness $p<0.05$

Of most interest is the data for the 8D gaussian analysis which indicates that cell activities during movement in the baseline and washout epochs are very similar. By comparison, activity in the force field epoch is significantly different. Changes in the cell's preferred direction demonstrates the same inter-epoch relationships; tuning sharpness also shows the same trend but at a slightly lower significance. This confirms the assessment made previously based on the raster plots, histograms, and tuning curves.

Tables 5.5 and 5.6 show the parameters and resulting analysis results for the activity of cell 1 during the peripheral target hold time. Data format is the same as the previous tables. The 8D gaussian analysis indicates that cell activities across the three behavioral epochs are not significantly different.

The principle conclusion drawn from the statistical analysis is that cell 1 activity significantly varies across the behavioral epochs only during the movement period. This change is characterized by a shift in the cell's preferred direction of activity during the force field epoch - a period when execution of the reaching task is affected by external dynamics.

For the activity of cell 2, Tables 5.7-5.8 and Tables 5.9-5.10 provide parameter and statistical summary data for movement time and peripheral target hold time periods, respectively. Again, of particular note are the relationships determined by the 8D gaussian analysis of cell activity during the movement time. Activities vary significantly between the baseline and force field epochs and between the baseline and washout epochs. Activities in the force field and washout epochs are very similar. These relationships, attributed to changes in the dynamic range and the average firing rate, confirm the trends seen in the graphical representations of the data.

The activities of 185 cells were recorded in the experiment paradigm. Of this total, 69 (37%) demonstrated average spike firing rates too low (<2Hz) to be considered relevant to the task or whose activity could not be recorded in a stable manner throughout the experiment session. The remaining 116 cells were analyzed in the manner just described. Table 5.11, which is included at the end of this chapter, provides a summary of the cell analyses. Following the cell identifier, the reaching task time periods during which each cell demonstrated significant activity are identified. Statistical analysis results comparing changes in cell activity between

Table 5.5 - Statistical parameters for activity during target hold period - Cell 1

Activity parameter	Behavioral epoch					
	Baseline		Force field		Washout	
	mean	variance	mean	variance	mean	variance
average rate	3.08	0.03	2.08	0.01	2.00	0.02
dynamic range	6.23	0.64	4.20	0.16	3.83	0.43
preferred direction	167.6	21.5	173.4	31.4	159.6	85.7
tuning sharpness	0.66	0.006	0.64	0.001	0.60	0.003

Table 5.6 - Significance tests across behavioral epochs for target hold activity - Cell 1

Parameter	Baseline vs Force field		Baseline vs Washout		Force field vs Washout	
	p-value	sig?	p-value	sig?	p-value	sig?
8D gaussian	0.82	no	1.00	no	1.00	no
average rate	0.00	yes	0.00	yes	0.68	no
dynamic range	0.02	yes	0.02	yes	0.64	no
preferred direction	0.43	no	0.44	no	0.21	no
tuning sharpness	0.79	no	0.50	no	0.52	no

Table 5.7 - Statistical parameters for activity during movement period - Cell 2						
	Behavioral epoch					
Activity parameter	Baseline		Force field		Washout	
	mean	variance	mean	variance	mean	variance
average rate	16.43	0.04	10.18	0.04	8.86	0.07
dynamic range	5.74	1.01	8.08	0.59	8.92	0.91
preferred direction	68.6	58.0	64.2	28.6	57.9	21.6
tuning sharpness	1.29	0.006	1.18	0.004	1.03	0.005

Table 5.8 - Significance tests across behavioral epochs for movement time activity - Cell 2						
Parameter	Baseline vs Force field		Baseline vs Washout		Force field vs Washout	
	p-value	sig?	p-value	sig?	p-value	sig?
8D gaussian	0.00	yes	0.00	yes	1.00	no
average rate	0.00	yes	0.00	yes	0.00	yes
dynamic range	0.06	no	0.02	yes	0.49	no
preferred direction	0.64	no	0.23	no	0.37	no
tuning sharpness	0.26	no	0.01	yes	0.10	no

Table 5.9 - Statistical parameters for activity during target hold period - Cell 2						
	Behavioral epoch					
Activity parameter	Baseline		Force field		Washout	
	mean	variance	mean	variance	mean	variance
average rate	7.72	0.10	3.17	0.03	2.17	0.03
dynamic range	9.53	1.67	4.50	0.70	6.71	1.10
preferred direction	50.5	34.4	60.3	71.8	61.1	19.3
tuning sharpness	1.01	0.003	0.65	0.002	0.69	0.003

Table 5.10 - Significance tests across behavioral epochs for target hold time activity - Cell 2						
Parameter	Baseline vs Force field		Baseline vs Washout		Force field vs Washout	
	p-value	sig?	p-value	sig?	p-value	sig?
8D gaussian	0.00	yes	0.26	no	0.96	no
average rate	0.00	yes	0.00	yes	0.00	yes
dynamic range	0.00	yes	0.09	no	0.10	no
preferred direction	0.34	no	0.15	no	0.94	no
tuning sharpness	0.00	yes	0.00	yes	0.53	no

pairs of behavioral epochs are listed in the next three columns. A zero in a column indicates there was no statistically significant difference in activity between the two epochs considered; a one implies a significant difference. When differences are indicated, the next column identifies the activity parameters contributing to the change. The final column of the table labels the cells in the categories to be described next.

5.3 Correlation of cell activity with task performance

Cells with significant firing rates were analyzed and classified according to the manner in which activity changed from baseline to force field to washout epochs. To appreciate the varied nature of activity changes and the significance of the cell categories, consider again the demands made by the reaching task on the neurological system controlling arm movement.

In all three behavioral epochs, the goal of the task is the same - move the manipulandum such that the cursor moves from the center target to a peripheral target. For a monkey well-trained in the task, this movement is approximately straight with a smooth, unimodal velocity history. For such a monkey, then, the kinematic parameters describing hand movements are the same across the three behavioral epochs. The dynamics of the task, the forces and torques required to bring about hand movement, are the same in the baseline and washout periods, but markedly different in the force field epoch. This is true even when the monkey is well-trained in the forces and his trajectories reflect the skilled performance seen in the baseline and washout epochs.

Given the kinematic and dynamic aspects of the reaching task within each behavioral epoch and noting the varied nature of changes in cell activity across these epochs, four categories of cells are defined:

- kinematic cells - cells that are directionally tuned in the baseline and preserve the same tuning and activity in the force field and washout epochs.
- dynamic cells - cells that are directionally tuned in the baseline, change their activity in the force field, and resume their baseline activity in the washout epoch.
- memory cells - cells whose activities change from the baseline to force field epochs and retain the force field activity through the washout period.
- "other" - cells with significant firing rates, but whose activities are not modulated by the task or whose changes in activities are other than those described by the three previous categories.

Kinematic cells are so named since changes in their activity are consistent with changes in kinematic parameters describing the reaching task - movement direction, hand path, hand velocity. As presented in the analysis of psychophysical data, for a well-trained monkey executing the task, kinematic parameters characterizing hand movements change significantly as a function of movement direction. There is minimal change in these parameters across the behavioral epochs. Figure 5.18 illustrates a typical kinematic cell. The three graphs show cell activity in the form of tuning curves for the baseline, force field, and washout epochs. There is significant modulation of cell activity as a function of movement direction; however, activity is not sensitive to the changes in external forces imposed during the force field epoch. Cell activity is clearly influenced by the task; the nature of this influence is a change in cell activity consistent with kinematic effects. Since kinematic cells demonstrate no significant activity changes across behavioral epochs, such cells are indicated by (0 , 0 , 0) in columns 3-5 of Table 5.11.

The activity of a dynamic cell is directly influenced by the force environment in which the reaching task is executed. Task dynamics in the baseline and washout epochs are the same; the dynamics of the force field epoch is different. Dynamic cell activity modulates in this same manner. An example of a dynamic cell is shown in Figure 5.19 where cell activity in the force field demonstrates a shift in direction of maximum activity compared to the baseline and washout epochs. In general, the changes in dynamic cell activity seen in the force field epoch may be reflected in changes in average firing rate, dynamic range, or preferred direction of activity. Cells with this activity are indicated by (0 , 1 , 0) in columns 3-5 of Table 5.11.

The activity of memory cells is initially like that of dynamic cells. Compared to the baseline period, memory cell activity in the force field epoch is modulated by the applied external forces. However, in memory cells, the modulated activity is retained in the washout epoch. This despite the fact that both the kinematic and dynamic demands of the reaching task in the washout period are the same as those of the baseline epoch.

Figure 5.20 illustrates three different cells with activity changes consistent with the definition of memory behavior. The cell in Figure 5.20a shows minimal activity during the baseline period and would be considered unrelated to the reaching task. However, once the external force field is applied, cell activity significantly increases and is modulated with movement direction. When the forces are removed in the washout epoch, cell activity remains high and retains its broadly-tuned nature. Figure 5.20b shows a cell that demonstrates broadly-tuned

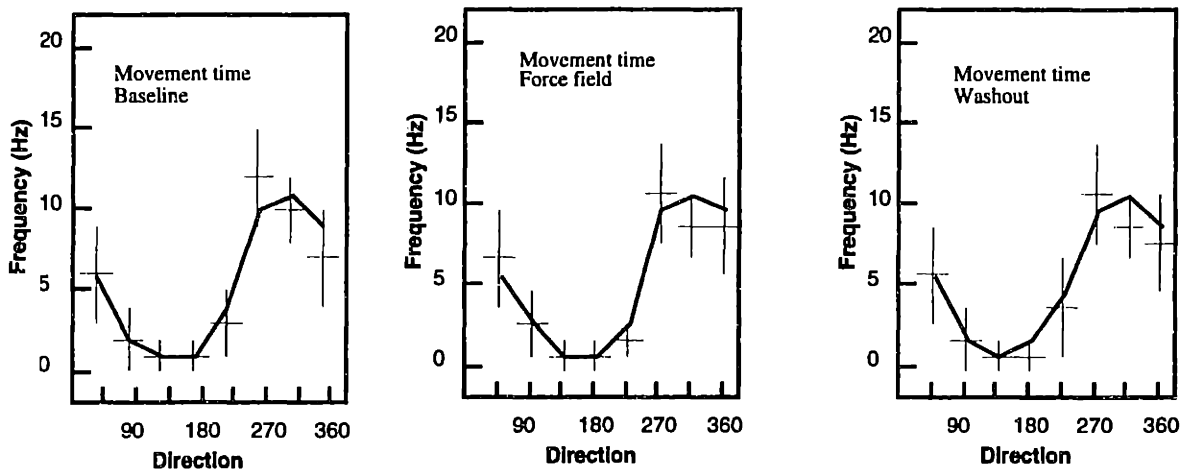

Figure 5.18 Kinematic cell showing constant activity across epochs

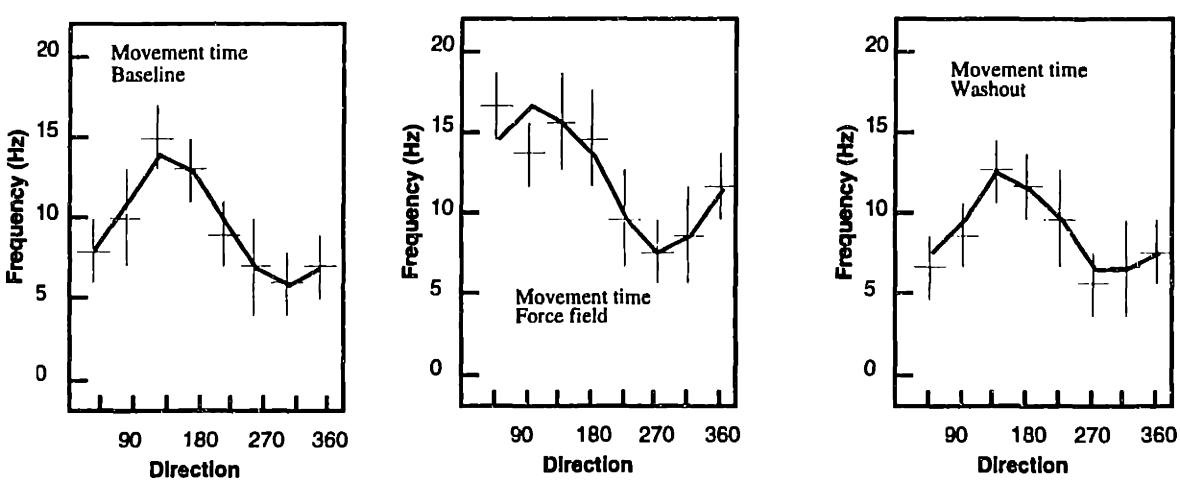

Figure 5.19 Dynamic cell showing modulation of activity with applied external force

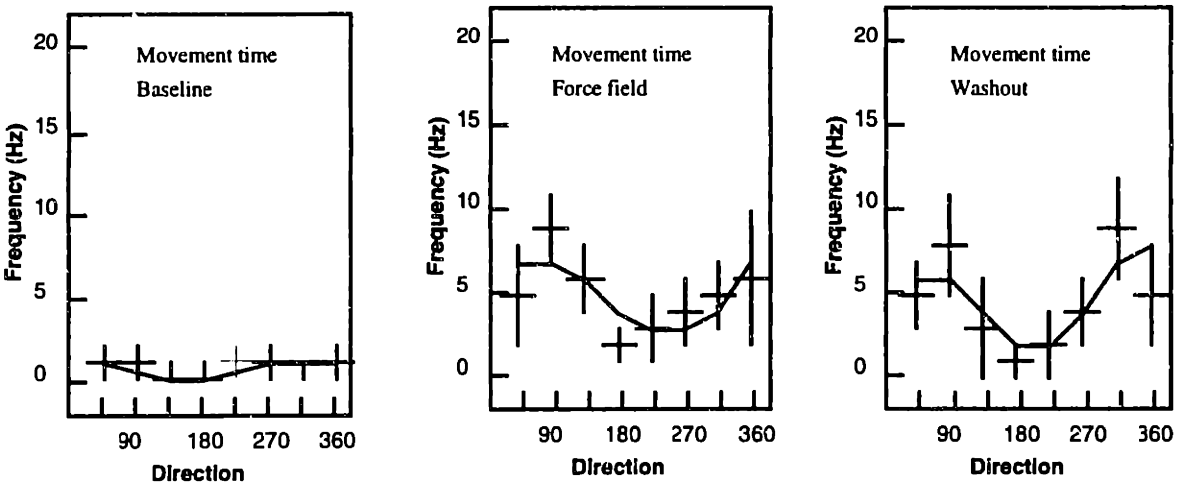

Figure 5.20a Memory cell exhibiting tune-in activity

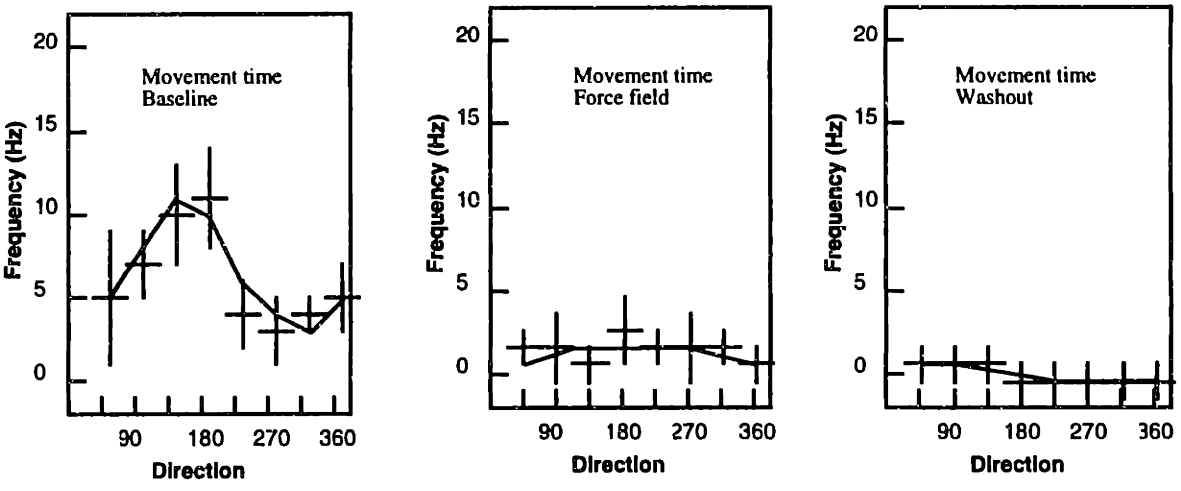

Figure 5.20b Memory cell exhibiting tune-out activity

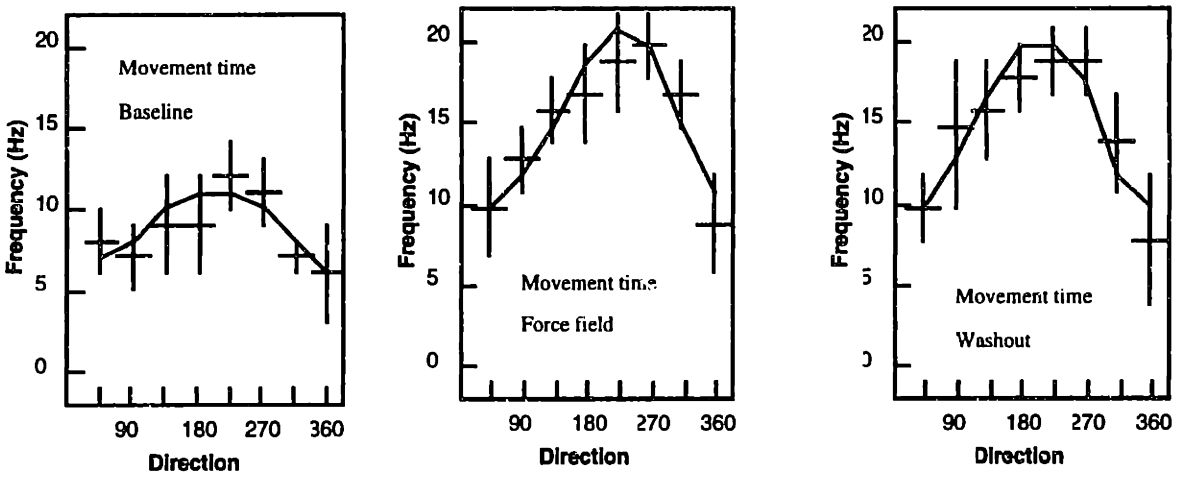

Figure 5.20c Memory cell exhibiting change in average rate and dynamic range

activity in the baseline epoch. With the onset of applied loads, cell activity drops and activity modulation with movement direction is lost. This low level of cell activity persists through the washout period. The cell in Figure 5.20c shows significant, broadly-tuned activity during all three behavioral epochs. However, compared to the baseline period, cell activity in the force field epoch has a higher average rate and a larger dynamic range. Again, the changes seen in the force field are retained in the washout period. Although the nature of the changes may vary among individual cells, all memory cells are characterized by a change in activity from baseline to force field and by persistence of the altered activity state through the washout period. In Table 5.11, such cells are indicated by a (1 , 1 , 0) in columns 3-5.

Some cells display significant activity in one or all of the behavioral epochs, yet changes in their activity are not readily explained by changes in the parameters or performance of the reaching task. An example would be a cell whose activity changes from baseline to force field epochs and changes in a different manner from the force field to the washout periods. These cells are labeled "other". Such a label does not imply that the cells are not related to the reaching task or to motor learning. Rather, the implication is that the nature of the relationship is not readily inferred from the changes in cell activity quantified here.

Of the 185 cells recorded in this experiment, 116 displayed activity at a sufficient level to be candidates for statistical analysis. Of these, 36 (31%) exhibited kinematic behavior, 10 (9%) dynamic behavior, and 21 (18%) memory behavior. The balance of the cells (49, 42%) displayed activity characteristics classified as "other".

5.4 Analysis of cell populations

The analyses described so far considered the activity of individual cells and the change in activity across the behavioral epochs. Internal representations of frames of reference and associated movement parameters can be emerging properties of neuronal populations. These constructs may not be evident at the level of the individual cell (Caminiti and Johnson 1992). To assess changes in the activity of cell populations across the three behavioral epochs, subsets of cells were identified based on the significance of activity parameters and analyses were conducted to quantify the systematic change in the parameters for the cell subset.

Kalaska et.al. (1989) showed that the preferred direction of cell activity shifts when a lateral static force is applied to a reaching task. The shift is in the direction of the bias force. A similar analysis was conducted here. A set of 45 cells was selected. This represented all cells

that demonstrated activity with a significant preferred movement direction in each of the three behavioral epochs. Both monkeys and recording sessions that used both the clockwise and counterclockwise force fields were represented in the cell set. The changes in preferred direction from baseline to force field, force field to washout, and baseline to washout were calculated. The change was measured in degrees. If the change in preferred direction was in the direction of the applied force, the value was positive. If the change was in the opposite direction, the value was negative. Data is presented in histogram form. Histograms uniformly distributed about zero would indicate no systematic shift in the preferred direction of cell activity between the two behavioral epochs considered. Histograms with a positive bias would suggest a shift in preferred movement direction in the direction of the applied force; a negative bias would indicate a shift away from the force.

Figure 5.21 shows the data for comparisons between a) baseline and force field, b) force field and washout, and c) baseline and washout epochs. In 5.21a there is a net shift in the preferred direction in the direction of the applied force. When the forces are removed, there is a shift away from the direction of the forces (Figure 5.21b). There is no overall change in preferred direction of activity when baseline and washout epochs are compared (Figure 5.21c). These results are consistent with those seen in Kalaska et.al. (1989).

A similar analysis was conducted for the tuning sharpness activity parameter. Here, a subset of 15 cells was selected. These represented all cells displaying memory activity that had significant sharpness across the three behavioral epochs. Histograms of data comparing the tuning sharpness between baseline-force field and baseline-washout were constructed. A negative shift in the data suggests that the tuning is sharper in the force field or washout epochs than in the baseline.

The results are shown in Figure 5.22a (comparing baseline to force field epochs) and 5.22b (comparing baseline to washout epochs). The magnitude of the change in the sharpness parameter is large - ranging to $\pm$ 180°. There does not appear to be a significant change in the sharpness parameter in the two paired-comparison analyses.

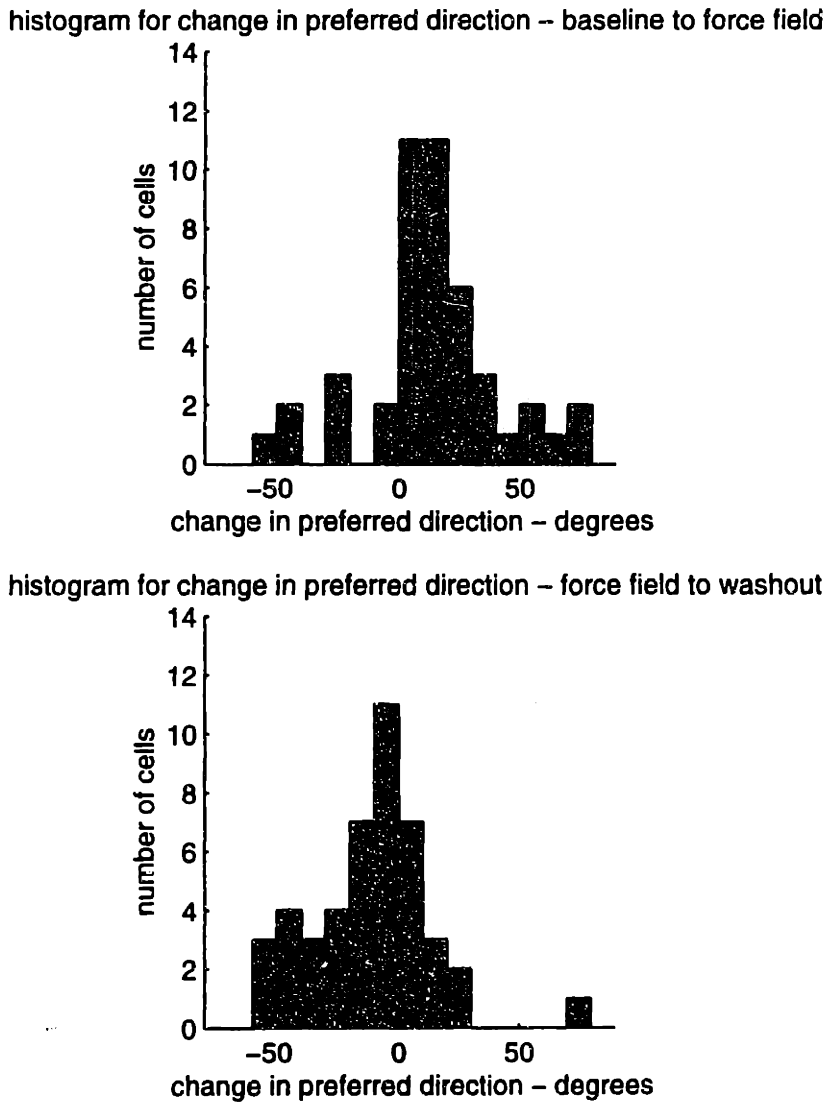

Figure 5.21a,b Change in preferred direction of activity

a) (upper graph) baseline to force field

b) (lower graph) force field to washout

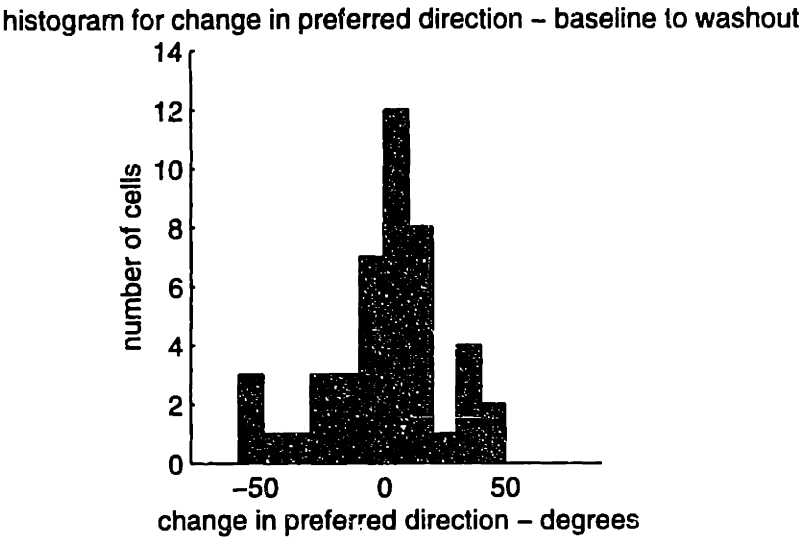

Figure 5.21c Change in preferred direction - baseline to washout

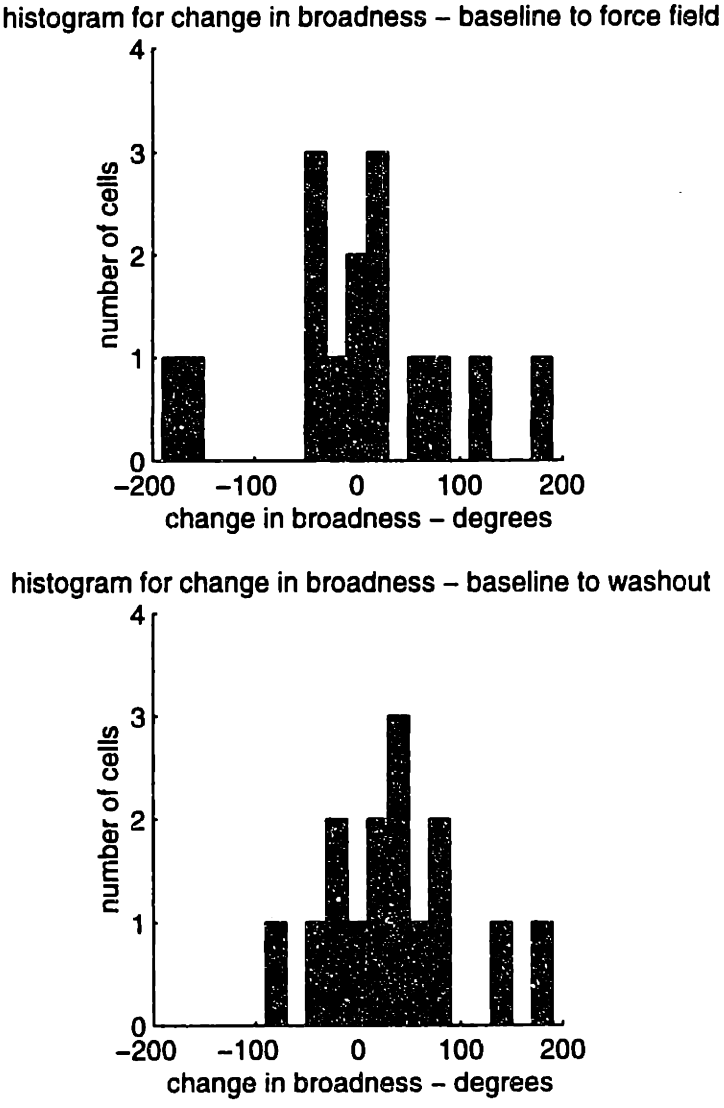

Figure 5.22 Change in tuning sharpness

a) (upper graph) baseline to force field

b) (lower graph) baseline to washout

cell ID	time period of significant activity	baseline vs force field	baseline vs washout	force field vs washout	contributing activity parameters	cell classification
0131_z_2	mt,tht	1	1	0	avg,pd	memory
0131_z_3	mt	1	1	0	avg,dr	memory
0203_z_2	tht,mt	0	0	0		kinematic
0203_z_3	mt,tht	1	1	0	avg,dr,pd	memory
0203_z_4	tht,mt	1	1	0	avg	memory
0204_z_2	mt,tht	1	1	0	avg,dr	memory
0206_z_2	mt	0	0	0		kinematic
0206_z_3	tht	0	0	0		kinematic
0206_z_4	mt,tht	0	0	0	avg	other
0207_z_2	mt,tht	0	0	0		other
0207_z_3	mt	0	0	0		other
0210_z_2	mt,tht	1	1	0	avg	memory
0211_z_2	mt,tht	0	0	0		kinematic
0212_z_2	tht,mt	0	0	0		kinematic
0213_z_2	tht	0	0	0		kinematic
0213_z_3	mt,tht	0	0	0		other
0214_z_2	mt,tht	0	0	0		kinematic
0217_z_2	tht,mt	0	0	0		kinematic
0218_z_2	mt	1	1	0	avg,pd	memory
0219_z_2	mt	0	0	0		other
0220_z_2	mt,tht,dt	1	1	0	avg	memory
0225_z_2	mt,tht	1	0	1	pd	dynamic
0226_z_2	mt	0	0	0		kinematic
0227_z_2	tht	0	0	0		other
0227_z_3	tht	1	1	0	avg,dr	memory
0305_z_2	tht	0	1	0	avg,dr	other
0305_z_3	mt	1	1	0	avg,dr	memory
0306_z_2	mt	0	0	0		kinematic
0307_z_3	mt,tht,dt	0	0	0		other
0311_z_2	mt,tht	0	0	0		kinematic
0313_z_3	mt	0	0	0		kinematic
0314_z_2	mt,tht	0	0	0		kinematic
0314_z_3	tht,mt	1	1	0	avg,dr	memory
0318_z_4	mt	1	1	1	avg,pd	other
0320_z_2	mt,tht	1	1	0	avg,dr	memory
0325_z_2						dynamic
0325_z_3						dynamic
0326_z_3	mt,tht	0	1	0	avg,pd	other
0327_z_3	mt,tht	0	0	0		other
0328_z_3	tht,mt	0	0	0		kinematic
0401_z_2	mt,tht	0	1	1	avg,pd	other
0410_z_3	tht,mt	0	0	0		kinematic
0414_z_2	mt,tht	0	0	1	avg,dr	other
0429_z_2	mt,tht	0	0	0		other
0429_z_3	mt,tht	1	1	0	avg,dr	memory
0430_z_2	tht	1	0	0		other

Legend:

dt = delay time
mt = movement time
tht = target hold time

avg = average firing rate
dr = dynamic range
pd = preferred direction
brd = tuning broadness

Table 5.11 Summary of cell statistical analyses

cell ID	time period of significant activity	baseline vs force field	baseline vs washout	force field vs washout	contributing activity parameters	cell classification
0430_z_3	tht,mt	0	0	0		kinematic
0501_z_2	mt,tht	0	0	0		kinematic
0502_z_2	mt,tht	1	1	0	avg	memory
0502_z_3	mt,tht	0	0	0		other
0508_z_2	mt,tht	0	0	0		other
0513_z_2	mt	0	0	0		other
0513_z_3	mt	1	0	1	avg	dynamic
0514_z_3	mt	0	1	1	avg,pd	other
0515_z_2	mt,tht	1	1	0	avg,pd,brd	memory
0516_z_2	tht,dt,mt	0	0	0		kinematic
0519_z_2	mt,tht,dt	1	1	0	avg	memory
0603_z_2	mt	0	0	0		kinematic
0603_z_3	tht	0	0	0		other
0603_z_4	tht	0	0	0		other
0604_z_2	mt,dt,tht	0	0	0		kinematic
0604_z_3	tht	0	0	0		other
0605_z_2	mt,dt	0	0	0		other
0605_z_3	tht,dt,mt	0	0	0		other
0605_z_4	mt	0	0	0		kinematic
0606_z_2	mt,dt,tht	0	1	1	avg	other
0626_z_2	mt,dt	1	0	1	avg,pd	dynamic
0626_y_2	mt,tht	0	0	0		other
0626_y_3	mt	0	0	0		other
0627_y_2	mt	1	0	1		dynamic
0630_z_2	tht,mt	0	0	0		kinematic
0630_y_2	mt	0	0	0		kinematic
0630_x_2	mt	0	0	1	avg	other
0630_x_3	mt	1	0	1	avg	dynamic
0701_z_2	tht,mt	0	0	0		kinematic
0701_y_2	mt	0	0	0		other
0701_x_2	mt	0	1	1	avg	other
0701_x_3	mt	0	0	0		other
0707_x_2	mt	1	1	0	avg	memory
0707_x_3	mt	0	1	0	avg	other
0710_z_2	tht,mt	0	0	0		kinematic
0710_z_3	mt	0	0	0		kinematic
0710_z_4	mt	0	0	0		other
0710_y_2	mt	1	0	0	avg	other
0710_y_3	mt	0	0	0		other
0710_x_2	mt	0	0	0		kinematic
0710_x_3	mt	0	0	0		kinematic
0715_z_3	mt,tht	1	1	0	avg	memory
0715_y_3	mt,dt,tht	1	1	0	avg,dr	memory
0716_z_4	dt,mt,tht	0	0	0		other
0717_z_2	mt,tht,dt	0	0	0		other
0717_x_2	mt	0	0	0		kinematic
0717_x_3	mt	1	0	1	avg,dr	dynamic

Legend:

dt = delay time
mt = movement time
tht = target hold time

avg = average firing rate
dr = dynamic range
pd = preferred direction
brd = tuning broadness

Table 5.11 Summary of cell statistical analyses (continued)

cell ID	time period of significant activity	baseline vs force field	baseline vs washout	force field vs washout	contributing activity parameters	cell classification
0723_z_3	mt	0	1	0	avg	other
0729_y_2	mt,dt,tht	1	0	0	avg,pd	other
0826_y_2	dt,mt,tht	1	1	0	avg	memory
0827_z_3	mt	0	0	0		kinematic
0828_z_2	dt	0	0	0		other
0829_z_2	mt,dt	0	0	0		kinematic
0829_y_2	mt	0	0	0		kinematic
0829_y_3	mt,dt	0	0	0		other
0829_y_4	mt	0	0	0		kinematic
0902_z_2	tht,mt,dt	0	0	0		kinematic
0902_y_2	mt,dt,tht	0	1	1	avg,dr,pd	other
0904_z_3	mt,dt	0	1	1	avg	other
0904_y_3	mt	0	0	0		other
0904_x_2	mt,tht,dt	1	0	1	avg,dr	dynamic
0904_x_3	mt	1	0	1	avg,dr	dynamic
0904_x_4	mt,tht	0	0	0		kinematic
0909_z_2	tht	0	0	0		kinematic
0909_y_2	mt	1	1	0	avg,pd	memory
0909_y_3	mt,tht,dt	0	1	1	avg,dr	other
0909_x_2	mt	0	0	1	pd	other
0911_z_2	mt	0	0	0		other
0911_y_2	mt	0	0	0		other
0911_x_2	dt,mt	0	0	0		other

Legend:

dt = delay time
mt = movement time
tht = target hold time

avg = average firing rate
dr = dynamic range
pd = preferred direction
brd = tuning broadness

Table 5.11 Summary of cell statistical analyses (continued)

6. Discussion

A major challenge to neurophysiologists in the investigation of motor learning and memory is to establish links between changes in behavior and changes in the activity of neurons in the central nervous system. The goal of this work was to develop and execute an experimental paradigm that brought together the two components required to address this challenge - a behavioral paradigm that creates the environment for motor learning and a physiological method that provides for stable recording of cortical cell activity. The behavioral paradigm developed for this work - a visually-guided, delayed reaching task executed in different force environments - created the environment for motor learning. Cell activity recorded from the arm-related area of the monkey primary motor cortex during execution of the reaching task provided the raw physiological data. Data obtained from the experimental paradigm was then analyzed to quantify task performance, to demonstrate motor learning, to quantify cell activity, and to establish relationships between parameters quantifying motor performance and cell activity.

Motor learning can be described as motor skill acquisition that occurs through practice and is characterized by improvement in the quality of task performance as measured by accuracy, speed, or minimum energy expenditure (Sanes, et.al. 1990). Motor learning involves the acquisition of new skilled movements and refers to the ability to acquire the temporal and spatial characteristics of movement patterns so that pattern execution is increasingly characterized by pre-programmed processes. The awkward, jerky movements seen in the earliest stages of motor learning can be associated with a feedback control system that relies on sensory-perceived errors to generate corrective motor commands. After practice, movements become smooth, coordinated, and often more rapid. This suggests acquisition and modification of motor programs that allow the performer to organize a sequence of movements in advance of the execution and to rely less on sensory feedback (Grafton et.al. 1992). Sensory-dependent, feedback mechanisms are replaced by feedforward programs. Skill acquisition in reaching movements is typically characterized by the appearance of single-peaked, bell-shaped velocity profiles and directed, straight-line hand paths (Halsband and Freund 1993).

Performance of the monkeys in the reaching task was consistent with these definitions of skill acquisition and clearly demonstrated motor learning. In the baseline behavioral epoch, reaching trajectories consistently demonstrated straight hand paths and smooth, unimodal velocity profiles. These accurate movements were initiated within the earliest trajectories of the baseline epoch and were maintained throughout this behavioral period. This performance was

maintained by both monkeys throughout weeks of executing the experimental paradigm. Such performance suggests that the baseline task is well-learned and is accomplished through the feedforward execution of an accurate, internal representation of the movement.

In the force epoch, application of a viscous curl force field changed the dynamics of the reaching task and created the environment for motor learning. Trajectories were significantly perturbed. Hand paths were deflected in the direction of the applied forces. Velocity histories showed multiple peaks and indicated longer movement times. Multiple corrective movements were made. These trajectories suggest that the task is accomplished, not by the feedforward execution of an internal movement model, but through the execution of multiple movement primitives selected and modified by sensory feedback. Performance is highly variable and is not consistent with that of a well-learned task.

With practice in the force field, task performance improves. Hand paths straighten; the number of velocity peaks diminish. There are fewer corrective movements. Although there is still considerable variability in the data, improved performance is demonstrated by a general increase in the correlation coefficient with increasing number of trials in the force field. This trend does not continue through the entire epoch but reaches a steady-state or plateau level. This characterization of improvement in task performance from initial trials in the force field epoch to late trials in the epoch was seen in every day of experimentation for both monkeys. The nature of this improved performance in the reaching task, then, is consistent with skill acquisition through motor learning.

There is an alternative explanation to such changes in task performance. The monkeys could simply be increasing the impedance of their arms - cocontracting agonist and antagonist muscle groups in response to the perturbing forces. Increased arm impedance would reject (diminish) the perturbing effect of the external forces and provide straighter movement trajectories. Increasing arm impedance through muscle co-contraction in response to external loads is an adaptive response not consistent with descriptions of motor learning presented here.

That improvement in reaching task performance with practice in the force field results from motor learning and not adaptation is supported by the trajectories seen early in the washout epoch. If the monkeys' response to the applied forces was simply adaptive co-contraction, once the forces were removed at the start of the washout period, hand paths should be straight. Indeed, since the perturbing forces are removed, trajectories in the washout epoch should be straighter and smoother than those seen at the end of the force field epoch. This was not the case. Trajectories early in the washout epoch exhibit "aftereffects" - perturbations in hand

paths executed in the null field that reflect the nature of the just-experienced forces. Aftereffects quantify the extent that the characteristics of the external forces have been incorporated into the internal representation of the reaching movement and demonstrate the transition from the sensory-guided, feedback controlled execution of a poorly-learned motor skill to the feedforward execution of a well-learned task. These two observations, the nature of task performance improvement in the force field and the demonstration of aftereffects in the reaching trials immediately following removal of the forces, support the conclusion of skill acquisition through motor learning.

Aftereffects are seen only in the first several trials in the washout period following removal of the external forces. The monkeys quickly select the movement paradigm appropriate for executing the reaching task in the null field. Performance of the reaching task throughout the washout period then remains at the same high level as that demonstrated in the baseline period. This suggests that practicing the reaching task in the force environment does not disrupt execution of the well-learned, baseline task. The development through motor learning of an internal model appropriate for movement within the altered force environment does not interfere with the existing cortical mechanism used to execute the baseline task in the null field.

The washout epoch is the last behavioral period of the experimental paradigm. That the monkeys' performance remains high throughout this period suggests that neither fatigue nor inattention play a significant role in the interpreting the results.

As has been described, for any given day, task performance in the force epoch improves from a low level in initial trials to a higher, plateaued level in later trials. Although this accurately describes changes in task performance for all experiment sessions, the nature of this change varies with increasing exposure to the perturbing force field. Two trends were seen. The number of trials required to achieve the day's plateau performance level decreased with increased exposure to the force field; fewer trials were required to reach maximum performance. The plateau level indicating maximum performance for a given day itself increased with increased exposure to the force field. This maximal performance also reached a steady-state level with time. Further exposure to the force field did not lead to continued task improvement. That the rate and extent of task improvement in the force field epoch varied between the two monkeys supports the belief that the capacity to acquire a motor skill represents an individual characteristic (Schlaug et.al. 1994).

Once monkey performance in the clockwise force field had reached its plateau, a counterclockwise force field was then applied. Average performance in the force epoch

dropped significantly, but quickly reached a plateau level comparable to that seen in the clockwise field. Initial performance in the counterclockwise force field was no better than that seen in initial performance within the clockwise field. This suggests that the motor skills acquired are specific to the individual force environments in which the task is executed. Nonetheless, performance improved in the counterclockwise force field at a rate faster than that seen in the original clockwise force field. This suggests a generalization or transfer of some aspect of task execution in the initial force environment to task execution in the subsequent force environment.

Taken in total, the analysis of psychophysical data demonstrates a change in task execution consistent with published definitions of motor learning. Performance after practice in a perturbing force field was characterized by reaching movements executed toward the target, with smoother velocity histories, and with less variability than those seen before practice. Two distinct time periods for learning were seen. For each day of experimentation, task performance improved from a low level early in the force field epoch to a higher, plateaued level late in the same epoch. Therefore, leaning was demonstrated during the time required by the monkeys to execute the force field epoch - about an hour. This short term improvement in task execution may be the "fragile" learning seen in human subjects by Brashers-Krug, et. al. (1995). For the initial, clockwise force field, average performance in the force epoch improved over a period of several weeks before reaching a plateau level. Such long-term improvement is consistent with "consolidated" learning (Brashers-Krug, et.al. 1995). The nature of task performance seen during early exposure to the novel counterclockwise force field and the rate of performance improvement suggest both a specificity and generality of the task. Identifying those characteristics of the reaching paradigm that contribute to such interesting learning behavior is left to future researchers.

The anatomical structures participating in motor learning belong to two classes: 1) structures that provide the motor areas somatosensory information in the early phase of learning, and 2) motor areas that modulate their activity during the course of learning (Seitz et.al. 1990). These areas include the primary motor cortex, premotor areas, basal ganglia, thalamus, and cerebellum. It is generally accepted that the primary motor cortex is active during motor learning. The extent of the involvement during the course of learning is still controversial. Salmon and Butters (1995) states that the primary motor cortex may be important initially, but becomes less so as motor behavior is instantiated in motor programs mediated by other brain structures. For subjects executing a finger tapping paradigm, Karni et.al. (1995) found that by week 4 of training, concurrent with asymptotic performance, the extent of primary motor

cortex activated by the practiced sequence enlarged. These changes persisted for several months.

In recording from cells in the primary motor cortex throughout the experimental paradigm here, a varied nature of cell activity changes was seen. Thirty-seven percent of recorded cells demonstrated no significant activity with any aspect of the task. This relatively high percentage is attributable to the approach to cell recording taken during the experimental paradigm. Once a cell in the arm area of primary motor cortex was isolated at the beginning of the session, no efforts were made to ensure that cell activity was modulated in an interesting way within the experiment or to find alternative cells should such modulation not develop. Had these efforts been made, the activity of cells that were initially uncommitted to the task but subsequently became involved would never have been recorded and characterized.

Three categories of cell activity were defined - kinematic, dynamic, and memory - based on changes in cell activity across the three behavioral epochs. Because an acute recording preparation was used in this work, it was impossible to return to a specific cell on subsequent days and determine whether its activity continued to support the given category classification. Since the recordings are not strictly repeatable, there is the potential to provide alternative explanations for the observed activity behaviors that lessen the significance of the findings. Once such explanation is an acute change in the recording state. Slight relative movement between the electrode and the recorded cell can irritate the cell and change its activity. If the change in activity occurred at the start of a behavioral epoch, the altered cell behavior would be inappropriately associated with the change in a control variable - task dynamics. Yet, in the analyses conducted here, stable cell activity in the center hold epoch across the three behavioral epochs was a prerequisite for subsequent analyses. Any experimental anomaly that caused an acute change in the cell activity would be observed as a change in cell behavior during the center hold period. Such cells would be excluded from classification due to poor recording stability.

Random changes in cell activity can be cited as an alternative explanation for the observed cell behavior. But the described cell activities were seen in both monkeys, and the activities were classified only after rigorous statistical analyses. In addition, both on individual cell and cell population bases, activities demonstrated systematic changes consistent with changes in experimental control variables that strongly argue against random behavior. To be classified as kinematic, dynamic, or memory, a cell's activity must be significantly modulated by movement direction and have a significant preferred direction of activity. The analysis of a population of cells indicated that, when a viscous curl force field is applied to the reaching task, there is a

systematic shift in the preferred direction of cell activity in the direction of the applied force. When the force is removed, there is again a systematic shift in preferred direction. The shift is now in the direction opposite that of the removed force. Systematic changes in cell activity, rigorous statistical analyses, and strong control criteria all suggest that the cell behaviors seen here are attributed to changes in the independent variables associated with the experimental design.

Forty percent of cells subject to statistical analysis displayed activity that was either kinematic or dynamic in nature. It is comparatively straightforward to describe the activity of these cells in terms of parameters associated with the reaching task. Well-learned reaching movements share common kinematic attributes; they are directed toward the respective targets and are made with consistent, smooth trajectories independent of the forces required to bring about the movements. When recording from a cortical area associated with planning and executing such similar movements, it is intuitively appealing to identify cells that demonstrate similar activity during these movements (kinematic cells). Although the kinematic aspects of the reaching task are similar across the behavioral epochs, the dynamics of the epochs are not. Different torques about the shoulder, elbow, and wrist joints are required to bring about successful movements in the force field compared to the baseline and washout epochs. Muscle strategies that bring about movement in the baseline and washout epochs could be similar; muscle strategies required to execute the task in the external force environment would be different. The primary motor cortex projects to spinal interneurons and associated motor neurons that innervate upper extremity musculature. Again, it is intuitively appealing to find cells that demonstrate changes in activity consistent with changes in task dynamics (dynamic cells).

Kinematic and dynamic cells exhibit activity similar to that seen by other researchers. Most notably, recording from cells in multiple motor areas while monkeys executed reaching movements, Georgopoulos and his colleagues demonstrated in many studies that cell activity strongly correlates with direction of movement - a kinematic parameter. Kalaska and associates, Thach and others found that cell activity is modulated by the application of a static, lateral load - a dynamic effect. The experimental paradigm performed here - execute reaching movements in the presence of velocity-dependent, external forces - is different than any used by previous researchers. Yet the two independent treatments of the paradigm - reaching movement direction and applied load - are common to other experiment methods. It is not surprising, then, that a subset of cells recorded here share characteristics similar to those reported previously.

The activity of cells demonstrated by "memory" cells represents behavior heretofore not described in the primary motor cortex. The interesting characteristics of such cells is that changes in their activity cannot be consistently explained by any kinematic or dynamic feature of the task being executed. Initial modulation of activity from baseline to force field epochs would suggest a cell sensitive to the dynamics of the reaching task. Yet, when the dynamics of the task again change and return to that seen in the baseline epoch, cell activity does not change. Memory cells, therefore, demonstrate "dynamic" behavior from baseline to force field epochs and "kinematic" behavior from force field to washout epochs.

Describing changes in cell activity solely in terms of kinematic or dynamic parameters of the reaching movement itself fails to recognize the effect that task execution may have on the neural systems controlling the movements. Psychophysical data analysis has already demonstrated that practice of the task within the force field brings about an improvement in performance seen both during a single experiment session and across multiple-session exposure to the field. Motor learning occurs. Therefore, even though the task executed by the monkey in the washout period is the same as that executed in the baseline epoch, the monkey is different. Specifically, the state of the neural mechanisms controlling the movements has been altered by the experience of the intervening force field epoch. This alteration in the state of the neural control system associated with motor learning could be reflected in the changes in activity seen in memory cells.

To explain an increase in the cortical area associated with executing a learned finger tapping paradigm, Karni et.al. (1995) speculated that motor practice induces the recruitment of additional M1 units into a network specifically representing the trained motor sequence. One substrate for the enlargement of cortical representations may be the unmasking of pre-existing lateral connections between populations of neurons whose outputs result in different sets of movements. Unmasking existing neural connections may subserve the fast or short-term learning seen daily within the experimental paradigm here. Karni et.al. continued that, to account for the gradual evolution of asymptotic performance in motor skill acquisition, improved synaptic connections between task-relevant cortical units subserving the execution of the skill are formed as the result of long-term practice.

In attempting to explain the neurobiological basis of motor learning in mammals, Asanuma and Pavlides (1997) echoed the belief that skilled movements result from the execution of a sequence of movement segments. The neural mechanisms associated with these segments are cortical efferent zones developed and reinforced through a type of long-term potentiation (LTP). Their results suggest that during repeated practice of a given movement, the sensory

input associated with movement could produce LTP in primary motor cortical neurons located in selected, related groups. In addition, they found that after repeated practice of a particular movement, excitability of a selected group of neurons in the ventrolateral thalamus (VL) increased, and original diffuse input from the VL became capable of producing excitation of selected zones in the primary motor cortex without input from the primary sensory cortex. Asanuma and Pavlides conclude that motor learning is based on increased excitability of efferent zones in the primary motor cortex by circulation of impulses in selected loop circuits.

The work here has found a subset of cells in the monkey primary motor cortex whose activity during a reaching task is not readily explained by movement parameters associated with the task itself. Indeed, the striking feature of memory cells is the difference in activity seen during execution of the task through epochs with the same kinematics and dynamics and the similarity in activity during execution of the task through epochs with similar kinematics but different dynamics. Explaining cell activity only in terms of parameters associated with task execution fails to recognize the change in state of the neural control system that results during motor learning. Previous research suggests that these changes can be detected on the individual neuron level. Motor learning might unmask new activation patterns that connect cells in a newly-defined, task-relevant unit. Through repeated practice of a task, a type of motor long-term potentiation may increase the excitability of these units by circulating impulses that reinforce and consolidate the units for a period after execution of the learned task. The activity of memory cells is consistent with such an explanation for the neural mechanisms of motor learning.

7. References

Alexander G.E. and Crutcher M.D. (1990) Preparation for movement: neural representations of intended direction in three motor areas of the monkey. J of Neurophysiol 64(1):133-150.

Asanuma H. and Pavlides C. (1997) Neurobiological basis of motor learning in mammals. NeuroReport 8, 4.

Brashers-Krug T., Shadmehr R. and Bizzi E. (1995) Consolidation of human motor learning. Department of Brain and Cognitive Sciences, Massachusetts Institute of Technology, Cambridge, MA 02129

Caminiti R. and Johnson P.B. (1992) Internal representations of movement in the cerebral cortex as revealed by the analysis of reaching. Cerebral Cortex July/August 2:269:276.

Caminiti R., Johnson P.B., Galli C., Ferraine S. and Burnod Y. (1991) Making arm movements within different parts of space: the premotor and motor cortical representation of a coordinate system for reaching to visual targets. J. Neurosci 11(5):1182-1197.

Caminiti R., Johnson P.B. and Urbano A. (1990) Making arm movements within different parts of space: dynamic aspects in primate motor cortex. J Neurosci 10(7):2039-2058.

Corkin S. (1968) Acquisition of motor skill after bilateral medial temporal lobe excision. Neuropsychologia 6:255-266.

DeLong M.R., Crutcher M.D. and Georgopoulos A.P. (1985) Primate globus pallidus and subthalamic nucleus: functional organization. J Neurophysiol 53(2)530-43.

di Pellegrino G., Fadiga L., Fogassi L., Gallese V. and Rizzolatti G. (1992) Understanding motor events: a neurophysiological study. Exp Brain Res 91:176-180.

Dizio P. and Lackner J.R. (1995) Motor adaptation to coriolis force perturbations of reaching movements: endpoint but not trajectory adaptation transfers to the nonexposed arm. J Neurophysiol 74(4):1787-1792.

Fisher N.I., *Statistical Analysis of Circular Data*, Cambridge University Press, 1993.

Fitts P.M. (1954) The information capacity of the human motor system in controlling the amplitude of movement. J of Exp Psychology 67, 381-391.

Flament D., Onstott D., Fu Q.G. and Ebner J.J. (1993) Distance- and error-related discharge of cells in premotor cortex of rhesus monkeys. Neurosci Lett 153(2)144-8.

Flanagan J.R. and Rao A.K. (1995) Trajectory adaptation to a nonlinear visuomotor transformation: evidence of motion planning in visually perceived space. J Neurophysiol Vol 74 No 5 2174-2178.

Flash T. and Gurevich I. (1991) Arm Stiffness and movement adaptation to external loads. Annual Internation Conference of the IEEE Engineering in Medicine and Biology Society, Vol 13, No. 2, 885-886.

Flash T. and Hogan N. (1985) The coordination of arm movements: an experimentally confirmed mathematical model. J Neurosci 5:1688-1703.

Fortier P.A., Kalaska J.F., and Smith A.M. (1989) Cerebellar neuronal activity related to whole-arm reaching movements in the monkey. J Neurophysiol 62:198-211.

Gandolfo F., Mussa-Ivaldi F.A. and Bizzi E. (1996) Motor learning by field approximation. Neurobiology (in press).

Georgopoulos A.P. and Ashe J. New concepts in generation of movement. Brain Sciences Center, Veterans Affairs Medical Center, One Veterans Drive, Minneapolis, MN 55455

Georgopoulos A.P., Ashe J., Smyrnis N. and Taira M. (1992) The motor cortex and the coding of force. Science Vol 256 1692-1695.

Georgopoulos A.P., Crutcher M.D. and Schwartz A.B. (1989) Cognitive spatial-motor processes. Exp Brain Res 75:183-194.

Georgopoulos A.P., Kettner R.E., and Schwartz A.B. (1988) Primate motor cortex and free arm movements to visual targets in three-dimensional space. II. Coding of the direction of movement by a neuronal population. J Neurosci 8(8):2928-2937.

Georgopoulos A.P., Schwartz A.B., and Kettner R.E. (1986) Neuronal population coding of movement direction. Science 233:1416-1419.

Georgopoulos A.P., Caminiti R. and Kalaska J.F. (1984) Static spatial effects in motor cortex and area 5: quantitative relations in a two-dimensional space. Exp Brain Res 54:446-454.

Georgopoulos A.P., Caminiti R., Kalaska J.F., and Massey J.T. (1983) Spatial coding of movement: A hypothesis concerning the coding of movement direction by motor cortical populations. Exp. Brain Res. Suppl. 7:327-336.

Georgopoulos A.P., Kalaska J.F., Caminiti R., and Massey J.T. (1982) On the relations between the direction of two-dimensional arm movements and cell discharge in primate motor cortex. J. Neurosci 2:1527-1537.

Ghilardi M.F., Gordon J. and Ghez C. (1995) Learning a visuomotor transformation in a local area of work space produces directional biases in other areas. J Neurophysiol 73(6):2535-2542.

Grafton S.T., Mazziotta J.C., Presty S., Friston K.J., Frackowiak R.S.J., and Phelps M.E. (1992) Functional anatomy of human procedural learning determined with regional cerebral blood flow and PET. J. Neurosci 12(7):2542-2548.

Halsband U. and Freund H.-J. (1993) Motor learning. Curr Op in Neurobiol 3:940-949.

Hogan N. (1984) An organizing principle for a class of voluntary movements. J Neurosci 4:2745-2754.

Kalaska J.F., Cohen D.A.D., Prud'homme M. and Hyde M.L. (1990) Parietal area 5 neuronal activity encodes movement kinematics, not movement dynamics. Exp Brain Res 80:351-364.

Kalaska J.F., Cohen D.A.D., Hyde M.L. and Prud'homme M. (1989) A comparison of movement direction-related versus load direction-related activity in primate motor cortex, using a two-dimensional reaching task. J. Neurosci 9:2080-2102.

Kalaska J.F., Caminiti R. and Georgopoulos A.P. (1983) Cortical mechanisms related to the direction of two-dimensional arm movements: relations in parietal area 5 and comparison with motor cortex. Exp Brain Res 53:247-260.

Karni A., Meyer G., Jezzard P., Adams M.M., Turner R., and Ungerleider L.G. (1995) Functional MRI evidence for adult motor cortex plasticity during motor skill learning. Nature Vol 377, 14 September 1995.

Kettner R.E., Schwartz A.B. and Georgopoulos A.P. (1988) Primate motor cortex and free arm movements to visual targets in three-dimensional space. III. Positional gradients and population coding of movement direction from various movement origins. J Neurosci 8(8):2938-2947.

Kihlstrom J.F. (1987) The cognition unconscious. Science 237:1445-1457.

Morasso P. (1981) Spatial control of arm movements. Exp Brain Res 42:223-227.

Mussa-Ivaldi F.A. (1988) Do neurons in the motor cortex encode movement direction? An alternative hypothesis. Neurosci Lett 91, 106-111.

Salmon, D.P. and Butters, N. (1995) Neurobiology of skill and habit learning. Curr Op in Neurobio 5:184-190.

Sanes J.N., Dimitrov B., and Hallet M. (1990) Motor learning in patients with cerebellar dysfunction. Brain 113:103-120.

Schlaug G., Knorr U., and Seitz R.J. (1994) Inter-subject variability of cerebral activations in acquiring a motor skill: a study with positron emission tomography. Exp Brain Res 98:523-534.

Schwartz A.B., Kettner R.E. and Georgopoulos A.P. (1988) Primate motor cortex and free arm movements to visual targets in three-dimensional space. I. Relations between single cell discharge and direction of movement. J Neurosci 8(8):2913-2927.

Scott S.H. and Kalaska J.F. (1995) Changes in motor cortex activity during reaching movements with similar hand paths but different arm postures. J Neurophysiol Vol 73 6:2563-2567.

Seitz R.J., Roland P.E., Bohm C., Greitz T., and Stone-Elander S. (1990) Motor learning in man: a positron emission tomography study. NeuroReport 1, 57-66.

Shadmehr R. and Mussa-Ivaldi F.A. (1994) Adaptive representation of dynamics during learning of a motor task. J Neurosci 14(5):3208-3224.

Shenoy K.V., Kaufman J., McGrann J.V., and Shaw G.L. (1993) Learning by selection in the trion model of cortical organization. Cerebral Cortex May/Jun V 3 N 3.

Soechting J.F. and Flanders M. (1989a) Sensorimotor representations for pointing to targets in three-dimensional space. J Neurophysiol 62:582-594.

Soechting J.F. and Flanders M. (1989b) Errors in pointing are due to approximations in sensorimotor transformations. J Neurophysiol 62:595-608.

Squire L.R. (1992) Memory and the hippocampus: a synthesis from findings with rats, monkeys, and humans. Psych Rev Vol. 99 2:195-231.

Tanji J. and Shima K. (1994) Role for supplementary motor area cells in planning several movements ahead. Nature 371:413-416.

Thach W.T. (1978) Correlation of neural discharge with pattern and force of muscular activity, joint position, and direction of intended next movement in motor cortex and cerebellum. J of Neurosci 41(3):654-676.

Uno Y., Kawato M. and Suzuki R. (1989) Formation and control of optimal trajectory in human multijoint arm movement. Biol Cybern 61:89-101.

Uno Y., Kawato M. and Suzuki R. (1987) Formation of optimum trajectory in control of arm movement - minimum torque-change model. Japan IEICE Technical Report, MBE86-79, 9-16.

Weinrich M., Wise S.P. and Mauritz K.-H. (1984) A neurophysiological study of the premotor cortex in the rhesus monkey. Brain 107:385-414.

Werner W., Bauswein E. and Fromm C. (1991) Static firing rates of premotor and primary motor cortical neurons associated with torque and joint position. Exp Brain Res 86:293-302.

Wolpert D.M., Ghahramani Z. and Jordan M.I. (1995) Are arm trajectories planned in kinematic or dynamic coordinates? An adaptive study. Exp Brain Res 103:460-470.

Appendix A. Calculating parameters for statistical analysis of cell activity

It is common in the analysis of neurophysiological data to plot the activity of cells in the motor cortex recorded during reaching movements as a function of movement direction. When plotted in this way, cell activity often exhibits a smooth variation from peak activity in the "preferred" direction of movement (Figure A.1). In this figure, the mean firing rate and the standard deviation about the mean are plotted for each direction of movement. The mean values are connected to demonstrate the variation across direction.

Such a graph provides a qualitative description of cell activity. When drawn across pairs of behavioral epochs from the current experiment - baseline, force field, or washout - changes in activity across epochs can be evident (Figure A.2). The goal of a statistical analysis is to quantify these changes and assess their significance.

Two separate analysis methods are applied to data here. Both were developed by Padoa Schioppa (1998); his informal memo documenting the analysis methods is essentially duplicated here. In the first method, the activity of a cell during a force epoch is characterized by an eight-dimensional (8D) vector. The components of the vector are the mean firing rates in the eight movement directions. The change in the 8D vector from one epoch to another forms the basis of the statistical analysis. This approach determines whether there is a significant change in cell activity between epochs and dictates the labeling of cells as kinematic, dynamic, or memory.

In the second statistical analysis method, the four parameters describing the nature of cell activity are analyzed. Given that the first analysis method determines a significant change in cell activity, this second method describes the nature of the change by identifying the contributing activity parameters.

A.1 Classification of cells - eight dimensional gaussian method

The activity of one cell across two behavioral epochs is to be compared. Within one epoch, the activity is characterized by an 8D vector with components equal to the mean firing rates of the cell in the eight movement directions. The monkey performs one movement at a time; therefore, the entire vector is not measured at once. Rather, multiple measures of each vector

component are made. Since the measures of the vector components are independent, the covariance matrix of the vector is diagonal.

For a direction of movement i, k_i measures of the firing rate n_i are made. ni is a random variable with expectation value $E(n_i)$ and variance $Var(n_i)$. An estimate of $E(n_i)$ and $Var(n_i)$ is determined by averaging across trials and computing the standard deviation.

$$m_i = \frac{1}{k_i}\sum_{j=1}^{k_i} n_{ij} \qquad \vec{m} = m_1, ..., m_8$$

$$s_i^2 = \frac{1}{k_i - 1}\sum_{j=1}^{k_i}\left(n_{ij} - m_i\right)^2 \qquad \vec{s}^2 = (s_1^2, ..., s_8^2)$$

where k_i is the number of trials in direction i and n_{ij} is the mean firing rate during trial j in direction i.

m_i itself is a random variable with expectation value $\mu_i = E(n_i)$ and variance $\sigma_i^2 = Var(n_i)/k_i$

$$m_i : N(\mu_i, \sigma_i^2) \qquad i = 1 \ldots 8$$

From the measures, an 8D vector $\vec{m}$ is obtained that has a gaussian distribution with unknown mean $\vec{\mu}$ and diagonal covariance matrix with estimated components

$$\sigma_i^2 = \frac{s_i^2}{k_i} \qquad i = 1 \ldots 8$$

It is now possible to compare cell activity across two force fields, F1 and F2, by performing an 8D z-test. Given

$$m_i^{F1} : N(\mu_i^{F1}, (\sigma_i^{F1})^2) \qquad i = 1 \ldots 8$$
$$m_i^{F2} : N(\mu_i^{F2}, (\sigma_i^{F2})^2) \qquad i = 1 \ldots 8$$

the null hypothesis H_o states that

$$H_o : \mu_i^{F1} = \mu_i^{F2} \qquad \text{for } i = 1 \ldots 8$$

A normalize variable, $\vec{r}$, is defined such that

$$r_i = \left(\frac{(m_i^{F1} - m_i^{F2})^2}{(\sigma_i^{F1})^2 + (\sigma_i^{F2})^2} \right)^{1/2} \qquad i = 1 \ldots 8$$

According to H_o, $\vec{r}$ is gaussian with normal distribution

$$r_i : N(0,1) \quad i = 1 \ldots 8$$

In fact, a finite value $\vec{R}$ is measured for $\vec{r}$ and H_o is rejected if the cumulative probability of values less probable than $\vec{R}$ is less than a threshold α.

Assuming that differences are completely random, a way to evaluate the difference between two gaussians is to compute the integral:

$$I(R) = \int_{C(\vec{R})} \prod_{i=1}^{8} \left(e^{-r_i^2/2} \frac{dr_i}{\sqrt{2\pi}} \right)$$

where $C(\vec{R})$ is the volume in 8D space of the values $\vec{r}$ "less probable" than $\vec{R}$. Ho is accepted/rejected by comparison of 1-I(R) with α.

This method is used to determine the significance of changes in a cell's activity across two behavioral epochs. By performing multiple-paired analysis, an assessment of changes from baseline to force field, baseline to washout, and force field to washout can be made. As shown in the table below, the nature of the changes dictates the cell's category.

Cell category	Are changes in activity across epochs significant?		
	Baseline to force field	Baseline to washout	Forcefield to washout
Kinematic	no	no	no
Dynamic	yes	no	yes
Memory	yes	yes	no

Table A.1 Changes in activity across epochs for cell categories

A.2 Parameter analysis of cell activity

The previous section described the method used to identify significant changes in cell activity across behavioral epochs. In this manner, a cell is classified by activity type. This method identifies cells whose activity changes; it does not identify the nature of the change.

In chapter 3, four activity parameters were defined that quantify the behavior of cortical cells for a given time period in a specific behavioral epoch (Figure A.3):

- mean or tonic firing rate across directions within the epoch
- dynamic range or modulation of activity about the mean
- preferred direction of activity
- sharpness of tuning.

General changes in cell activity across behavioral epochs identified by the 8D gaussian method should also be evident in changes to a subset of these activity parameters. A statistical analysis using the activity parameters, then, would provide additional information about the nature of cell activity.

Although these parameters quantify changes in activity across epochs, the parameters themselves are not sufficient to perform a statistical analysis. Variations in the parameters are required. The problem is that the activity parameters are calculated, not measured directly in

the experiment. Rather, average firing rates during specific time periods for each reaching movement are measured. It is necessary, then, to cast the parameters in terms of the measured variable and to propagate the variation in the measured variable to variations of the calculated parameters. An analysis method was developed (Padoa Schioppa 1998). The mathematical basis of the method and its application to a generic parameter $P(m_i)$ is described first. The method is then applied specifically to the parameters describing cell activity for a typical data set.

A.2.1. Mathematical development for a generic cell activity parameter

Consider cell activity during a single trial time period (movement time) for a single behavioral epoch (baseline). The monkey makes k_i trials in movement direction ϕ_i so that there are k_i measures of the cell firing rate during movement time, n_{ij}. The mean activity, m_i, and the variance, s_i^2, for the direction are calculated as:

$$m_i = \frac{1}{k_i}\sum_{j=1}^{k_i} n_{ij} \qquad \vec{m} = m_1, \ldots, m_8$$

$$s_i^2 = \frac{1}{k_i - 1}\sum_{j=1}^{k_i}\left(n_{ij} - m_i\right)^2 \qquad \vec{s}^{\,2} = (s_1^2, \ldots, s_8^2)$$

The mean values, m_i, can be plotted as a function of movement direction to give the graph shown in Figure A1. A parameter, p, describing cell activity is defined as a function of m_i: $p=P(m_i)$. The desire is to propagate the variability of the measured variable, n_i, through m_i to p. The following assumptions/observations are made:

- n_i is a random variable described by a normal distribution

$$n_i : \quad N(\mu_i, \sigma_i^2)$$

- m_i is a random variable described by a normal distribution

$$m_i : \quad N(\mu_i, \frac{\sigma_i^2}{k_i})$$

- The functional description of the parameter, p, is approximately linear in the region of $\vec{\mu}$ and can be expressed in a Taylor series as:

$$P(\vec{m}) \approx P(\vec{\mu}) + \sum_i \left.\frac{\partial P}{\partial m_i}\right|_{\mu_i} (m_i + \mu_i) \qquad (1)$$

- Given a random variable, m, with normal distribution

$$m: \qquad N(\mu, \sigma^2)$$

a second random variable can be defined

$$f = \alpha + \beta m \qquad (2)$$

with normal distribution

$$f: \qquad N(\alpha + \beta\mu, \beta^2 \sigma^2) \qquad (3)$$

Comparing the functional forms of equations (1) and (2) and noting equation (3), the parameter $p=P(m_i)$ can be written as a random variable with normal distribution

$$p: \qquad N\left(P(\vec{\mu}), \sum_i \left(\left.\frac{\partial P}{\partial m_i}\right|_{\mu_i} \right)^2 \frac{\sigma_i^2}{k_i} \right) \equiv N(\mu_p, \sigma_p^2) \qquad (4)$$

μ_p and σ_p^2 are estimated from the values of $\vec{m}$ and $\vec{s}^2$. This method can be applied to data from the three behavioral epochs. The resulting sets of statistical parameters can be used in standard methods to assess differences in cell activity across the epochs.

A.3. Method as applied to specific cell activity parameters

Four parameters have been identified to quantify cell activity: tonic firing rate, dynamic range, preferred direction of activity and sharpness of tuning. Using the mathematical method just described, the statistical parameters for each activity parameter are determined.

A.3.1. Tonic firing rate

Cast in terms of the mean spike frequency in each direction of movement, m_i, the tonic firing rate is given as

$$\varpi = \frac{1}{8}\sum_i m_i$$

The variance of the tonic firing rate is determined from the derivative of the functional expression and the variance of m_i

$$\sigma_\varpi^2 = \frac{1}{8^2}\sum_{i=1}^{8}\frac{\sigma_i^2}{k_i}$$

A.3.2. Dynamic range

The dynamic range is the modulation of cell activity about the tonic rate as a function of movement direction. Mathematically stated,

$$\omega_{dr} = m_{\theta_{max}} - m_{\theta_{min}}$$

where $m_{\theta max}$ and $m_{\theta min}$ are the mean spike rate in the directions of maximum and minimum activity, respectively. The variance for dynamic range is the sum of the variances for mean spike rates in the directions associated with the directions of maximum and minimum activity:

$$\sigma_{\omega dr}^2 = \left(\frac{\sigma^2}{k}\right)_{\theta_{max}} + \left(\frac{\sigma^2}{k}\right)_{\theta_{min}}$$

A.3.3. Preferred direction of activity

The cell activity parameter, preferred direction, identifies the movement direction of maximum cell activity. If activity in direction ϕ_i is characterized by a vector with amplitude m_i and unit vector in the given direction, then the mean preferred direction of cell activity is direction of the resultant vector summed over all eight directions of movement:

$$\phi_{pd} = P_{pd}(m_i) = \arctan\left(\frac{\sum_{i=1}^{8} m_i \sin\phi_i}{\sum_{i=1}^{8} m_i \cos\phi_i}\right)$$

From equation (4), the variance of the activity parameter is determined from the derivative of the parameter function and the variance of $\vec{m}$. It is given by

$$\sigma^2_{\phi_{pd}} = \sum_{i=1}^{8} \left(\frac{\sin\phi_i \sum_j m_j \cos\phi_j - \cos\phi_i \sum_j m_j \sin\phi_j}{\left(\sum_j m_j \sin\phi_j\right)^2 + \left(\sum_j m_j \cos\phi_j\right)^2} \right)^2 \frac{\sigma_i^2}{k_i}$$

A.3.4 Sharpness of tuning

As shown in Figure A.2, tuning sharpness is calculated as the difference between the two movement direction angles defined by the intersection of a line at the tonic firing rate and the tuning curve itself. The value for tuning sharpness is determined through a computational algorithm; the parameter does not lend itself to a simple mathematical expression. In the algorithm, the tuning curve is defined as a series of eight line segments connecting the mean firing rates for each direction of movement. The algorithm finds the two line segments, one on either side of the direction of maximum activity, that intersects the tonic or average firing rate value. For each of the two segments, the specific angle whose corresponding rate value equals the tonic value is determined through interpolation. The sharpness parameter is then defined as the difference between the two angles. The variance of the tuning sharpness is calculated as a function both of the variances associated with the mean firing rates in the movement directions that delimit the sharpness parameter and of the variance associated with the tonic firing rate.

Cell activity as a function of movement direction is often characterized relative to the broadly tuned behavior described by a cosine curve. A cell whose tuning curve approximates a cosine function would have a sharpness parameter equal to 180°. The data presented here for this parameter is normalized by dividing the calculated angle value by 180°. Therefore, parameter values greater than one indicate tuning broader than that of a cosine curve; parameter values less than one indicate a sharper response.

A.3.5 Numerical example

A numerical example is provided to illustrate application of the statistical analysis method. Figure A-4a-c shows histograms of single cell activity in the baseline, force field, and washout epochs, respectively. Recall that histograms demonstrate the temporal nature of cell activity by dividing the reaching task into discreet time bins and summing spike activity within each bin over multiple executions of the reaching trial. The ordinate is spike frequency in Hertz; the abscissa is time in milliseconds. Monkey movement toward a peripheral target starts at time

t=0ms. The effect of movement direction is seen by plotting separate histograms for each direction.

The trends seen in Figure A.4a suggest that nominal cell activity for the baseline epoch during the movement period is 7-10Hz. The direction of maximum firing, the cell's preferred direction, is approximately 135°-180°. Figure A.4b shows comparable data during the force field epoch. Average cell activity does not apparently change. However, compared to baseline data, a decrease in spike activity for movements to 225° and an increase in activity for movements to 45°-90° suggest a shift in the cell's preferred direction. Figure A.4c, activity of the cell during the washout epoch, shows a slight decrease in average firing rate and a direction of maximum activity again approximately 135°-180°. Figure A.5 shows mean cell firing rate during movement time for the baseline, force field, and washout epochs overlaid on a single plot. Again, the direction of maximum activity seems to shift during the force field epoch. The statistical analysis methods will demonstrate whether this trend is significant.

Raw spike frequency data in the movement period is used to calculate the mean frequencies and corresponding variances in each direction of movement for the three behavioral epochs:

$$m_{baseline} = \{\ 7.71 \quad 8.02 \quad 8.85 \quad 10.63 \quad 12.35 \quad 13.03 \quad 9.64 \quad 8.14\ \}$$

$$\sigma_{i\ baseline}^2 = \{\ 3.90 \quad 4.73 \quad 5.76 \quad 7.20 \quad 5.44 \quad 5.44 \quad 10.05 \quad 5.83\ \}$$

$$m_{forcefield} = \{\ 9.63 \quad 8.44 \quad 5.99 \quad 10.49 \quad 12.64 \quad 12.30 \quad 10.88 \quad 11.63\ \}$$

$$\sigma_{i\ forcefield}^2 = \{\ 14.72 \quad 7.87 \quad 4.18 \quad 9.00 \quad 8.40 \quad 7.84 \quad 8.59 \quad 7.09\ \}$$

$$m_{washout} = \{\ 5.89 \quad 5.55 \quad 6.79 \quad 9.13 \quad 11.17 \quad 10.39 \quad 8.52 \quad 6.58\ \}$$

$$\sigma_{i\ washout}^2 = \{\ 5.49 \quad 3.36 \quad 4.75 \quad 5.85 \quad 4.38 \quad 8.08 \quad 6.95 \quad 4.50\ \}$$

Applying the method of the previous section, the mean and variance for each cell activity parameter over the three epochs are given below:

Activity parameter	Behavioral epoch					
	Baseline		Force field		Washout	
	mean	variance	mean	variance	mean	variance
tonic rate	9.80	0.04	10.25	0.05	8.00	0.04
dynamic range	5.32	0.55	6.63	0.53	5.62	0.47
preferred direction	165.5	49.7	120.3	57.4	162.3	37.2
tuning sharpness	0.86	0.007	1.19	0.010	0.94	0.008

Table A2. Statistical parameters for activity parameters over behavioral epochs

Considering activity across pairs of behavioral epochs, the following statistics are calculated:

Parameter	Baseline vs forcefield		Baseline vs Washout		Forcefield vs Washout	
	p-value	sig?	p-value	sig?	p-value	sig?
8D gaussian	0.03	yes	0.88	no	0.00	yes
tonic rate	0.14	no	0.00	yes	0.00	yes
dynamic range	0.20	no	0.76	no	0.30	no
preferred direction	0.00	yes	0.73	no	0.00	yes
tuning sharpness	0.01	yes	0.50	no	0.06	no

Table A3. Significance tests across behavioral epochs

The relationship among force epochs indicated by the 8D gaussian method suggests that this is a dynamic cell - cell activity changes in the force field epoch compared to baseline and washout. The same relationship is seen in the preferred direction parameter, confirming the trend that seemed evident from visual assessment of the data. This is also seen in tuning sharpness; however, the trend fall just short of statistical significance. Changes in the tonic rate demonstrate a different trend. Due to the large number of reaching movements made in each direction, tonic rate is statistically a very sensitive parameter. The small change in tonic rate across epoch, although statistically significant, does not change the conclusion as to the labeling of this cell as kinematic.

A.4. References

Padoa Schioppa, C. (1998) Report on data analysis. Personal communication.

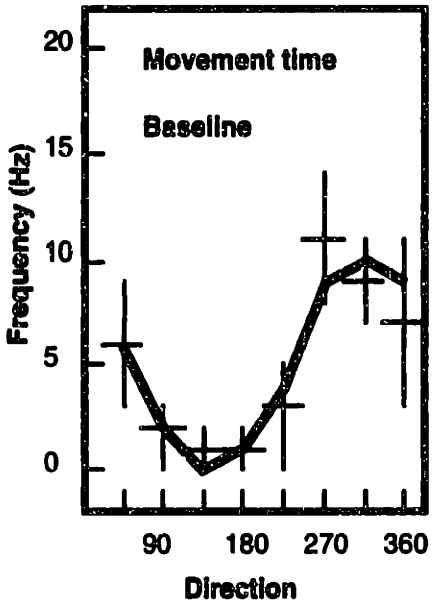

Figure A1. Cell activity broadly tuned with movement direction

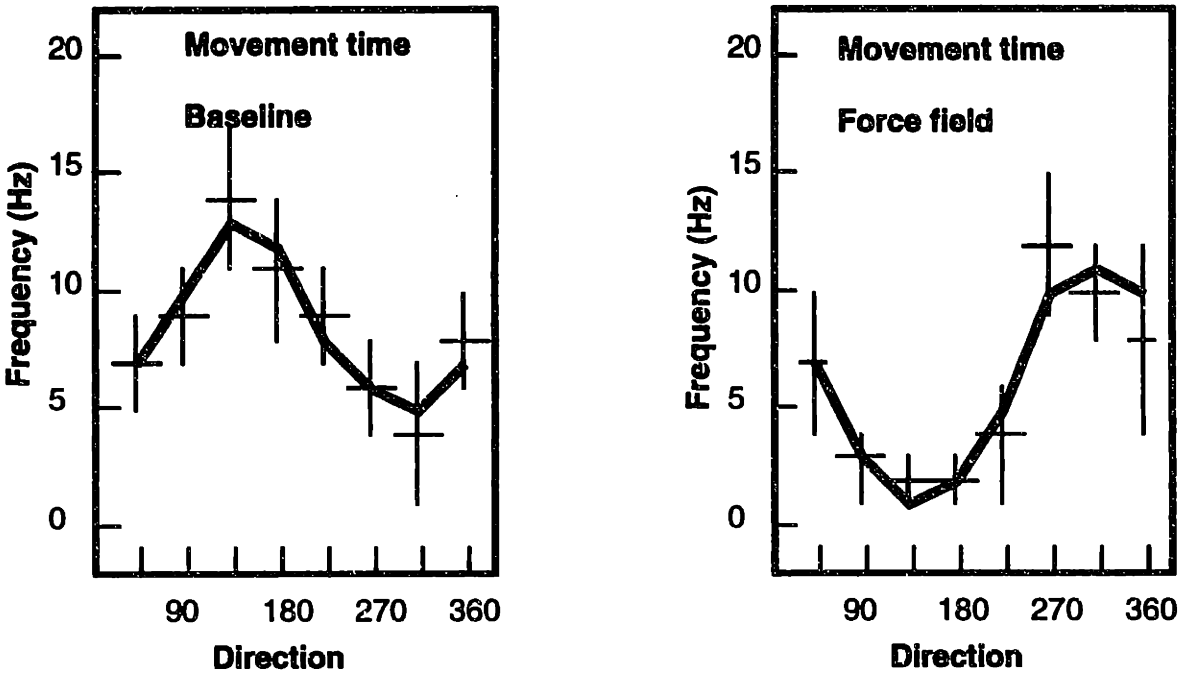

Figure A2. Change in cell activity from baseline to force field epochs

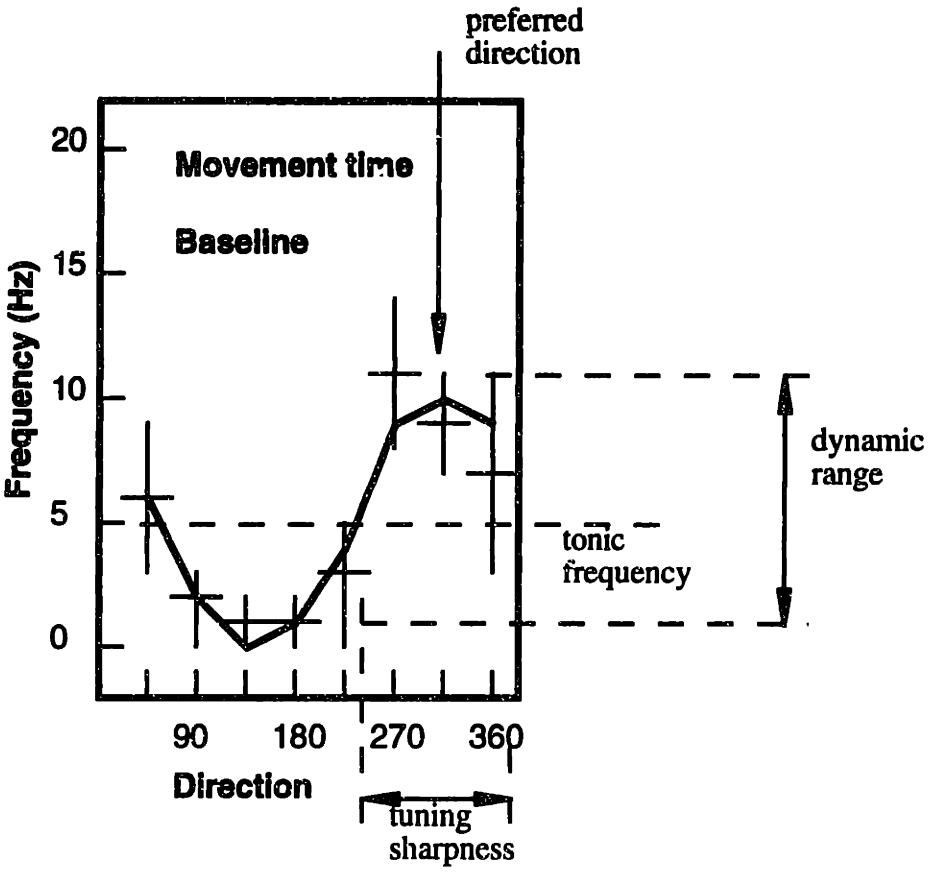

Figure A3. Parameters describing cell activity

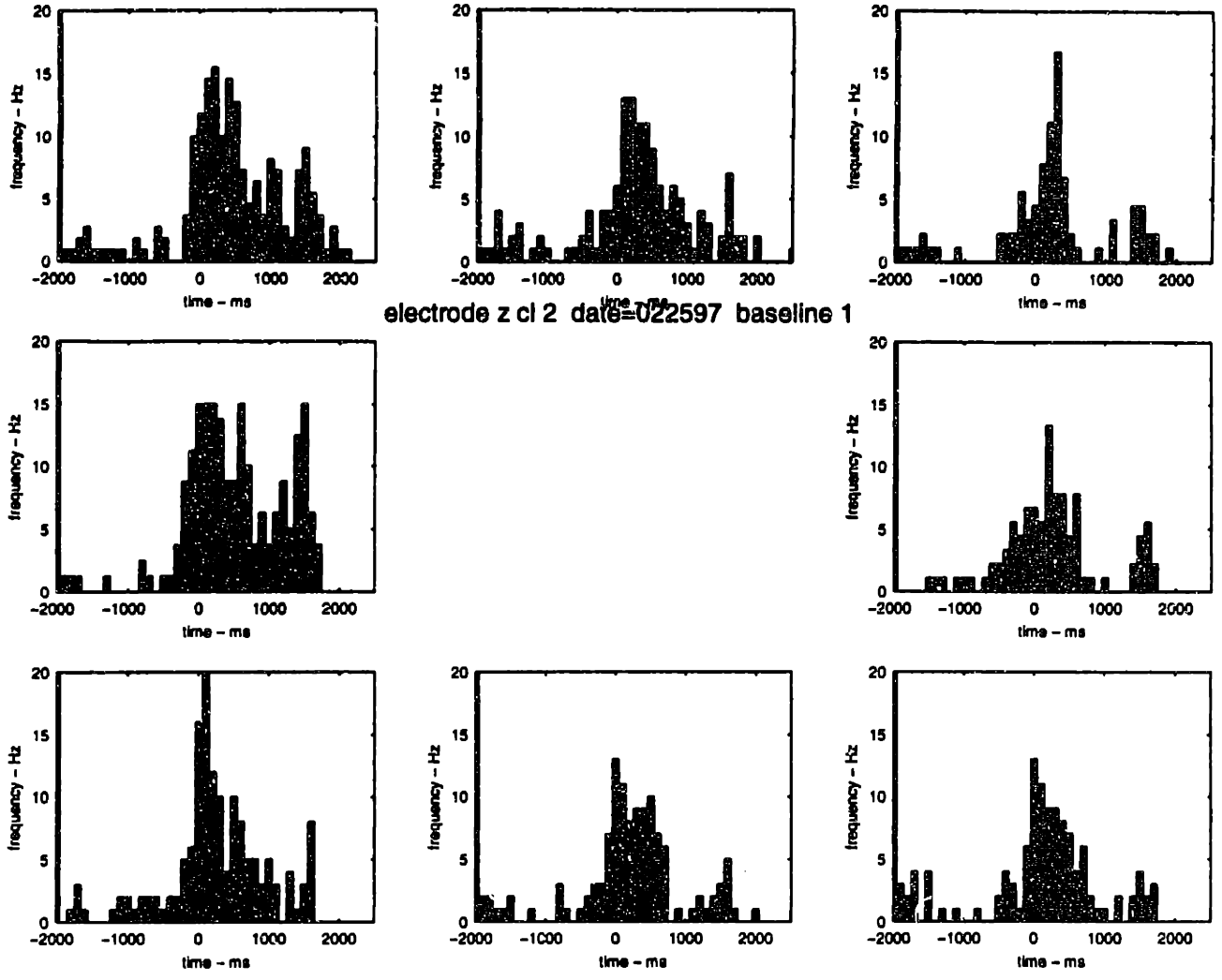

Figure A.4a Histogram of cell activity during baseline epoch

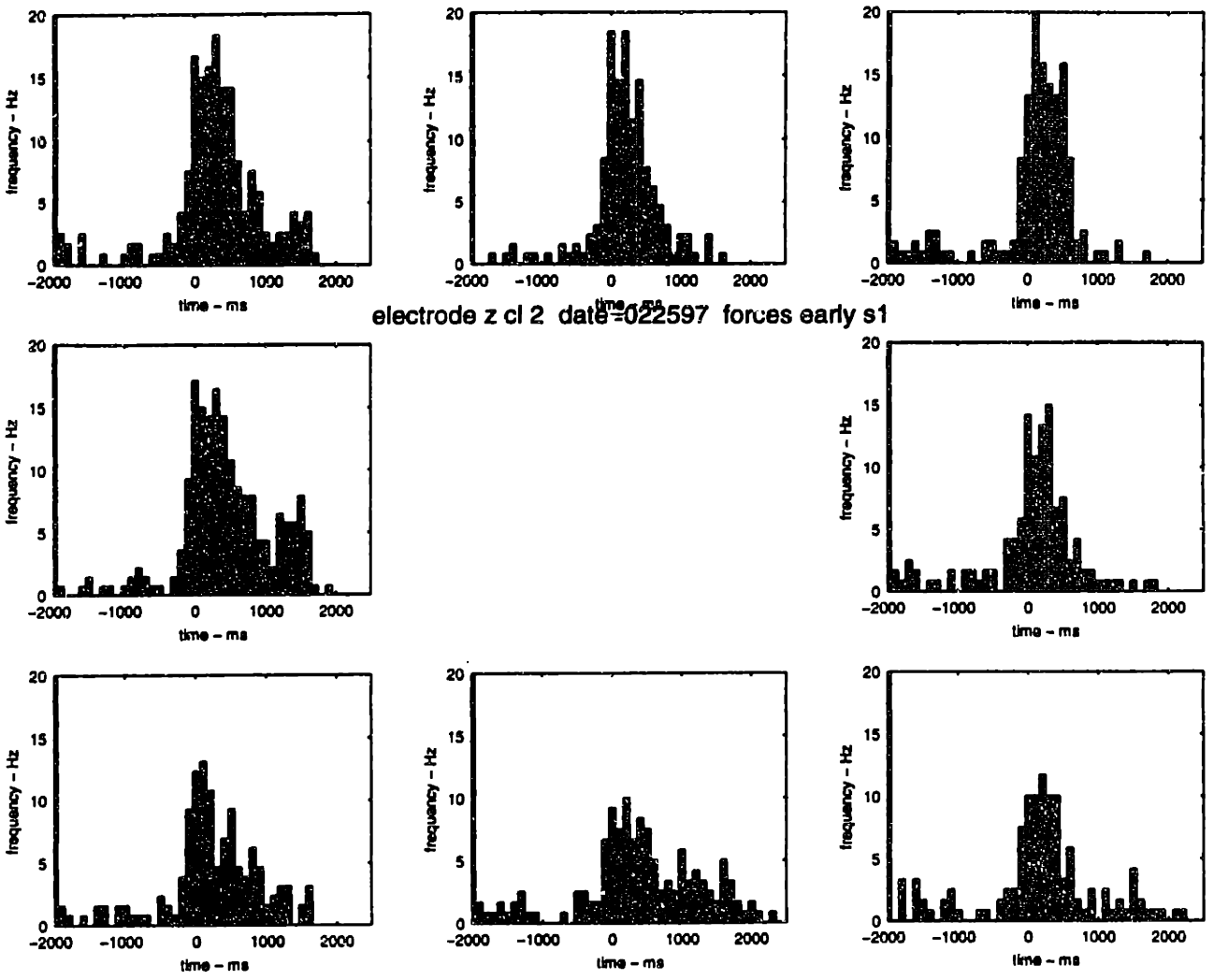

Figure A.4b Histogram of cell activity during force field epoch

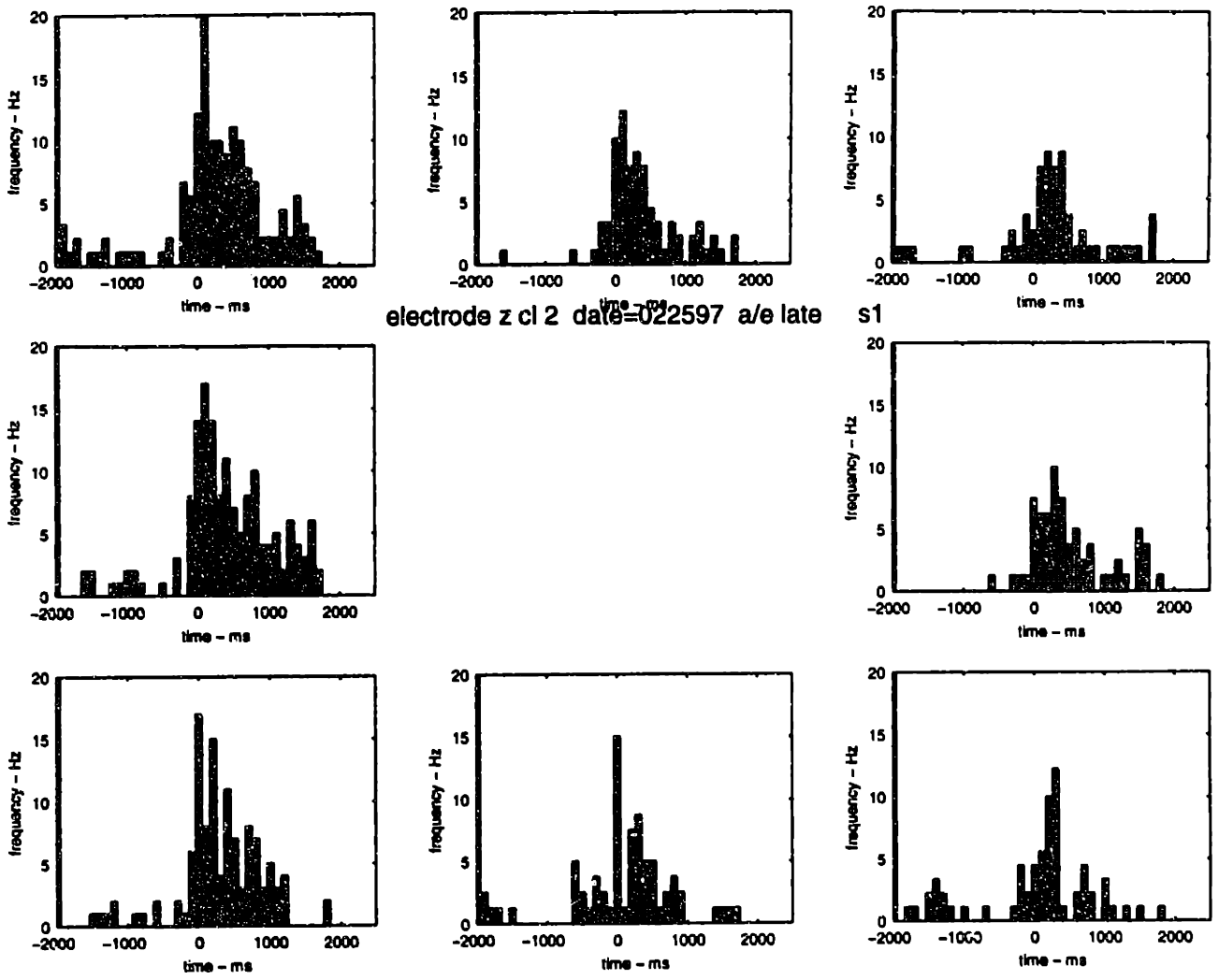

Figure A.4c Histogram of cell activity during washout epoch

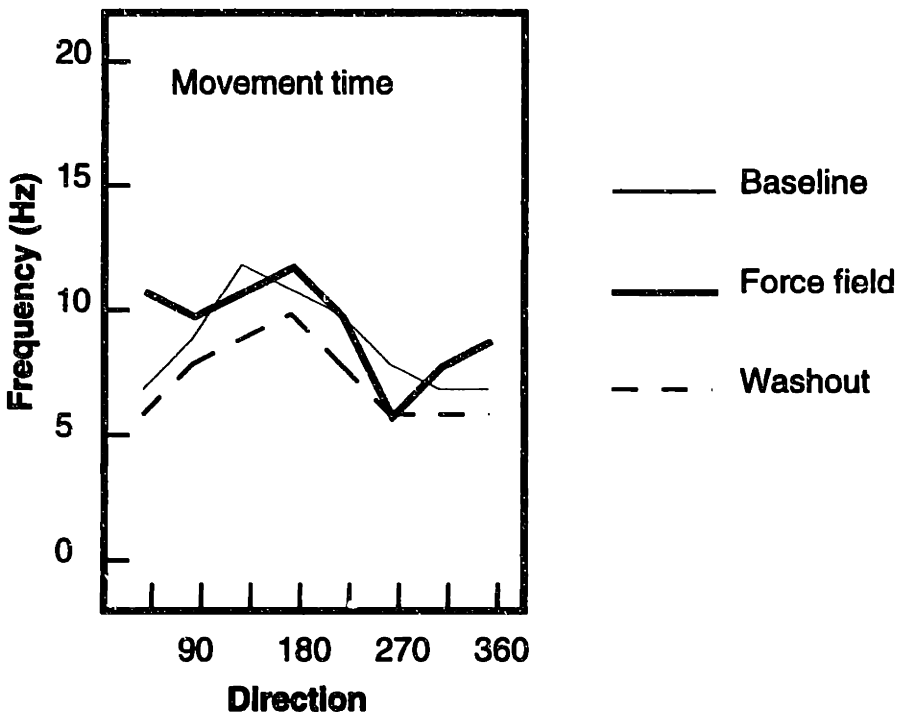

Figure A5. Cell activity for three behavioral epochs